The optimal mix of flexibility from an integrated energy system

Qikun Chen

School of Engineering

Cardiff University

A thesis submitted for the degree of

Doctor of Philosophy

Aug 2024

Acknowledgements

This research project would not have reached fruition without the generous and unwavering support of many dedicated individuals. I am deeply grateful to my supervisors, Prof. Meysam and Prof. Nicholas Jenkins. Their insightful guidance, constant support, and encouragement have been instrumental in shaping the direction and success of my work.

In addition, I sincerely thank the CIREGS group for the stimulating discussions, constructive feedback, and collaborative environment, which enriched my understanding and academic growth. Our rigorous weekly meetings were consistently enlightening and invaluable to my research.

My deepest appreciation goes to my family. Their endless patience, unconditional love, and constant encouragement have sustained me throughout this journey. They have been my pillar of strength and a source of motivation during challenging times.

I am also grateful for the failures, discrimination, neglect, and countless sleepless nights along this journey, as they have significantly enhanced my resilience while preserving my courage to question, my passion for exploration, and my pursuit of liberty, justice, and impartiality.

Finally, thanks to my cat, Cosmo, for his companionship during my PhD.

Abstract

Quantifying the value of energy system flexibility is becoming increasingly complex due to the growing interconnections and interactions among diverse energy infrastructures. To address this challenge, a modelling framework of an integrated energy system is developed. This framework incorporates the coordinated operation of various units, to optimise the whole energy system's operation and identify the role of different flexibility sources.

It was shown by the results that, compressor units within the gas network can offer flexibility by using linepack as a gas storage buffer, and the coordinated operation of gas-driven and electric-driven compressors can significantly reduce operational costs and emissions.

Flexible operation of electrolysers and electric storage units enables the power system to accommodate more variable renewable generation. In addition, residential heating systems can contribute flexibility by using the thermal inertia of building fabrics to adjust indoor temperatures adaptively. These flexibilities lead to substantial reductions in operational costs compared to systems lacking such capabilities.

The magnitude of available flexibility that can be offered by various electric-side units was quantified, and Locational Marginal Prices (LMP) were calculated

for busbars throughout the electric power system. A correlation analysis explored the relationship between upward flexibility and LMP at each busbar. Results showed that by harnessing this flexibility, the system can more effectively manage increasing demand by optimally dispatching renewable resources across time steps.

Table of contents

List of Figures

List of Tables

Nomenclature

1. Set (index)	Description
Gas system	
$GP(gp)$	Sources of gas provision
$EL(gp)$	Networked Electrolysers ($EL \subset GP$)
$S(s)$	Gas storage sites
$P(p)$	Pipelines
$N(n)$	Nodes
$C(c)$	Compressor units
$GC(c)$	Gas-driven compressor units ($GC \subset C$)
$EC(c)$	Electric-driven compressor units ($EC \subset C$)
Electricity system	
$OTH(g)$	Power generator, including nuclear, bioenergy and other renewable sources (waste, ground thermal, etc)
$GT(g)$	Gas turbines
$VRE(g)$	Renewable generators including wind farms and PV panels
$I(i)$	Interconnectors
$L(l)$	Transmission lines (wires)
$B(b)$	Busbars
$ES(es)$	Electrical energy storage units
Heating system	
$BD(bd)$	Buildings
$HP(bd)$	Buildings installed with heat pumps ($HP \subset BD$)
$GB(bd)$	Buildings installed with gas boilers ($GB \subset BD$)
Others	
$T(t)$	Time resolution (hour)

2. Variables	Description
Gas system	
$Q_{gp,t}^{\mathrm{GP}}$	Gas provision at t (mcm/h)
$Q_{s,t}^{\mathrm{S}}$	Gas discharging from a storage at t (mcm/h)
$Q_{p,t}^{\mathrm{av}}$	Average gas flow within a pipe at t (mcm/h)
$Q_{p,t}^{\mathrm{in+/out+}}$	Positive* inflow/outflow of gas within a pipe at t (mcm/h)
$Q_{p,t}^{\mathrm{in-/out-}}$	Negative inflow/outflow of gas within a pipe at t (mcm/h)
$\Pi_{n,t}$	Pressure at a gas node at t (bar)

* In the model, the direction gas flow from n_p^{start} to n_p^{end} is considered positive, while flow from n_p^{end} to n_p^{start} is considered negative. n_p^{start} and n_p^{end} are both ends of a pipe, or suction node and discharge node of a compressor.

$Q_{n,t}^{\mathrm{sup/dem}}$	Cumulative gas supply/ demand at a gas node at t (mcm/h)
$Q_{n,t}^{\mathrm{flexdem}}$	Flexible gas supply at a gas node at t (mcm/h)
$Q_{n,t}^{\mathrm{LS}}$	Gas load shedding at a gas node at t (mcm/h)
$Q_{c,t}^{\mathrm{tp}}$	Gas throughput of a compressor at t (mcm/h)
$E_{c,t}$	Energy consumption of a compressor at t (MWh)
$Q_{c,t}^{\mathrm{u}}$	Gas consumption by a compressor at t (mcm/h)
$Q_{c,t}^{\mathrm{in/out+}}$	Positive inflow/outflow of gas within a compressor at t (mcm/h)
$Q_{c,t}^{\mathrm{in/out-}}$	Negative inflow/outflow of gas within a compressor at t (mcm/h)
$L_{p,t}$	Volumetric value of linepack in a pipe at t (mcm)
$\alpha_{c,t}$	Compression ratio
$Q_{g,t}^{\mathrm{G}}$	Gas consumed by a gas turbine at t (mcm/h)
$x_{p,t}$	Binary variables denoting the gas flow direction in a pipe at t

Electricity system

$P_{gp,t}^{\mathrm{GP}}$	Power consumption of an electrolyser at t (MW)
$P_{g,t}^{\mathrm{G}}$	Power generation from a generator at t (MW)
$P_{g,t}^{\mathrm{U}}$	Power from a renewable power station can be utilised at t (MW)
$P_{g,t}^{\mathrm{C}}$	Curtailed renewable at a renewable power station at t (MW)
$P_{i,t}^{\mathrm{IM}}$	Power import from an interconnector at t (MW)
$P_{l,t}$	Power flow in a wire at t (MW)
$\theta_{b,t}$	Voltage angle at a busbar at t (rad)
$P_{b,t}^{\mathrm{sup/dem}}$	Cumulative power supply/demand at a busbar at t (MW)
$P_{b,t}^{\mathrm{flexdem}}$	Flexible power demand at a busbar at t (MW)
$P_{b,t}^{\mathrm{LS}}$	Power load shedding at a busbar at t (MW)
$P_{es,t}^{\mathrm{ES}}$	Power charging/discharging of a storage unit at t (MW)
$E_{es,t}^{\mathrm{ES}}$	Stored electrical energy in a storage unit at t (MWh)
$y_{g,t}$	Binary variable denoting the start-up process of a turbine at t
$z_{g,t}$	Binary variable denoting the shut-down process of a turbine at t
$u_{g,t}$	Binary variable denoting the ON/OFF process of a turbine at t

Heating system

$T_{bd,t}^{\mathrm{in}}$	Indoor temperature of a building at t (K)

$P_{bd,t}^{\mathrm{HP}}$	Power consumption of the building installed with heat pumps at t (MW)
$Q_{bd,t}^{\mathrm{GB}}$	Gas consumption of the building installed with gas boilers at t (mcm/h)

3. Parameters	**Description**
Gas system	
$\underline{Q_{gp}^{\mathrm{GP}}}/\overline{Q_{gp}^{\mathrm{GP}}}$	Min/max gas provision (mcm/h)
$\overline{\eta^{\mathrm{EL}}}$	Efficiency of an electrolyser
$\underline{\mathrm{Q}_s^{\mathrm{S}}}/\overline{\mathrm{Q}_s^{\mathrm{S}}}$	Min/max gas discharging from an underground storage site (mcm/h)
$\mathrm{K_p}$	Coefficient of gas flow of a pipe
T^{b}	Base temperature of the gas system (°R)
P^{b}	Base pressure of the gas system (psia)
γ	Specific gravity of gas
T^{av}	Average temperature in pipelines (°R)
Z	Compressibility of gas at base temperature and pressure
Len_p	Length of a pipe (km)
D_p	Diameter of a pipe (m)
$Q_{n,t}^{\mathrm{nflexdem}}$	Predefined non-flexible gas demand (mcm/h)
S_p	Linepack coefficient of a pipe
ρ	Density of gas (kg/m^3)
L_p^0	Initial linepack volume (mcm/h)
B, B′	Fitted coefficients of a linear expression by simplifying the nonlinear equation of compressors energy consumption
$\underline{\alpha_c}/\overline{\alpha_c}$	Min/max value of compression ratio
HV	Energy content of gas (MWh/mcm)
Electricity system	
δ_g	Load factor of generator
$\underline{\mathrm{P}_g^{\mathrm{G}}}/\overline{\mathrm{P}_g^{\mathrm{G}}}$	Min/max generation at generator (MW)
$\overline{u_g^0}$	Initial ON/OFF status of CCHT
$\mathrm{RU}_g/\mathrm{RD}_g$	Ramp-up/down rate of a gas turbine (MW/h)
$\mathrm{SU}_g/\mathrm{SD}_g$	Start-up/shut-down rate of CCHT(MW/h)
$\mathrm{L}^{\mathrm{MU/MD}}$	Min-up/Min-down time of a turbine (MW)
η^{G}	Efficiency of a generator
$\mathrm{P}_{g,t}^{\mathrm{A}}$	The available amount of renewable generation at a renewable power station
$\underline{P_i^{\mathrm{IM}}}/\overline{P_i^{\mathrm{IM}}}$	Min/max power import from an interconnector
$\overline{\bar{P}_l}$	Maximum power flow
X_l	Reactance of branch (ohm)
$P_{b,t}^{\mathrm{nflexdem}}$	Predefined electricity demand (MW)
ES_{es}^0	Initial amount of energy stored in an electrical energy storage unit (MWh)

δ_g	Load factor of generator
$\mathrm{P}_g^{\mathrm{G}}/\overline{\mathrm{P}_g^{\mathrm{G}}}$	Min/max generation at generator (MW)
$\overline{u_g^0}$	Initial ON/OFF status of CCHT
Heating system	
T_{bd,t_0}^{in}	Initial indoor temperature of a building (K)
$\mathrm{T}_{bd,t}^{\mathrm{amb}}$	Ambient temperature (K)
U_{bd}	Thermal conductivity (K/MW)
C_{bd}	Thermal capacity (MJ/K)

Chapter 1 Introduction

1.1 Background

1.1.1 Decarbonisation target and the transition to a Net Zero energy system

Global warming presents a significant challenge worldwide. It is estimated that the average global surface temperature was 1.06°C warmer than pre-industrial level in 2022 [1]. This led to a multitude of severe consequences, including rising sea levels, the intensification of extreme weather events such as droughts and floods, and a great reduction in biodiversity.

A primary contributor to global warming is greenhouse gas (GHG) emission, largely due to the burning of fossil fuels such as oil and gas. Approximately, annual carbon dioxide (CO_2) emissions worldwide exceeded 37 billion metric tons in 2022, a 64% increase from the 1990 level [2]. To combat climate change and mitigate the effects of global warming, it is essential to reduce these emissions globally.

The United Kingdom has established an ambitious target to reach Net Zero by 2050, a goal that necessitates the widespread adoption of renewable energy sources to decarbonise the energy system [3]. As of the third quarter of 2023, renewables account for approximately 44.5% of the UK's total electricity generation [4]. Future projections indicate that renewable energy could fulfil between 75% and 90% of the UK's electricity demand by 2050 [5]. This requires the installation of up to 157 GW of wind turbines and 90 GW of PV panels [6].

The substantial increase in renewable energy sources significantly alters the energy supply landscape. Figure 1.1 illustrates the differences in energy flow across supply and demand between the current state and the projected mix for 2050. It can be found that fossil fuels such as gas and oil remain the predominant sources for meeting energy demands currently while renewables such as wind, and PV are expected to play an essential role in the future.

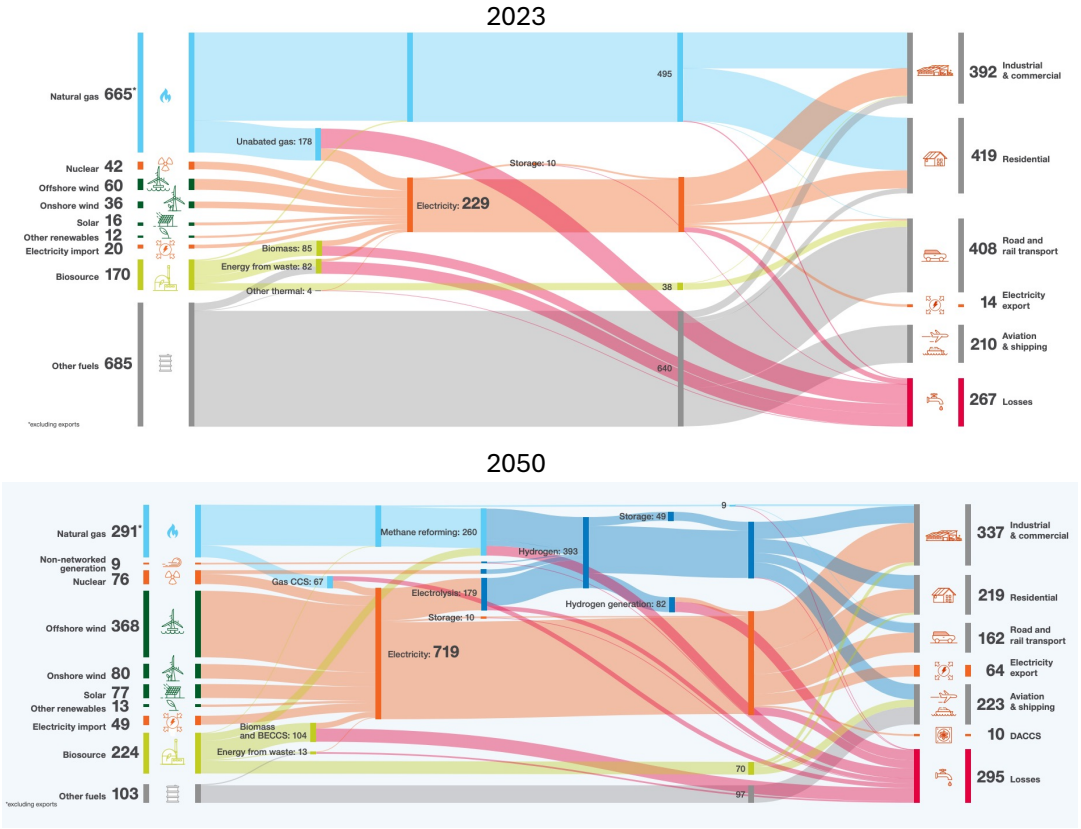

1**Figure 1.1** Energy flow across supply and demand in 2023 and 2050. (data from FES [7] ,unit: TWh)

1.1.2 Flexibility requirements for the future energy system

Higher renewable energy penetration brings challenges such as intermittency, grid stability risks, and increased flexibility requirements due to the variable nature of wind and solar power. It also demands upgrades to transmission and distribution networks, rethinking market designs to incentivise flexibility and backup capacity, and solutions to manage energy curtailment during low-demand periods.

One of these challenges arises from the operational requirement to timely balance electricity demand and supply, which is necessary for ensuring the stability and reliability of the electric power system. Unlike conventional sources such as fossil fuels that offer controllable output, renewable sources are intermittent and fluctuating, making achieving this balance more complicated.

Flexibility, defined as the electric power system's capacity to balance supply and demand [8], plays a significant role in ensuring the reliability and stability of the power grid. Insufficient flexibility within the system hampers its capability to integrate a substantial proportion of renewable energy technologies. For instance, in Great Britain (GB), approximately 5.8 terawatt-hours (TWh) of wind-generated power had to be curtailed across 2020 and 2021, which could have powered around 0.8 million households [9]. The corresponding cost of curtailing wind power was nearly one billion Pounds in 2023[10]. Such cases underscore the critical need for enhanced system flexibility in the transition to Net Zero. The requirement for different levels and types of flexibility for the future is shown in Figure 1.2.

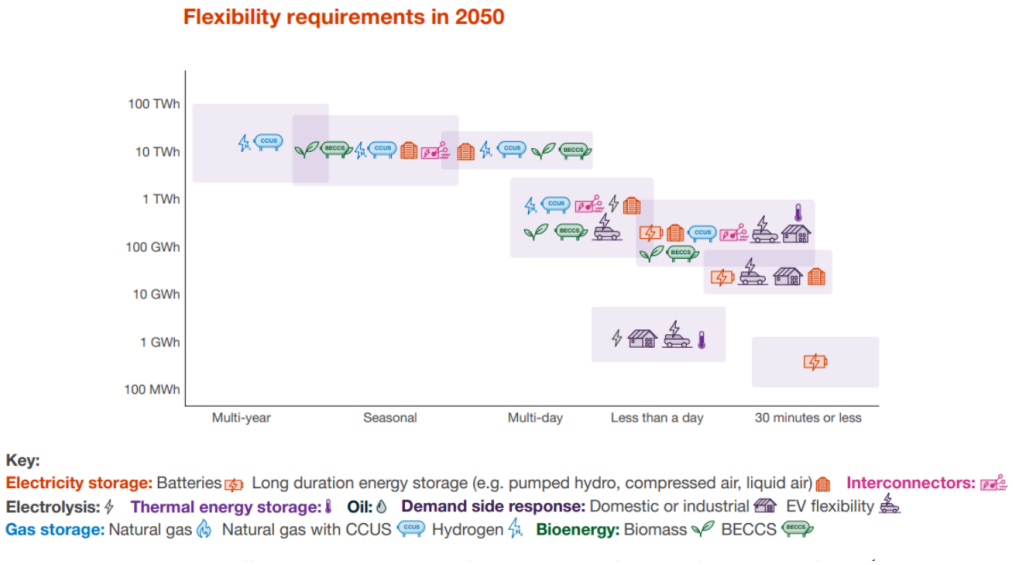

2**Figure 1.2** Different levels and types of energy system flexibility for the year of 2050[11]. The flexibility requirements for energy systems in 2050 is categorised across different timescales. For instance, gas storage, hydrogen, natural gas with carbon capture (CCUS), and bioenergy are key enablers to provide long term flexibility, while demand side response and batteries tend to provide short term flexibility.

A more flexible electric power system holds the key to accommodating a higher share of renewable generation, thereby reducing both curtailments and their associated costs. It is estimated that by leveraging system flexibility, the UK could save up to £10 billion annually by 2050 [12].

1.1.3 Enhanced flexibility via energy systems integration

To enhance the flexibility of the GB electric power system, it is envisioned that up to 50 GW of energy storage capacity is required by 2050 [6]. While a continuous reduction of electrical energy storage costs [13–15] has been observed over the recent years, battery storage is still an expensive technology and there are concerns about their life cycle environmental impacts [16–20]. Therefore, instead of solely relying on battery storage, coordinated operation of multiple energy vectors allows us to leverage energy storage [21,22] and demand response potentials [23,24] available in the other energy vectors such as heat, natural gas and hydrogen.

Hydrogen infrastructures can offer flexibility to the electric power system by supplying hydrogen-fired power plants [25,26] and providing large-scale within-pipe storage (linepack) and underground storage to absorb hydrogen produced by electrolysers [27–30]. Hydrogen-fired power plants can help compensate for the shortfall of electricity when renewable generation is unable to meet the electricity demand. Additionally, when renewable generation exceeds electricity demand, surplus renewable electricity can be utilised by electrolysers to produce green hydrogen, which can be stored within the hydrogen system.

Furthermore, the electric power system can gain demand-side flexibility through the strategic use of low-carbon heating devices, like heat pumps, which leverage the thermal inertia of buildings [31–35]. Such flexibility allows for the

reduction of electricity consumption, particularly during peak demand periods, while maintaining the comfort of building occupants. By utilising buildings' inherent thermal storage capacity, these heating systems can adapt to renewable generation. For instance, during periods of high renewable generation, the heat pumps can be boosted to raise the indoor temperature without jeopardising thermal comfort. The indoor temperature can be maintained for hours due to thermal inertia of the building material, allowing for the heat pumps to be scaled back or turned off during subsequent periods of lower renewable generation. This not only helps in smoothing out the curve of electricity demand but also aids in integrating renewable energy sources more effectively into the power grid, thereby contributing to a more sustainable and efficient energy system.

1.2 Challenges

Large-scale integration of diverse low-carbon technologies introduces great operational challenge to the whole energy network. Specifically, these challenges include:

(1) Variable Renewable Energy (VRE) such as wind and solar are intermittent and hard to predict accurately. Integrating a high volume of renewable energy into the electricity network poses a significant operational challenge to the network to balance demand and supply in real-time.

(2) Integrating a large number of facilities into the energy system complicates its operation due to the need to consider diverse factors such as varying capacities, maintenance requirements, and energy outputs. To achieve minimal operational costs, it is crucial to optimise these facilities' operations simultaneously through strategic coordination.

(3) Quantifying the flexibility available to the electric power system is challenging as different flexible sources offer varying degrees of flexibility subject to their capacity and operational limitations. Additionally, the level of system flexibility is also influenced by other factors such as transmission capacity. A comprehensive assessment that considers the operational constraints of all units and their complex interactions is essential to accurately quantify the system's total flexibility.

(4) There is an increasing need for the installation of flexible resources due to the higher penetration of renewable energy. However, such investment decisions must be made with careful consideration. The demand for flexibility can vary greatly between different locations, some may require a high level of flexibility, whereas others might need significantly less. Without appropriately tailored consideration, this can result in over-installation of flexibility resources in certain areas, leading to unnecessary and potentially wasteful investments.

Optimising the operation of an energy system requires a comprehensive model that accounts for the physical constraints of networks and infrastructures.

However, the intricate interdependencies between various energy facilities and the unique operational characteristics of certain units significantly increase the complexity of the optimisation problem, for example, introducing integer variables and nonlinear constraints. To address this complexity and reduce the computational burden, approximation techniques are necessary.

1.3 Research aims

The primary aim of this investigation is to explore the role of energy systems integration in optimising the operation of the system and enhancing system flexibility. The key objectives of this thesis are outlined as follows:

(1) Provide a detailed representation of the integrated energy system with diverse energy supplies, transmission networks and storage facilities. The model is generic and can be applied to diverse scenarios, including different regions and countries.

(2) Explore the intricate interactions between different energy facilities within the energy system and optimise the operation of the system via the coordinated operation of these facilities.

(3) Identify how various flexible energy sources offer flexibility to the electric power system, considering their distinct operational characteristics, and elucidate the impact each type of flexibility has on the system's operation.

(4) To quantify the magnitude of flexibility offered by various electric-side units and clarify its economic significance.

1.4 Thesis outline

This section outlines the thesis structure, providing a summary of each chapter.

Chapter 1 introduces the research, detailing its background, objectives, and primary challenges.

Chapter 2 introduces the integrated energy system (IES) model, providing a detailed representation of each component within the IES, in addition to the expressions of coupling components between different systems.

In Chapter 3, the IES model was applied to the gas network of South Wales and Southwest England. This analysis aimed to optimise the operation of the gas networks by utilising flexibility from linepack and compressor units. Nonlinear hydraulic equations were reformulated using Second-Order Cone Programming (SOCP) and McCormick envelopes. Additionally, an efficient algorithm was implemented to enhance the model's accuracy.

In Chapter 4, a case study was analysed, applying the IES model to the whole GB gas network while considering the flexible operation of compressor units. Different scenarios were considered to explore the benefits of coordinated operation of gas-driven compressors and electric-driven compressors. The potential of electric-driven compressors to provide flexibility to the electric power system was also analysed. Moreover, a Cost Benefit Analysis (CBA) was carried

out in this chapter to evaluate the investment viability of installing electric-driven compressor units.

Chapter 5 investigates the value of flexibility through energy system integration. The model was applied to an integrated hydrogen-electricity-heating system in 2050 in GB. This chapter emphasises the economic and operational benefits of various flexibility sources, comparing the performance of energy systems with and without such flexibility.

Chapter 6 quantifies the flexibility magnitude and impacts of flexibility locational marginal prices (LMP) in the electric power system. It contrasts the LMPs in scenarios with and without sufficient flexibility, discussing the impact of unlocking flexibility on reducing LMP. Additionally, it explores the correlation between the LMP and the available flexibility magnitude of the electric power system.

Chapter 7 summarises the research, highlighting its main findings and describing directions for future work.

1.5 Summary of Achievements

A summary of the main achievements of this work included in the thesis is given below:

(1) A model of the gas network considering the compressor units was developed. The model was formulated as a Mixed-Integer Second-

Order-Cone Programming (MISOCP), using a bound-tightening algorithm to improve the computational performance of optimisation The model was applied to the gas network of South Wales and Southwest of England, to optimise the operation of compressor units to reach a minimum cost. This work was published as "*Optimal Operation of Compressors in an Integrated Gas and Electricity System—An Enhanced MISOCP Method"* in the IEEE Access journal (DOI: 10.1109/ACCESS.2022.3227859) [36].

Contributions:

Qikun Chen: Modelling, programming, data collection, analysis, writing, editing, visualisation.

Meysam Qadrdan: Conceptualisation, review & editing, supervision.

Nicholas Jenkins: Review & editing, supervision.

Yongning Zhao: Modelling, review & editing.

(2) An optimisation model of Great Britain's high-pressure gas transmission network with 24 compressor stations was developed, to analyse the optimal operation of the value of flexibility from the hybrid compressor stations (compressor stations in which both electric-driven and gas-driven compressor units exist). Furthermore, a cost-benefit analysis was carried out to assess the investment viability of installing electric-driven compressor units. This work was published as "*Assessing Techno-Economic and Environmental Impacts of Gas Compressor Fleet as a*

Source of Flexibility to the Power System" in the IEEE Transactions on Energy Markets, Policy and Regulation journal (DOI: 10.1109/TEMPR.2023.3276308)[37].

Contributions:

Qikun Chen: Modelling, programming, data collection, analysis, writing, editing, visualisation.

Meysam Qadrdan: Conceptualisation, review & editing, supervision.

Tong Zhang: Review & editing.

(3) An optimisation model of the integrated electricity and heating system was developed and applied to a case study for GB. Various scenarios with different indoor temperature constraints were defined, to clarify the value of heat pump flexibility. The results reveal that by leveraging thermal inertia, heat pumps can be reasonably adjusted in operation to achieve cost savings through maximising the use of renewable energy. This work was submitted as "*Flexible operation of heat pumps in a decarbonised power system"* to the IEEE PES ISGT Europe Conference 2024 (Accepted).

Contributions:

Qikun Chen: Modelling, conceptualisation, programming, data collection, analysis, writing, editing, visualisation.

Meysam Qadrdan: Conceptualisation.

(4) A modelling framework to quantify the amount of flexibility available through energy systems integration was developed. Using an integrated electricity, hydrogen and heat supply system for Great Britain in 2050 as a case study, the impacts of flexibility on the operational costs of the whole system, locational marginal prices of the electric power system and renewable energy curtailment were investigated. This work is submitted as "*The optimal mix of flexibility in a future integrated energy system*" to the journal *Cell Reports Sustainability,* under peer review.

Contributions:

Qikun Chen: Modelling, programming, data collection, analysis, writing, editing, visualisation.

Meysam Qadrdan: Conceptualisation, review & editing, supervision

Chapter 2 Modelling of the integrated energy system

2.1 Introduction

To investigate the interactions between different energy facilities, a comprehensive model that provides a detailed representation of the entire energy system is essential. Numerous models have already been developed, focusing on the integration of components across various energy networks, such as gas and electricity networks[38–40], electricity and heating [41–43] networks. However, many of these models are case-specific, lack generality, and are challenging to apply in broader contexts.

Some planning models, such as MESSAGE model[44], TIMES model[45], Calliope model[46], focus on national or even larger scales. These models aim to provide high level economic and policy insights, rather than detailed analyses of the operational dynamics of energy systems. For instance, aspects such as electricity transmission and the operational status of different units are often simplified or neglected. However, the lack of detailed representation in these

models can make it challenging to accurately quantify the flexibility that the entire energy system can provide.

In this investigation, the integrated energy systems (IES) model is a least-cost optimisation tool designed to investigate the optimal operation of the whole energy system. Similar to other energy system modelling frameworks such as Combined Gas and Electricity Model (CGEN)*, it encompasses a diverse array of energy production technologies, energy consumers, transmission networks, and flexibility solutions, allowing for a detailed examination of how different energy components interact and support the overall infrastructure's efficiency.

Three main modules are incorporated within the IES model, comprising the gas*, electricity and the residential heating system. Gas and electricity systems are modelled as the network, denoted by numerous nodes and branches. Those nodes stand for different energy facilities or offtake points while branches specify pipelines or wires. They are interconnected through various facilities such as

* CGEN was designed to optimise the operation of the gas and electricity system. Compared to CGEN, IES model introduces several enhancements, including formulations for electrical energy storage units, electrolysers, and residential heating systems. In addition, IES model employs a more time-efficient approach to address the nonlinearity of the optimisation problem.

* The modelling of the gas system is applicable to both natural gas and hydrogen networks, and it can be adapted to various geographical scales, from regional to national levels.

networked electrolysers, gas-fired power generator and electric-driven compressor units.

Furthermore, the residential heat system, i.e. heat demand and heating technologies in residential buildings, is connected to the electricity and gas networks through heat pumps and gas boilers, respectively.

2.2 Objective function of IES

The objective function of the IES model is to minimise the total operational cost of integrated energy systems while adhering to the physical constraints imposed by technologies and networks, as specified in Eq. (2.1). Details for each variable are outlined in Table 2.1. The model operates with hourly time steps and daily time horizons. Note that, each term in Eq. (2.1) represents the total cost associated with a specific type of element. For example, C^{GP} denotes the total cost of gas provision, calculated as the total gas supply across the entire gas network multiplied by the hourly gas price, summed over all time steps.

$$\mathrm{Min}\ C^{\mathrm{T}} = C^{\mathrm{GP}} + C^{\mathrm{S}} + C^{\mathrm{G}} + C^{\mathrm{IM}} + C^{\mathrm{LS}} + C^{\mathrm{R}} \tag{2.1}$$

1**Table 2.1** The description of Variables in Eq. (2.1).

Variable	Description, unit (£)
C^{T}	Total operational cost of the whole system
C^{GP}	Total cost of gas provision
C^{S}	Total cost of gas storage utilisation
C^{G}	Total cost of power generation by different technologies
C^{IM}	Total cost of electricity import
C^{LS}	Total cost of load shedding
C^{R}	Total cost of renewable curtailment

2.3 Modelling of the gas system

In the formulation of the gas system, different sources of gas provision, pipelines across different regions, compressor units and storage facilities are considered. The model does not account for the transportation of mixed gases, as the complexities of multi-phase flow are beyond the scope of this investigation. Therefore, due to this limitation, only one type of gas supply can be considered at a time.

2.3.1 Sources of gas provision

Gas provisions from different sources are denoted by Eq. (2.2).

$$\underline{Q_{gp}^{\mathrm{GP}}} \leq Q_{gp,t}^{\mathrm{GP}} \leq \overline{Q_{gp}^{\mathrm{GP}}}, \forall gp \in GP, t \in T \tag{2.2}$$

Where GP specifies different types of gas provisions while gp denotes each specific type. $Q_{gp,t}^{\mathrm{GP}}$ denotes the rate of gas provision while $\underline{Q_{gp}^{\mathrm{GP}}}/\overline{Q_{gp}^{\mathrm{GP}}}$ represent min/max rate of gas provision. If the model is applied to natural gas systems, gp could present gas supplied from gas terminals. For hydrogen systems, gp could refer to blue hydrogen, which is produced by steam methane reforming (SMR) and supplied from gas terminals, or green hydrogen which is produced via electrolysers.

The networked electrolyser serves as a coupling component between the gas and electricity systems. The amount of hydrogen produced by these electrolysers is determined by the amount of electricity they consume, as described in Eq. (2.3).

$$\mathrm{HV}^{\mathrm{H}} Q_{gp,t}^{\mathrm{GP}} = \eta^{\mathrm{EL}} P_{gp,t}^{\mathrm{GP}} \Delta\tau, \forall gp \in EL, t \in T \tag{2.3}$$

Where HV^{H} is the heat value of hydrogen, η^{EL} is the efficiency of networked electrolysers, $P_{gp,t}^{\mathrm{GP}}$ is the power generation and $\Delta\tau$ denotes the time interval (time resolution is one hour in this model and $\Delta\tau = 1$).

2.3.2 Gas storage

The underground gas storage is modelled, which is applicable for both natural gas and hydrogen systems. Note that, in this short-term operational model,

gas storage servers as the backup option, offering additional provision in cases where gas supply falls short of demand, albeit at a higher cost. Therefore, only the gas withdrawal from the storage facility is considered. The withdrawal capacity from storage sites is represented by Eq. (2.4)

$$\underline{\mathrm{Q}_s^{\mathrm{S}}} \leq Q_{s,t}^{\mathrm{S}} \leq \overline{\mathrm{Q}_s^{\mathrm{S}}}, \forall s \in S, t \in T \tag{2.4}$$

Where S denotes the set of storage sites, $Q_{s,t}^{\mathrm{S}}$ is the amount of gas that can be withdrawn from the storage, $\underline{\mathrm{Q}_s^{\mathrm{S}}}$ and $\overline{\mathrm{Q}_s^{\mathrm{S}}}$, represent the min/max withdrawal rate at each time step, respectively.

2.3.3 Gas flow and nodal balance

Since the direction of gas flow within the pipe is uncertain at each time step, bi-directional flow is formulated in the model. Figure 2.1 presents the bi-directional gas in a pipe. Note that, n_p^{start}, n_p^{end} are two ends of a pipe, it is assumed that, the direction gas flow from n_p^{start} to n_p^{end} is considered positive, while flow from n_p^{end} to n_p^{start} is considered negative.

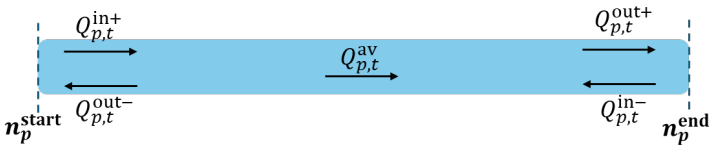

.3**Figure 2.1** Bi-directional gas flow in a pipe.

Where $Q_{p,t}^{\text{in/out+}}$ denote the positive inflow/outflow of gas while $Q_{p,t}^{\text{in/out−}}$ represent the negative inflow/outflow rate of gas through a pipe p. $Q_{p,t}^{\text{av}}$ is the average gas flow rate in pipe p, and can be calculated by Eq. (2.5)

$$Q_{p,t}^{\text{av}} = 0.5(Q_{p,t}^{\text{in+}} + Q_{p,t}^{\text{out+}}) - 0.5(Q_{p,t}^{\text{in−}} + Q_{p,t}^{\text{out−}}), \forall\, p \in P, t \in T \qquad (2.5)$$

To ensure that gas flows in only one direction, a set of binary variables is required, making the model a mixed-integer problem. The formulation of bi-directional flow will be detailed in Chapter 3.

The hydraulic flow equation which is used to clarify the relationship between flow rate and pressure drop within a pipe, is considered and denoted by Eq. (2.6).

$$Q_{p,t}^{\text{av}}\left|Q_{p,t}^{\text{av}}\right| = \mathrm{K}_p^2(\Pi^2_{n_p^{\text{start}},t} - \Pi^2_{n_p^{\text{end}},t}),\ \forall p \in P, \forall t \in T \qquad (2.6)$$

Where $\Pi_{n_p^{\text{start}}}$ and $\Pi_{n_p^{\text{end}}}$ are pressure value at node both ends of a pipe, respectively. K_p is the flow coefficient calculated by Eq. (2.7) [47].

$$\mathrm{K}_p = \sqrt{\frac{2.33\mathrm{D}_p^{2.53}(\frac{\mathrm{T^b}}{\mathrm{P}b})^{1.02}}{\mathrm{T^{av}}\times\mathrm{Z}\times\mathrm{Len}_p\times\gamma^{0.961}}}, \forall p \in P, t \in T \quad (2.7)$$

Within the gas network, the mass conservation (also referred to as nodal balance) is taken into account. Eq. (2.8) is the nodal balance equation for the pipeline network, ensuring that the gas inflow at each node n is equal to the gas outflow from that same node at all timesteps. Figure 2.2 graphically illustrates an example of nodal balance.

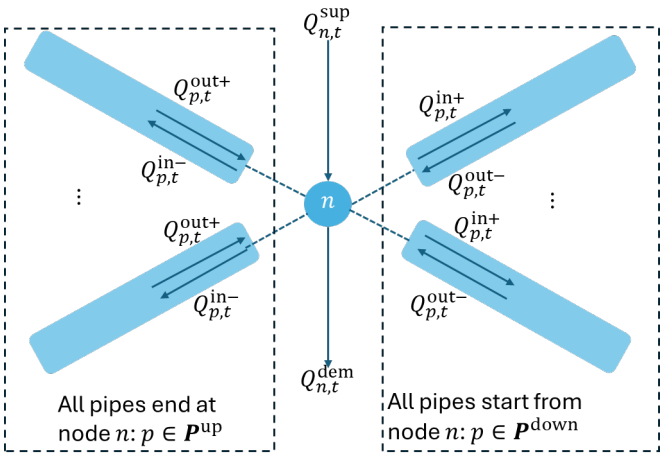

4**Figure 2.2** Diagram of nodal balance in the gas network

$$Q_{n,t}^{\mathrm{sup}} - Q_{n,t}^{\mathrm{dem}} + \sum_{p\in P^{\mathrm{up}}}(Q_{p,t}^{\mathrm{out+}} - Q_{p,t}^{\mathrm{in+}}) + \sum_{p\in P^{\mathrm{down}}}(Q_{p,t}^{\mathrm{out-}} - Q_{p,t}^{\mathrm{in-}}) = 0, \forall n \in N, t \in T \quad (2.8)$$

Where $Q_{n,t}^{\mathrm{sup}}$ represents the cumulative gas provision at node n at time t, sourced from gas terminals, electrolysers, and gas storage facilities. The gas demand $Q_{n,t}^{\mathrm{dem}}$ represents the comprehensive gas demand at the same node.

2.3.4 Gas demand

The cumulative gas demand at each node, represented by $Q_{n,t}^{\mathrm{dem}}$, is divided into two distinct categories: 'flexible' and 'non-flexible' demands, as outlined in Eq. (2.9). The value of flexible demand is case-specific and is determined endogenously within the model to achieve a cost-optimal operational strategy. For instance, when the model is applied to the gas network (as in Chapters 3 and 4), the flexible demand corresponds to the gas demand of gas-driven compressor units. Alternatively, when applied to the integrated hydrogen, electricity, and heating system (case study in Chapter 5), the flexible demand includes hydrogen demand for power generation and heating. The remaining energy demands are assumed to be non-flexible and predetermined and are inputs to the model.

$$Q_{n,t}^{\mathrm{dem}} = Q_{n,t}^{\mathrm{flexdem}} + Q_{n,t}^{\mathrm{nflexdem}}, \forall n \in N, t \in T \tag{2.9}$$

Where $Q_{n,t}^{\mathrm{flexdem}}$ denotes flexible demand while $Q_{n,t}^{\mathrm{nflexdem}}$ represents the ‘non-flexible’ demand. Load shedding is considered, to prevent the system from overloading, as denoted by Eq. (2.10).

$$Q_{n,t}^{\mathrm{LS}} \leq Q_{n,t}^{\mathrm{nflexdem}}, \forall n \in N, t \in T \quad (2.10)$$

Where $Q_{n,t}^{\mathrm{LS}}$ represents the rate of gas load shedding. A high penalty cost for gas load shedding is considered, to ensure its minimisation by the optimisation model.

2.3.5 Linepack formulation

Within the pipeline system, the linepack which refers the amount of gas that can be temporarily stored within the pipeline and is formulated by Eq. (2.11) - Eq. (2.15).

Eq. (2.11) describes the relationship between linepack in pipeline p and pressure at both ends of the pipe.

$$L_{p,t} = \mathrm{S}_p \frac{\Pi_{n_p^{\mathrm{start}},t} + \Pi_{n_p^{\mathrm{end}},t}}{2}, \forall p \in P, t \in T \quad (2.11)$$

Where $L_{p,t}$ is the linepack volume of pipeline p at time t and S_p is the linepack coefficient determined by Eq. (2.12).

$$\mathrm{S}_p = \frac{\pi \times \mathrm{Len}_p \times \mathrm{D}_p^2}{4 \times \mathrm{Z} \times \mathrm{T}^{\mathrm{b}} \times \rho}, \forall p \in P, t \in T \quad (2.12)$$

Eq. (2.13) and Eq. (2.14) establish the continuity of linepack across time steps t (current timestep) and previous timestep.

$$L_{p,t_1} = \mathrm{L}_p^0 + Q_{p,t_1}^{\mathrm{in}+} - Q_{p,t_1}^{\mathrm{out}+} + Q_{p,t_1}^{\mathrm{in}-} - Q_{p,t_1}^{\mathrm{out}-}, \forall p \in P, t = t_1 \qquad (2.13)$$

$$L_{p,t} = L_{p,t-1} + Q_{p,t}^{\mathrm{in}+} - Q_{p,t}^{\mathrm{out}+} + Q_{p,t}^{\mathrm{in}-} - Q_{p,t}^{\mathrm{out}-}, \forall p \in P, t \neq t_1 \qquad (2.14)$$

Where $L_{p,t}$ is the volumetric value of linepack in a pipe p, L_p^0 represents the predefined initial linepack indicating the original linepack volume before optimisation.

Eq. (2.15) indicates the linepack at the end of day should be equal or greater than initial volume, ensuring the level of it is enough for the next day. This equation can be modified to impose any other target for the end-of-day linepack.

$$L_{p,t24} \geq \mathrm{L}_p^0, \forall p \in P \qquad (2.15)$$

2.3.6 Compressor units

To ensure sufficient flow, compressor units which are installed along pipelines are considered in the modelling of transmission system. These units are capable of boosting pressure, addressing the critical need for ensuring a safe operation.

Two types of compressor units are considered: Electric-driven Compressor (EDC) and Gas-driven Compressor (GDC). The energy consumption of each compressor can be expressed by Eq. (2.16).

$$E_{c,t} = \mathrm{B}Q_{c,t}^{\mathrm{tp}} + \mathrm{B}'\alpha_{c,t}, \forall\, c \in C, t \in T \tag{2.16}$$

Where $E_{c,t}$ is the energy consumption of a compressor unit c, B and B' are fitted coefficients to linearise the original nonlinear formulation, $Q_{c,t}^{\mathrm{tp}}$ is the gas throughput and $\alpha_{c,t}$ is the compression ratio, which is restricted by Eq. (2.17).

$$\underline{\alpha_c} \leq \alpha_{c,t} \leq \overline{\alpha_c}, \forall\, c \in C, t \in T \tag{2.17}$$

Eq. (2.18) and Eq. (2.19) are employed so that negative flow (flow from discharge node to suction node) is not allowed within a compressor.

$$Q_{c,t}^{\mathrm{in}-} = 0, \forall\, c \in C, t \in T \tag{2.18}$$

$$Q_{c,t}^{\mathrm{out}-} = 0, \forall\, c \in C, t \in T \tag{2.19}$$

The pressure increases after being boosted by the compressor is denoted by Eq. (2.20).

$$\Pi_{n_c^{\mathrm{end}},t} = \Pi_{n_c^{\mathrm{start}},t}\alpha_{c,t}, \forall\, c \in C, t \in T \tag{2.20}$$

Where n_c^{end} is the discharge node of a compressor c while n_c^{start} is the suction node of it.

The amount of gas throughput should be equivalent to that of gas positive outflow, expressed as Eq. (2.21).

$$Q_{c,t}^{\mathrm{tp}} = Q_{c,t}^{\mathrm{out+}}, \forall\, c \in C, t \in T \tag{2.21}$$

Mass conservation of gas through a compressor unit is maintained, as denoted by Eq. (2.22). If the compressor runs on gas, the amount of gas consumed by the compressor can be calculated by Eq. (2.23). If the compressor is driven by electricity, $Q_{c,t}^{\mathrm{u}} = 0$ and the gas inflow of the compressor equals to gas outflow of this compressor, as denoted by denoted by Eq. (2.24).

$$Q_{c,t}^{\mathrm{out+}} + Q_{c,t}^{\mathrm{u}} = Q_{c,t}^{\mathrm{in+}}, \forall\, c \in C, t \in T \tag{2.22}$$

$$Q_{c,t}^{\mathrm{u}} = \frac{E_{c,t}}{\mathrm{HV}}, \forall\, c \in GC, t \in T \tag{2.23}$$

$$Q_{c,t}^{\mathrm{in+}} = Q_{c,t}^{\mathrm{out+}}, \forall\, c \in EC, t \in T \tag{2.24}$$

2.4 Modelling of the electricity system

In the modelling of the electricity system, different types of power generator, transmission wires and electric energy storage units are considered.

2.4.1 Power generation

Within the electricity system, the power generation from different types of power stations is modelled by Eq. (2.25) and Eq. (2.26). Eq. (2.25) denotes the power generation including nuclear, bioenergy and other renewable sources (e.g., ground thermal energy, waste, etc), which is fixed over optimisation timesteps.

$$P_{g,t}^{\mathrm{G}} = \delta_g \overline{\mathrm{P}_g^{\mathrm{G}}}, \ \ \forall g \in OTH, t \in T \tag{2.25}$$

Where $P_{g,t}^{\mathrm{G}}$ is the power generation, $\overline{P_g^{\mathrm{G}}}$ is the capacity of the power station g and δ_g is the capacity factor.

Eq. (2.26) represents the power generation from gas turbines, considering its operational status.

$$u_{g,t}\underline{\mathrm{P}_g^{\mathrm{G}}} \leq P_{g,t}^{\mathrm{G}} \leq u_{g,t}\overline{\mathrm{P}_g^{\mathrm{G}}}, \ \forall g \in GT, t \in T \tag{2.26}$$

Where $u_{g,t}$ is a set of binary variables, denoting ON/OFF status of gas turbine g. For instance, when $u_{g,t}$=1, the turbine is working within the operational bounds $[\underline{P_g^{\mathrm{G}}}, \overline{P_g^{\mathrm{G}}}]$, and when $u_{g,t} = 0$, it is offline and $P_{g,t}^{\mathrm{G}} = 0$.

The detailed representation of the operational status of gas turbines are given by Eq. (2.27) – Eq. (2.29). These constraints are employed to ensure that the turbine cannot be in both start-up and shut-down state at the same time.

$$y_{g,t} + z_{g,t} \leq 1, \ \forall g \in GT, t \in T \tag{2.27}$$

$$y_{g,t_1} - z_{g,t_1} = u_{g,t_1} - u_g^0, \ \forall g \in GT, t = t_1 \tag{2.28}$$

$$y_{g,t} - z_{g,t} = u_{g,t} - u_{g,t-1,}, \ \forall g \in GT, t \in T \backslash t_1 \tag{2.29}$$

Where $y_{g,t}$ and $z_{g,t}$ are sets of binary variables associated with turbine's start-up and shut-down processes, respectively. If $y_{g,t} = 1$, the turbine g is starting up; if $z_{g,t} = 1$, it is shutting down. It is not possible for the turbine to be in both start-up and shut-down states simultaneously, as constrained by Eq. (2.27).

$u_{g,t}$ is a set of binary variables denoting the ON/OFF status of a turbine and u_g^0 is the initial ON/OFF status of it. Eq. (2.28) delineates the relationship between

the start-up process, shut-down process and ON/OFF status of a turbine at the first time step t_1, while Eq. (2.29) details this relationship for all other timesteps.

Eq. (2.30) and Eq. (2.31) constrain the ramp-up rate and ramp-down rate of turbine within an allowable range, respectively.

$$P_{g,t}^{\mathrm{G}} - P_{g,t-1}^{\mathrm{G}} \leq \mathrm{RU}_g\left(1 - y_{g,t}\right) + \mathrm{SU}_g y_{g,t},\ \forall g \in GT, t \in T \qquad (2.30)$$

$$P_{g,t-1}^{\mathrm{G}} - P_{g,t}^{G} \leq \mathrm{RD}_g(1 - z_{g,t}) + \mathrm{SD}_g z_{g,t},\ \forall g \in GT, t \in T \qquad (2.31)$$

Where RU_g is ramp-up rate, SU_g is the start-up rate, RD_g is ramp-down rate and SD_g is shut-down rate.

Eq. (2.32) to Eq. (2.35) specify the minimum up time and minimum down time constraints for the turbine. In the operation of turbine, minimum up time is the minimum period that a turbine must be kept running once it has been started up while minimum up time refers to the minimum period that a power plant must remain offline once it has been turned off.

$$\sum_{t=t_k}^{t=t_{k+(\mathrm{L}^{\mathrm{MU}}-1)}} u_{g,t} \geq \mathrm{L}^{\mathrm{MU}} \times y_{g,t_k}, 1 \leq k \leq 21,\ \forall g \in GT, t \in T \qquad (2.32)$$

$$\sum_{t=t_k}^{t=t_{24}} (u_{g,t} - y_{g,t_k}) \geq 0, 22 \leq k \leq 24,\ \forall g \in GT, t \in T \qquad (2.33)$$

$$\sum_{t=t_k}^{t=t_{k+(\mathrm{L}^{\mathrm{MD}}-1)}}(1-u_{g,t}) \geq \mathrm{L}^{\mathrm{MD}} \times z_{g,t_k}, 1 \leq k \leq 21,\ \forall g \in GT, t \in T \quad (2.34)$$

$$\sum_{t=t_k}^{t=t_{24}}(1-u_{g,t}-z_{g,t_k}) \geq 0, 22 \leq k \leq 24,\ \forall g \in GT, t \in T \quad (2.35)$$

Where L^{MU} is the minimum up time and L^{MD} is the minimum down time.

The gas turbine serves as a linkage between the gas system and the electricity system, since the amount of electricity it can generate is determined by its gas consumption, as specified in Eq. (2.36).

$$P_{g,t}^{\mathrm{G}}\Delta\tau = \eta^{\mathrm{G}}\mathrm{HV}^{\mathrm{G}}Q_{g,t}^{\mathrm{G}}, \forall g \in GT, t \in T \quad (2.36)$$

Eq. (2.37) is the constraint governing power generation from VRE sources, encompassing both wind generation and solar generation.

$$P_{g,t}^{\mathrm{U}} + P_{g,t}^{\mathrm{C}} = \mathrm{P}_{g,t}^{\mathrm{A}}, \forall g \in VRE, t \in T \quad (2.37)$$

Where $P_{g,t}^{\mathrm{U}}$ is the amount of power injected into the grid from the power station g, $P_{g,t}^{\mathrm{C}}$ is the curtailed renewable generation and $\mathrm{P}_{g,t}^{\mathrm{A}}$ specifies the available amount of renewable generation at this power station, which is predetermined as input data.

Furthermore, Equation (2.38) serves as the constraint governing electricity import via interconnectors. In this case study, we simplify the analysis by not delving into the intricate energy markets for import and export. Instead, we assign a relatively high value to the import cost. This ensures that electricity is imported only when domestic supply falls short of meeting demand.

$$\underline{P_i^{\mathrm{IM}}} \leq P_{i,t}^{\mathrm{IM}} \leq \overline{P_i^{\mathrm{IM}}}, \forall i \in I, t \in T \tag{2.38}$$

Where $P_{i,t}^{\mathrm{IM}}$ is the amount of power imported to the power system from other countries via interconnectors.

2.4.2 Power flow and nodal balance

The DC power flow is formulated in the modelling of the electricity transmission network. The DC flow is simplified from the AC power flow based on the following assumptions:

1. In high-voltage transmission systems, line resistance is much smaller than line reactance, so resistance and system losses can be ignored.

2. The phase voltage angle difference in a high-voltage line is very small.

3. The bus voltage per unit is close to the nominal value.

A linear power flow equation is employed to in the model, as denoted by Eq. (2.39) and Eq. (2.40).

$$-\bar{P}_l \leq P_{l,t} \leq \bar{P}_l, \forall l \in L, \forall t \in T \tag{2.39}$$

$$P_{l,t} = \left(\theta_{b_l^{\text{start}},t} - \theta_{b_l^{\text{end}},t}\right) / \mathrm{X}_l, \forall l \in L, \forall t \in T \tag{2.40}$$

Where$P_{l,t}$ is the power flow at wire l while $\bar{P}_l$ is the transmission capacity of l, $\theta_{b_l^{\text{start}},t}$ and $\theta_{b_l^{\text{end}},t}$ are the voltage angles at the start and end of this wire, respectively, and X_l is the reactance of the wire l.

The nodal balance (energy conservation) is considered, as denoted by Eq. (2.41). This constraint ensures that the inflow of power at each busbar b must be equal to the power outflow from that same busbar. Figure 2.3 presents a simple example of the nodal balance within the electric power system.

$$P_{b,t}^{\text{sup}} - P_{b,t}^{\text{dem}} + \sum_{l \in l^{\text{up}}} P_{l,t} - \sum_{l \in l^{\text{down}}} P_{l,t} = 0, \forall b \in B, t \in T \tag{2.41}$$

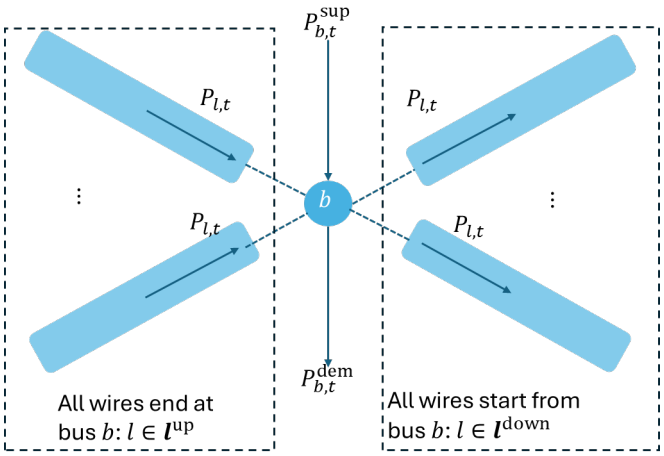

5**Figure 2.3** Diagram of nodal balance in the electric power system

Where $P_{b,t}^{\mathrm{sup}}$ denotes the total amount of power injected into the busbar b, from all generators and discharged power from the batter/pump storage that connected with b. $P_{b,t}^{\mathrm{dem}}$ represents the total amount of power demand from this node.

2.3.3 Power demand

Similar to the modelling of the gas system, flexible and non-flexible power demands are incorporated in the electricity model, as denoted by Eq. (2.42).

$$P_{b,t}^{\mathrm{dem}} = P_{b,t}^{\mathrm{flexdem}} + P_{b,t}^{\mathrm{nflexdem}}, \forall b \in B, t \in T \tag{2.42}$$

Where $P_{b,t}^{\mathrm{flexdem}}$ denotes flexible power demand, which includes demand for heating, electrolysers and electric-driven compressor units. It is optimised

endogenously by the model. $P_{b,t}^{\mathrm{nflexdem}}$ represents the remaining power demand classified as 'non-flexible' power demand, which is pre-determined as input data.

Load shedding is considered, to prevent the electricity system from overloading, as denoted by Eq. (2.43).

$$P_{b,t}^{\mathrm{LS}} \leq P_{b,t}^{\mathrm{nflexdem}}, \forall b \in B, t \in T \tag{2.43}$$

Where $P_{b,t}^{\mathrm{LS}}$ denotes the rate of load shedding. Similar to the modelling of the gas system, the optimisation considers a high penalty cost for electricity load shedding to ensure its minimisation.

2.4.4 Electrical energy storage

Eq. (2.44) - Eq. (2.46) represent the operation of the electricity storage units (including battery storage and pumped storage). Eq. (2.44) - Eq. (2.45) establish the continuity of energy storage across adjacent timesteps.

$$E_{es,t_1}^{\mathrm{ES}} = \mathrm{ES}_{es}^{0} + P_{es,t_1}^{\mathrm{ES}} \Delta\tau, \forall es \in ES, t = t_1 \tag{2.44}$$

$$E_{es,t}^{\mathrm{ES}} = ES_{es,t-1}^{\mathrm{ES}} + P_{es,t}^{\mathrm{ES}} \Delta\tau, \forall es \in ES, t \neq t_1 \tag{2.45}$$

Where $ES_{es,t}$ is the amount of energy stored in units es, $P^{\mathrm{ES}}_{es,t_1}\Delta t$ denotes the amount of electrical energy being charged (when $P^{\mathrm{ES}}_{es,t} \geq 0$) or discharged (when $P^{\mathrm{ES}}_{es,t} \leq 0$). ES_{es,t_0} represents the predefined initial level of energy stored in the unit es. ES^0_{es} is the initial amount of energy stored in the unit es.

Eq. (2.46) signifies that the energy storage of the unit es at the end of the day must be equal to or greater than its initial value, ensuring that the stored energy level is sufficient for the next day's requirements.

$$ES^{\mathrm{ES}}_{es,t_{24}} \geq \mathrm{ES}^0_{es}, \forall es \in ES \tag{2.46}$$

2.5 Modelling of the residential heating system

2.5.1 Thermal balance of the building

Within the IES model, the energy consumption of residential heating is considered. Multiple buildings in different locations are simplified to a single building, where they share the same averaged value for thermal characteristics of building materials, such as thermal capacity and thermal conductivity.

Thermal balance [48] of the building is considered and outlined as Eq. (2.47) and Eq. (2.48). Eq. (2.47) establishes the relationship between indoor

temperature at t_0 (initial timestep before optimisation) and t_1, ambient temperature ($T_{b,t}^{\mathrm{amb}}$) and heat load $H_{b,t}$ in buildings at busbar b.

$$T_{bd,t_1}^{\mathrm{in}} = e^{-\frac{3600\mathrm{U}_{bd}}{\mathrm{C}_{bd}}} T_{bd,t_0}^{\mathrm{in}} + \left(1 - e^{-\frac{3600\mathrm{U}_{bd}}{\mathrm{C}_{bd}}}\right) \mathrm{T}_{bd,t_1}^{\mathrm{amb}} + \frac{1}{U_{bd}} \left(1 - e^{-\frac{3600\mathrm{U}_{bd}}{\mathrm{C}_{bd}}}\right) H_{bd,t} \quad , \forall bd \in BD, t = t_1 \quad (2.47)$$

Where U_b is the averaged value of thermal conductivity of buildings at b and C_b is the averaged value of thermal capacity of these buildings. Eq. (2.48) applies similar considerations for other time steps beyond t_1. $\mathrm{T}_{bd,t_1}^{\mathrm{amb}}$ is the ambient temperature as predefined as input data, while the indoor temperature is variable which can be affected by ambient temperature and heat supply $H_{bd,t}$.

$$T_{bd,t}^{\mathrm{in}} = e^{-\frac{3600\mathrm{U}_{bd}}{\mathrm{C}_{bd}}} T_{bd,t-1}^{\mathrm{in}} + \left(1 - e^{-\frac{3600\mathrm{U}_{bd}}{\mathrm{C}_{bd}}}\right) \mathrm{T}_{bd,t}^{\mathrm{amb}} + \frac{1}{U_{bd}} \left(1 - e^{-\frac{3600\mathrm{U}_{bd}}{\mathrm{C}_{bd}}}\right) H_{bd,t} \quad , \forall bd \in BD, t \neq t_1 \quad (2.48)$$

2.5.2 Electricity consumption of buildings installed with heat pumps

The required energy for residential buildings equipped with air source heat pumps (expressed by $\forall b \in HP$) to satisfy the heat demand is calculated by Eq. (2.49).

$$H_{bd,t}^{\mathrm{HP}} = \mathrm{COP}_{bd,t} P_{bd,t}^{\mathrm{HP}} \Delta\tau, \forall bd \in HP, t \in T \quad (2.49)$$

Where $\mathrm{COP}_{bd,t}$ is the coefficient of performance impacted by the ambient temperature and can be calculated by Eq. (2.50).

$$\mathrm{COP}_{bd,t} = 3 + (\mathrm{T}_{bd,t}^{\mathrm{amb}} - 270.5)/15, \forall bd \in HP, t \in T \quad (2.50)$$

2.5.3 Gas consumption of buildings installed with boilers

The amount of natural gas/hydrogen required to satisfy the heat demand for residential buildings with boilers (expressed by $\forall b \in GB$) are identified by Eq. (2.51).

$$H_{bd,t} = \mathrm{HV}^{\mathrm{NG}} \eta^{\mathrm{GB}} Q_{bd,t}^{\mathrm{GB}}, \forall bd \in GB, t \in T \quad (2.51)$$

Where η^{GB} denotes the efficiency for all boilers, $Q_{bd,t}^{\mathrm{GB}}$ stands for the required volume of natural gas for the natural gas boiler or hydrogen for the hydrogen boiler.

2.6 Summary

This chapter details the formulation of the IES model, including the objective function and constrains of the whole system. IES model is generic and can be

applied across various case studies. Chapter 3 utilises the IES model to analyse the natural gas transmission system in South Wales and Southwest England, while Chapter 4 extends its application to the entire natural gas network in Great Britain. In these two chapters, only the gas network model in section 2.3 is used, while all constraints in the power system model remain inactive. The objective function of the model in these chapters is to minimise the operational cost of the gas network only.

Chapters 5 and 6 explore the value of energy systems integration, applying the IES model to evaluate the hydrogen network and electricity under the 2050 scenario. Instead of revamping the modelling framework, switching case studies only requires adjusting parameters through input data.

Note that this chapter focuses on detailing the fundamental framework employed across all case studies. Other formulations, such as methods for flexibility quantification, approximations for nonlinear constraints, and calculations for locational marginal prices, will be detailed in their respective chapters.

Chapter 3 Optimal operation of compressor units in an integrated gas and electricity system

3.1 Introduction

3.1.1 Background

Compressor units are essential components of natural gas networks, responsible for directing flows, boosting gas pressure, and maintaining the linepack level, thereby facilitating the long-distance transportation of gas through pipelines. These units are pivotal in ensuring the efficient and reliable delivery of gas across extensive networks.

The national transmission system (NTS) of natural gas in GB has 24 compressor sites with more than 70 compressor units [49]. Mainly, gas-driven compressor (GDC) units are employed which results in the emission of various greenhouse gases and pollutants [50]. Under the Industrial Emission Directive (IED) [50], the network operator is required to reduce emissions from the compressor fleet. One option is to replace gas-driven compressors with electric-driven

compressors (EDCs). There are nine electric-driven compressor units installed in the NTS with a total power capacity of approximately 200 MW [51].

Strategic management of these compressor units is crucial for optimising the operation of the gas network and thus reducing the operational cost. This necessitates an efficient approach to analysing the optimal operation of the system.

3.1.2 Stat-of-art of approaches for reformulating nonlinear optimisation problems

Some constraints within the IES model, such as the hydraulic flow equation Eq. (2.8), are nonlinear and nonconvex, posing a great computational challenge for optimisation processes [52,53]. To reduce the complexity of the problem, a range of approaches have been devised to simplify the nonlinear formulation.

This section introduces four approximation methods commonly employed to address the nonlinear constraints of gas flow in pipes.

3.1.2.1 Piecewise Linearisation (PWL)

Piecewise linearisation (PWL) is a mathematic technique to approximate the complex nonlinear function with a series of linear segments, as shown in Figure 3.1.

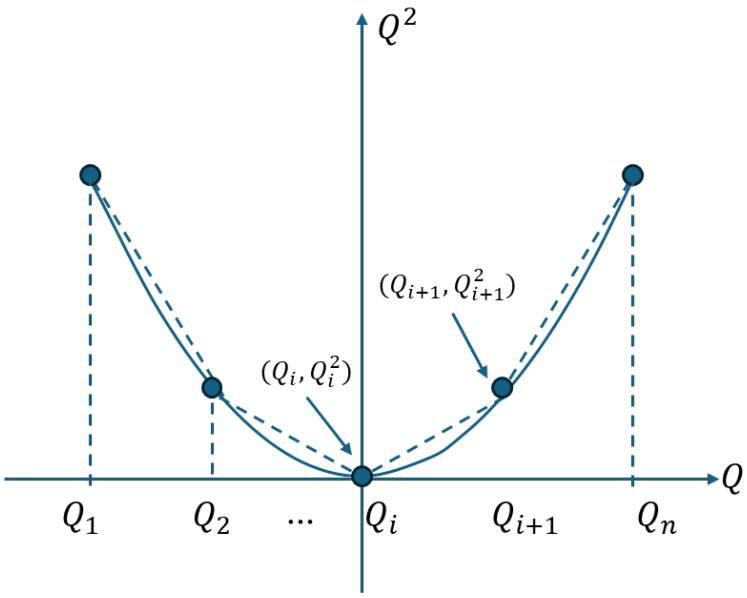

6**Figure 3.1** Approximating nonlinear flow equation using PWL

For instance, a quadratic expression $f(Q) = Q^2$, with Q ranging between $[Q_1, Q_n]$ (where Q^2 has n sampling points to evaluate the function values) can be approximated by a series of linear segments as $[(Q_i, Q_i^2), (Q_{i+1}, Q_{i+1}^2)]$, where i=1,2…$n-1$.

Then any given value Q between Q_i and Q_{i+1} can be expressed by Eq. (3.1) and $g(Q)$, which is used to approximate Q^2 can be expressed by Eq. (3.2).

$$Q = uQ_i + (1-u)Q_{i+1}, u \in [0,1] \tag{3.1}$$

$$g(Q) = uQ_i^2 + (1-u)Q_{i+1}^2, u \in [0,1] \quad (3.2)$$

Where u is a fraction describe how far Q is along the interval from Q_i and Q_{i+1}. This method demonstrates a strong performance in approximating nonlinear equations and has found widespread application in energy system optimisations [54–59].

While Piecewise Linearisation (PWL) is efficient and applicable to various case studies, there exists an inherent trade-off between accuracy and computational complexity when employing this approach. Achieving higher accuracy in the approximation demands a sufficient number of segments, yet this leads to an increase in the number of integer variables, thereby imposing a greater computational burden [36,37,60].

3.1.2.2 Second-Order-Cone Programming (SOCP)

In comparison to PWL, Second Order Cone programming (SOCP) is generally faster [61] in solving complex nonlinear optimisation problems [62–66]. A SOCP problem can be expressed as:

$$\min (f^{\mathrm{T}} x) \quad (3.3)$$

$$\text{s.t.} \|A_i x + b_i\| \leq c_i^T x + d_i, i = 1,2 \dots N, \tag{3.4}$$

Where $x \epsilon \mathbb{R}^n$ is the variable of optimisation, and $f \epsilon \mathbb{R}^n$, $A \epsilon \mathbb{R}^{(n_i - 1)n}$, $b_i \epsilon \mathbb{R}^{n_i - 1}$, $d_i \epsilon \mathbb{R}$ are parameters. $\|A_i x + b_i\| \leq c_i^T x + d_i$ is a SOCP of dimension n.

The standard form of the SOCP (also called Lorentz cone) of dimension k can be defined as Eq. (3.5) and can be further expressed by Eq. (3.6).

$$\ell_k = \left\{ \begin{bmatrix} u \\ t \end{bmatrix} \middle| \, u \epsilon \mathbb{R}^{k-1}, t \epsilon \mathbb{R}^n, \|u\| \leq t \right\} \tag{3.5}$$

$$\|A_i x + b_i\| \leq c_i^T x + d_i \Leftrightarrow \begin{bmatrix} A_i \\ c_i^T \end{bmatrix} x + \begin{bmatrix} b_i \\ d_i \end{bmatrix} \epsilon \ell_{k_i} \tag{3.6}$$

3.1.2.3 McCormick Envelope

The McCormick Envelope, proposed by Garth McCormick [67], serves as a convex relaxation technique employed in the optimisation of bilinear and other non-linear programming (NLP) problems. A derivation of the McCormick Envelopes for a given bilinear function was given by Eq. (3.7) - Eq. (3.11).

Eq. (3.7) is a bilinear function, where $x^{\mathrm{L/U}}$ are lower/upper bounds of x and $y^{\mathrm{L/U}}$ are lower/upper bounds of y.

It is known that $(x - x^{\mathrm{L}})(y - y^{\mathrm{L}}) \geq 0$, therefore, one of lower bounds of Eq. (3.7) can be denoted by Eq. (3.8). Similarly, other bounds of this bilinear function can be found as denoted by Eq. (3.9)-Eq. (3.11).

$$z = xy, x \in [x^{\mathrm{L}}, x^{\mathrm{U}}], y \in [y^{\mathrm{L}}, y^{\mathrm{U}}] \tag{3.7}$$

$$z \geq xy^{\mathrm{L}} + yx^{\mathrm{L}} - x^{\mathrm{L}}y^{\mathrm{L}} \tag{3.8}$$

$$z \geq xy^{\mathrm{U}} + yx^{\mathrm{U}} - x^{\mathrm{U}}y^{\mathrm{U}} \tag{3.9}$$

$$z \leq xy^{\mathrm{L}} + yx^{\mathrm{U}} - x^{\mathrm{U}}y^{\mathrm{L}} \tag{3.10}$$

$$z \leq xy^{\mathrm{U}} + yx^{\mathrm{L}} - x^{\mathrm{L}}y^{\mathrm{U}} \tag{3.11}$$

Using an approximated feasible region enclosed by the McCormick Envelope generally decreases computational time, compared to directly solving a nonlinear problem. Nonetheless, the accuracy of this envelope is determined by the tightness of the bounds. While tighter bounds yield a more precise solution, they also increase the time required for computation [68,69].

3.1.2.4 Polyhedral Outer-Approximation

The Polyhedral Outer-Approximation (POA) is a mathematical approach primarily used for approximating quadratic formulations in nonlinear optimisations [70]. This method revolves around the approximation of a non-linear feasible region using a polyhedral set. Outer tangent lines are constructed at select points along the curve of the non-linear function, establishing its lower bounds. Concurrently, a straight line connecting both ends of this curve is employed to define the upper bound. Figure 3.2 provides a graphical representation of an example using this approximation technique on a quadratic function $f(x) = x^2$.

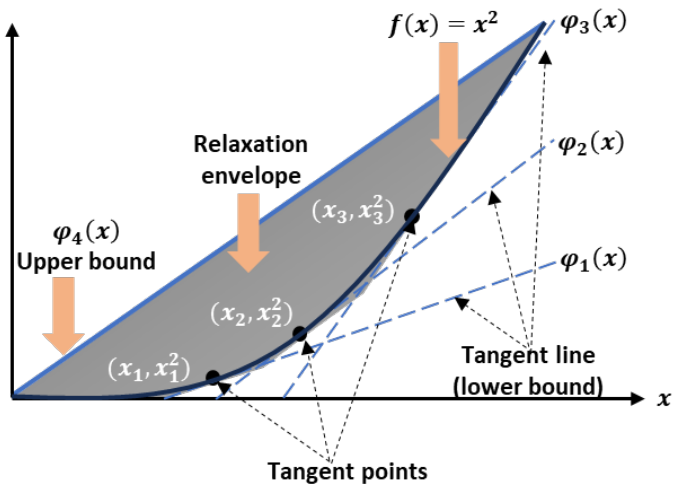

7**Figure 3.2**. Approximating a quadratic function using POA.

Firstly, choosing three points along the curve (x_1, x_1^2), (x_2, x_2^2), (x_3, x_3^2), and then creating outer tangents at these points as described by Eq. (3.12). These

tangent lines serve as the lower boundary of $f(x)$, as expressed by Eq. (3.13). The upper bound of $f(x)$ can be denoted by Eq. (3.14) where (x_s, x_s^2), (x_e, x_e^2), represent both ends of the curve.

$$\varphi_i(x) - f(x_i) = \frac{df(x_i)}{dx_i}(x - x_i), i = 1,2,3 \tag{3.12}$$

$$f(x) \geq \varphi_i(x), i = 1,2,3 \tag{3.13}$$

$$f(x) \leq \frac{f(x_e)-f(x_s)}{x_e-x_s}(x - x_e) + f(x_e) \tag{3.14}$$

3.2 Case study

Section 3.1.2 summarised different mathematic techniques that can be used to approximate the nonlinear expressions in optimisations. In this section, a case study on the high-pressure natural gas transmission system of South Wales and Southwest of England in the UK was carried out, using SOCP and McCormick Envelope to reformulate the hydraulic flow equation. The aim of the optimisation is to minimise the operational cost of the gas network considering energy consumption of compressor units.

3.2.1 The configuration of a compressor station

This gas network consists of seven pipelines, nine gas nodes, one gas terminal and two compressor stations as shown in Figure 3.3.

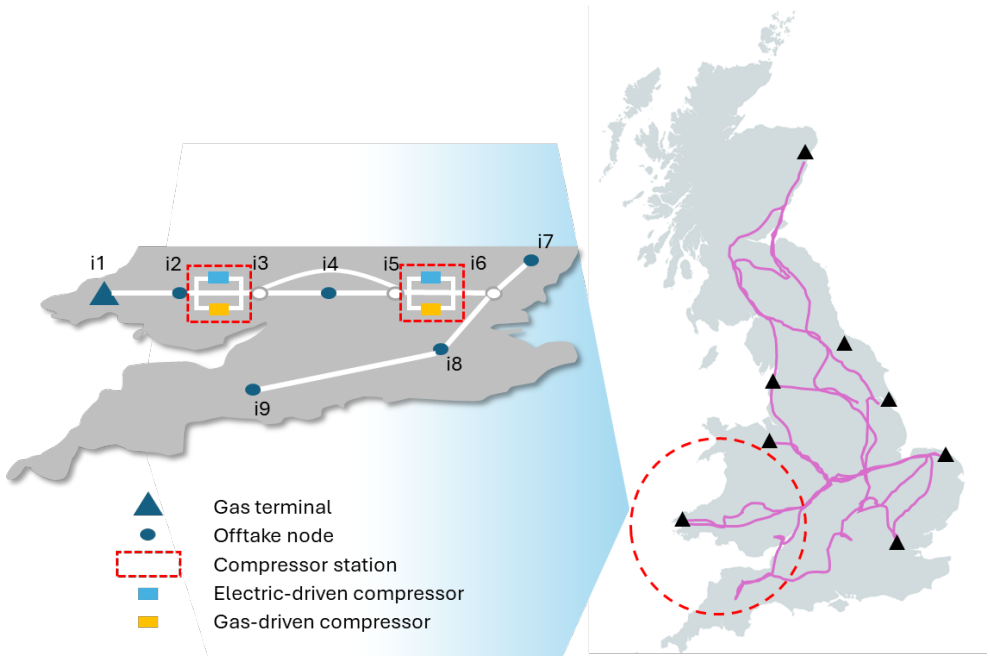

8**Figure 3.3** The gas network of South Wales and Southwest England.

In the case study, two types of compressor units operating in parallel were modelled as shown in Figure 3.4. There are three valves that are used to control the direction of gas flow. If the compressor units are in the OFF state, valve 1 allows gas flow though the bypass line only. If the compressor station operates to boost the pressure, gas flow will be directed to either of the compressor units

(gas-driven compressor (GDC) or electric-driven compressor (EDC)) under the control of valve 2 and valve 3.

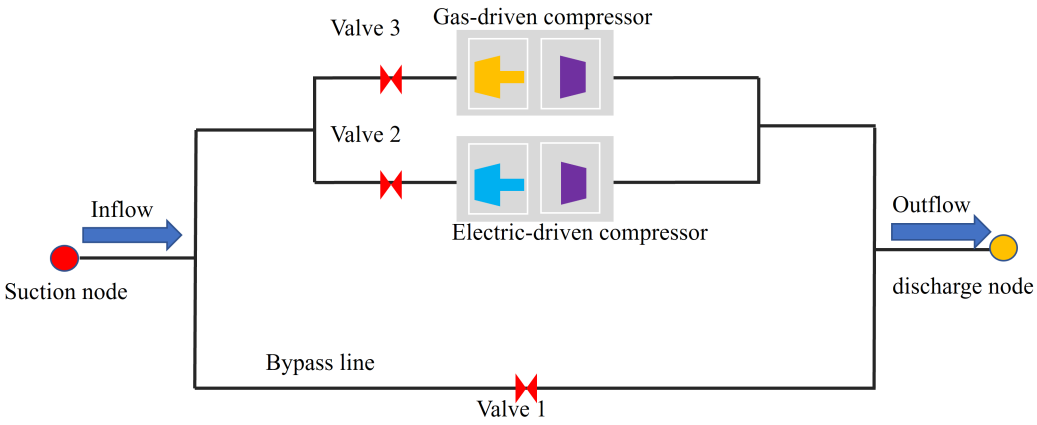

9**Figure 3.4** Parallel configuration of compressor units

The ON/OFF status of each compressor unit is denoted by a set of binary variables $w_{c,t}$. The original expression of the compressor unit Eq. (2.21) was reformulated by Eq. (3.15) – Eq. (3.18)

$$E_{c,t} \geq \mathrm{B}Q_{c,t}^{\mathrm{tp}} + \mathrm{B}'\alpha_{c,t} - \mathrm{M}^{\mathrm{c}}\left(1 - w_{c,t}\right), \forall\, c \in C, t \in T \tag{3.15}$$

$$E_{c,t} \leq \mathrm{B}Q_{c,t}^{\mathrm{tp}} + \mathrm{B}'\alpha_{c,t} + \mathrm{M}^{\mathrm{c}}\left(1 - w_{c,t}\right), \forall\, c \in C, t \in T \tag{3.16}$$

$$0 \leq E_{c,t} \leq \mathrm{M}^{\mathrm{c}} w_{c,t}, \forall\, c \in C, t \in T \tag{3.17}$$

$$0 \leq \alpha_{c,t} - 1 \leq \overline{\alpha_c} w_{c,t}, \forall\, c \in C, t \in T \tag{3.18}$$

Where $\mathrm{M^c}$ is a sufficient large number*. If $w_{c,t} = 1, E_{c,t} = \mathrm{B}Q_{c,t}^{\mathrm{tp}} + \mathrm{B}'\alpha_{c,t}$, and $\alpha_{c,t} \geq 1$, otherwise, $E_{c,t} = 0$ and $\alpha_{c,t} = 1$.

If the compressor is working, then the option for operating GDC or EDC is expressed by Eq. (3.19) – Eq. (3.21).

$$E_{c,t} = E_{c,t}^{\mathrm{EC}} + E_{c,t}^{\mathrm{GC}}, \forall\, c \in C, t \in T \tag{3.19}$$

$$0 \leq E_{c,t}^{\mathrm{EC}} \leq \mathrm{M^c} v_{c,t}, \forall\, c \in EC, t \in T \tag{3.20}$$

$$0 \leq E_{c,t}^{\mathrm{GC}} \leq \mathrm{M^c}(1 - v_{c,t}), \forall\, c \in GC, t \in T \tag{3.21}$$

Where $E_{c,t}^{\mathrm{EC}}$ is the energy consumption of the electric-driven compressor while $E_{c,t}^{\mathrm{EC}}$ denotes the energy consumption of the gas-driven compressor. $v_{c,t}$ is the binary variable denoting the ON/OFF status of the electric-driven compressor.

* Big M method is a mathematical technique used in linear programming to solve problems with constraints containing inequalities and equality constraints.

3.2.2 Input data

The profile of the hourly gas demand of a typical winter day, and the day-ahead prices of both gas and electricity are shown in Figure 3.5. Pressure at gas terminal was fixed to 55 bar during 24 hours. The gas price was assumed to be constant during the day while the electricity price was fluctuating (the variation in electricity price is slightly exaggerated to test its impacts on the optimal operation of the compressors).

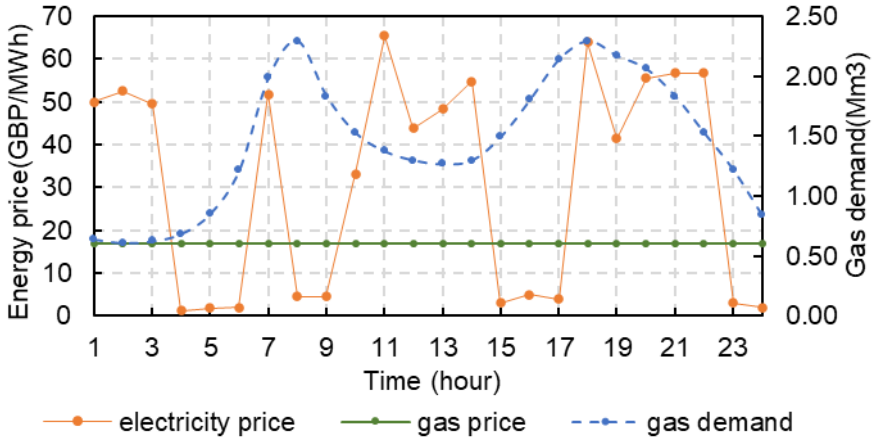

10**Figure 3.5** Day-ahead gas and electricity prices and gas demand

3.2.3 Scenarios definition

Three scenarios were studied in this chapter to investigate the optimal operation of the compressor units. These scenarios were defined as follows:

• **Scenario 1:** Only GDCs are allowed to work while all EDCs are in OFF status.

• **Scenario 2**: Only EDCs are allowed to work while all GDCs are in OFF status.

• **Scenario 3**: All GDCs and EDCs are allowed to work.

3.3 Simplifications of the nonlinear equations in the model

3.3.1 Reformulation of the nonlinear equation using SOCP and McCormick Envelope

Due to the nonlinear and nonconvex nature of Eq. (2.6) (See section 2.3.3), which characterises the intricate bidirectional flow within the pipeline, solving it presents a substantial computational challenge for optimisations. To address this, SOCP and McCormick Envelope were employed to approximate the hydraulic expression.

To formulate the bidirectional flow, a set of auxiliary variables and binary variables were introduced as Eq. (3.22) - Eq. (3.26). $Q_{p,t}^{+}$ in Eq. (3.22) represents averaged flow from m to n (defined as positive flow) in pipe a while $Q_{p,t}^{-}$ in Eq. (3.23) denotes averaged flow from n to m (defined as negative flow).

$$Q_{p,t}^{+} = 0.5(Q_{p,t}^{\mathrm{in}+} + Q_{p,t}^{\mathrm{out}+}), \forall p \in P, \forall t \in T \tag{3.22}$$

$$Q_{p,t}^{-} = 0.5(Q_{p,t}^{\mathrm{in}-} + Q_{p,t}^{\mathrm{out}-}),\ \forall p \in P, \forall t \in T \tag{3.23}$$

Then, a sufficiently large value M^{F} was employed, with a set of binary variables $x_{p,t}$ in Eq. (3. 24) and Eq. (3. 25), to ensure either $Q_{p,t}^{+}$ or $Q_{p,t}^{-}$ is active, that is, when $x_{p,t} = 1$, $Q_{p,t}^{+}$ is active and $Q_{p,t}^{-} = 0$, otherwise, $Q_{p,t}^{-}$ is active and $Q_{p,t}^{+} = 0$. Consequently, the bidirectional flow $Q_{p,t}$ can be expressed by Eq. (3.26).

$$0 \le Q_{p,t}^{+} \le \mathrm{M}^{\mathrm{F}}\, x_{p,t},\ \forall p \in P, \forall t \in T \tag{3.24}$$

$$-\mathrm{M}^{\mathrm{F}}\, x_{p,t} \le Q_{p,t}^{+} \le 0,\ \forall p \in P, \forall t \in T \tag{3.25}$$

$$Q_{p,t}^{\mathrm{AV}} = Q_{p,t}^{+} - Q_{p,t}^{-},\ \forall p \in P, \forall t \in T \tag{3.26}$$

Then, using SOCP to reformulate the bidirectional flow, by replacing Eq. (2.6) to Eq. (3.27) – Eq. (3.28).

$$(Q_{p,t}^{+})^2 \le \mathrm{K}_{p,t}^2 \left(\Pi_{n^{\mathrm{start}},t}^2 - \Pi_{n^{\mathrm{end}},t}^2\right) + (\mathrm{M}^{\mathrm{F}})^2(1 - x_{p,t}),\ \forall p \in P, \forall t \in T \tag{3.27}$$

$$(Q_{p,t}^{-})^2 \leq -\mathrm{K}_{p,t}^2 \left(\Pi_{n^{\mathrm{start}},t}^2 - \Pi_{n^{\mathrm{end}},t}^2\right) + (\mathrm{M}^{\mathrm{F}})^2(x_{p,t}),\ \ \forall p \in P, \forall t \in T \qquad (3.28)$$

Introducing two sets of auxiliary variable $\psi_{p,t}^{-} = \Pi_{n^{\mathrm{start}},t} - \Pi_{n^{\mathrm{end}},t}$ and $\psi_{p,t}^{+} = \Pi_{n^{\mathrm{start}},t} + \Pi_{n^{\mathrm{end}},t}$, then the nonlinear term $\Pi_{n^{\mathrm{start}},t}^2 - \Pi_{n^{\mathrm{end}},t}^2$ can be converted to a bilinear term by using $\varphi_{p,t} = \psi_{p,t}^{-}\psi_{p,t}^{+}$. Afterwards, using McCormick Envelope to reformulate the $\varphi_{p,t}$ as denoted by Eq. (3.29) – Eq. (3. 32).

$$\varphi_{p,t} \leq \overline{\psi_{p,t}^{-}}\psi_{p,t}^{+} + \psi_{p,t}^{-}\underline{\psi_{p,t}^{+}} - \overline{\psi_{p,t}^{-}}\underline{\psi_{p,t}^{+}}, \forall p \in P, \forall t \in T \qquad (3.29)$$

$$\varphi_{p,t} \leq \psi_{p,t}^{-}\overline{\psi_{p,t}^{+}} + \underline{\psi_{p,t}^{-}}\psi_{p,t}^{+} - \overline{\psi_{p,t}^{+}}\underline{\psi_{p,t}^{-}}, \forall p \in P, \forall t \in T \qquad (3.30)$$

$$\varphi_{p,t} \leq \psi_{a,t}^{-}\overline{\psi_{p,t}^{+}} + \underline{\psi_{p,t}^{-}}\psi_{p,t}^{+} - \overline{\psi_{p,t}^{+}}\underline{\psi_{p,t}^{-}}, \forall p \in P, \forall t \in T \qquad (3.31)$$

$$\varphi_{p,t} \geq \psi_{p,t}^{-}\overline{\psi_{p,t}^{+}} + \overline{\psi_{p,t}^{-}}\psi_{p,t}^{+} - \overline{\psi_{p,t}^{+}}\overline{\psi_{p,t}^{-}}, \forall p \in P, \forall t \in T \qquad (3.32)$$

Where $\underline{\psi_{p,t}^{-}}$ is the lower bound of $\psi_{p,t}^{-}$ and $\overline{\psi_{p,t}^{-}}$ denotes the upper bound of it, and $\underline{\psi_{p,t}^{+}}$ specifies the lower bound of $\psi_{p,t}^{+}$ while $\overline{\psi_{p,t}^{+}}$ is the upper bound of $\psi_{p,t}^{+}$.

Using additional auxiliary variables $w_{p,t}^{+}$, $w_{p,t}^{-}$ to approximate $(Q_{p,t}^{+})^2$ and $(Q_{p,t}^{-})^2$ as expressed by Eq. (3.33)-Eq. (3.36).

$$w_{p,t}^{+} \geq (Q_{p,t}^{+})^2, \forall p \in P, \forall t \in T \tag{3.33}$$

$$w_{p,t}^{+} \leq \left(\overline{Q_{p,t}^{+}} + \underline{Q_{p,t}^{+}}\right) Q_{p,t}^{+} - \overline{Q_{p,t}^{+}}\,\underline{Q_{p,t}^{+}}, \forall p \in P, \forall t \in T \tag{3.34}$$

$$w_{p,t}^{-} \geq (Q_{p,t}^{-})^2, \forall p \in P, \forall t \in T \tag{3.35}$$

$$w_{p,t}^{-} \leq \left(\overline{Q_{p,t}^{-}} + \underline{Q_{p,t}^{-}}\right) Q_{p,t}^{-} - \overline{Q_{p,t}^{-}}\,\underline{Q_{p,t}^{-}}, \forall p \in P, \forall t \in T \tag{3.36}$$

Additionally, McCormick Envelope was used to approximate the expression of compressing ratio Eq. (2.16) (see section 2.3.6) through an envelope bounded by Eq. (3.37)-Eq. (3.40).

$$\Pi_{n^{\text{end}},t} \leq \overline{\alpha_c}\,\Pi_{n^{\text{start}},t} + \alpha_{c,t}\underline{\Pi_{n^{\text{start}},t}} - \overline{\alpha_c}\,\underline{\Pi_{n^{\text{start}},t}}, \forall p \in P, \forall t \in T \quad \text{Eq. (3.37)}$$

$$\Pi_{n^{\text{end}},t} \leq \underline{\alpha_c}\,\Pi_{n^{\text{start}},t} + \alpha_c\overline{\Pi_{n^{\text{start}},t}} - \underline{\alpha_c}\,\overline{\Pi_{n^{\text{start}},t}}, \forall p \in P, \forall t \in T \quad \text{Eq. (3.38)}$$

$$\Pi_{n^{\text{end}},t} \geq \overline{\alpha_c}\,\Pi_{n^{\text{start}},t} + \alpha_c\overline{\Pi_{n^{\text{start}},t}} - \overline{\alpha_c}\,\overline{\Pi_{n^{\text{start}},t}}, \forall p \in P, \forall t \in T \quad \text{Eq. (3.39)}$$

$$\Pi_{n^{\text{end}},t} \geq \underline{\alpha_c}\ \Pi_{n^{\text{start}},t} + \alpha_c \underline{\Pi_{n^{\text{start}},t}} - \underline{\alpha_c}\ \underline{\Pi_{n^{\text{start}},t}}, \forall p \in P, \forall t \in T \qquad \text{Eq. (3.40)}$$

3.3.2 An enhanced MISOCP using Bound-Tightening algorithm

The original mixed-integer nonlinear problem (MINLP) was reformulated to mixed-integer Second-Order Cone problem (SOCP), however, as there is a trade-off between the accuracy of the solution and the computational time: over-relaxed bounds of SOC constraints give fast calculation but may produce inaccurate solutions while over-tightening bounds of them results in increased time though increased accuracy.

To address this, an enhanced SOCP with a bound-tightening algorithm proposed in reference [60] can be helpful. By using this method, the bound of SOC constraints which are over relaxed can be gradually tightened until reaching the satisfying tolerance. The principle of this algorithm is graphically shown in Figure 3.6.

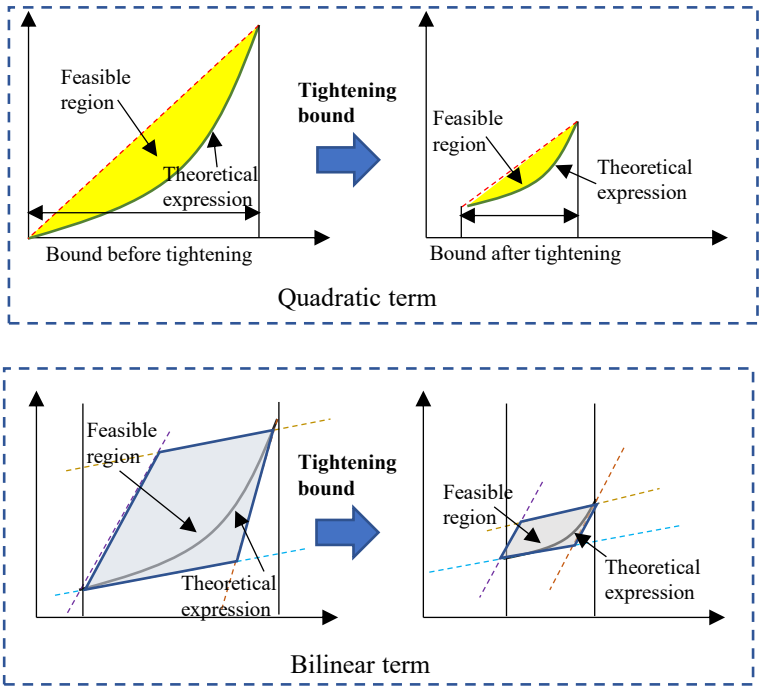

11**Figure 3.6** Tightening the bound of the nonlinear terms.

The function of the bound-tightening algorithm was clarified in this section as illustrated in Algorithm 1. A set of control parameters γ_k (unique for each pipeline at each iteration) which were used to increase the value of the lower bound or decrease the value of the upper bound, were introduced firstly. Initially, the bounds of each SOC constraint $\{\overline{Q_{p,t}^{+}}, \underline{Q_{p,t}^{+}}, \overline{Q_{p,t}^{-}}, \underline{Q_{p,t}^{-}}, \overline{\psi_{p,t}^{+}}, \underline{\psi_{p,t}^{+}}, \overline{\psi_{p,t}^{-}}, \underline{\psi_{p,t}^{-}}\}$ were created in relatively wide ranges. Then the optimisation will be solved repeatedly until the defined error is less than the set convergence tolerance δ or

a number of iterations (N_{it}) were completed. The error used to control the repetition was defined as $e_{p,t} = \left|\frac{\mathrm{K}_p^2(\Pi^2_{n^{\mathrm{start}},t} - \Pi^2_{n^{\mathrm{end}},t}) - (Q_p^{\mathrm{AV}})^2}{\mathrm{K}_p^2(\Pi^2_{n^{\mathrm{start}},t} - \Pi^2_{n^{\mathrm{end}},t})}\right|$.

Algorithm 1: An enhanced MISCOP algorithm

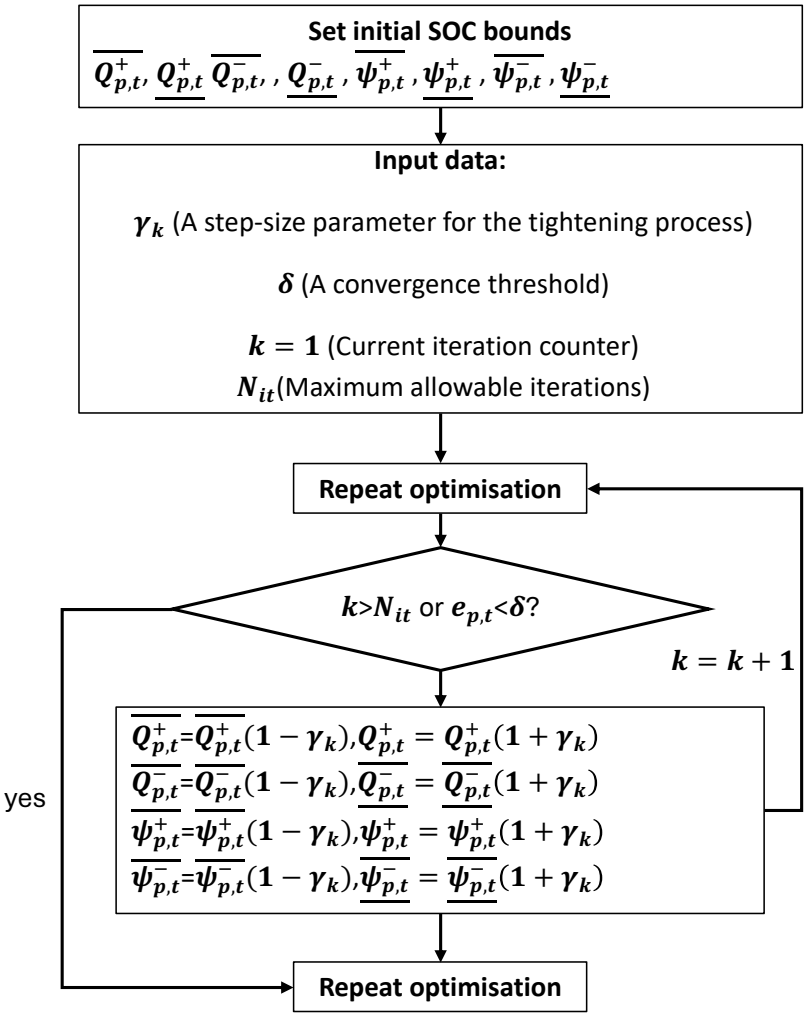

3.4 Results

3.4.1 Performance of the solution algorithm

The accuracy of the model using bound-tightening algorithm was analysed. The number of iterations *k* was set to three (the algorithm was not used when *k*=1). $e_{a,t}$ is the error between the value of gas flow in theoretical and that of the solution. $e_{a,t}^{av}$ in Eq. (3.41) is the average value of $e_{a,t}$ over time steps which was used to indicate the quality of the solution.

$$e_p^{av} = \frac{\sum_{t=1}^{T} e_{p,t}}{T}, \forall p \in P \tag{3.41}$$

Figure 3.7 shows the $e_{i,j}^{av}$ of each pipe after each iteration. Introducing $u^{av} = \frac{e_p^{av}}{N_A}$ to formulate the average value of the defined error e_p^{av} of each pipeline, where N_A is the number of pipelines. Table 3.1 summarises control parameters γ_k and results for each iteration. It can be found that the better solution with smaller u^{av} was obtained via tightening bound by the algorithm- decreased average value of defined error from 14.5% to 2.7%, while the computational time is acceptable. However, it is noted that, this algorithm may not be suitable to be used for the large-scale optimisation, since the number of iterations will be increased due to more variables.

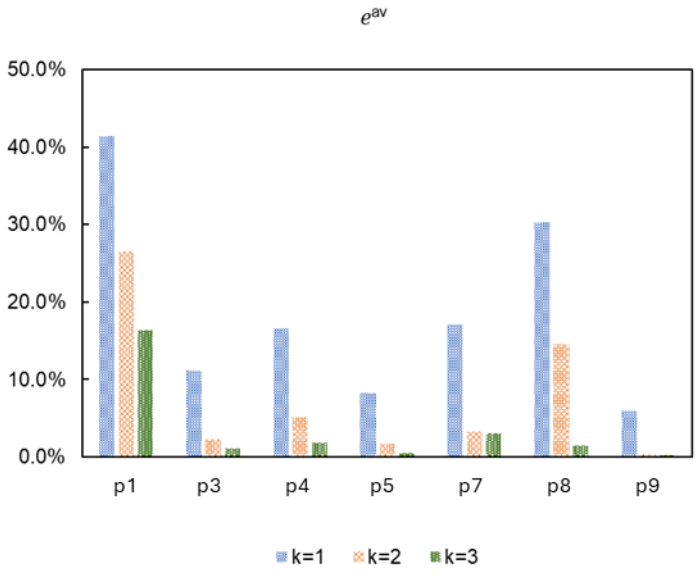

12**Figure 3.7** Improving solutions via using the bound-tightening algorithm

2**Table 3.1** Parameters and results of each iteration

Iteration	γ_k	u^{av}	**Time**
k=1	-	14.54%	3s
k=2	0.2	3.1%	18s
k=3	0.15	2.7%	31s

3.4.2 The value of coordinated operation of GDC and EDC

Three scenarios were investigated to determine the value of the combined operation of EDC and GDC. Profiles of the energy consumption in these scenarios are shown in Figure 3.8 - Figure 3.10.

It can be found from Figure 3.8, when only GDCs are allowed to work, the compressors have to work harder in period of higher gas demand (e.g., at hour 8, 17 and 18, gas demand profile see Figure 3.6).

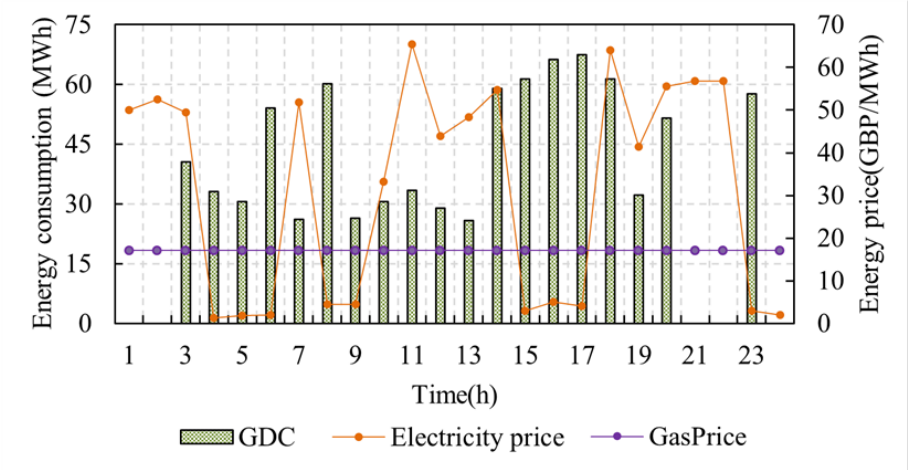

13**Figure 3.8** Energy consumption of compressors in Scenario 1

However, when only EDCs are available, their operation is affected by the electricity price. As shown in Figure 3.9, when electricity price is relatively lower (e.g., at hour 4, 5 and 6), compressor units will work harder to increase linepack.

When electricity price is higher, the linepack can maintain the pressure for several hours to reduce workload of these compressors to save energy consumption.

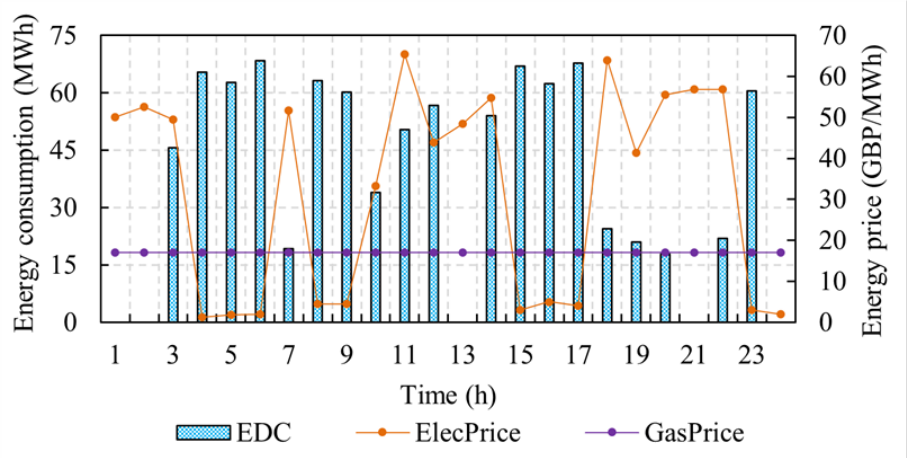

14**Figure 3.9** Energy consumption of compressors in Scenario 2

Figure 3.10 shows that the operation of GDCs and EDCs in Scenario 3 is sensitive to the relative price of electricity and gas: when the electricity cost is lower than that of gas (e.g., at hour 4, 5 and 6), EDCs are working (GDCs are OFF) and when the gas cost is lower (e.g., at hour 11, 13, 15), GDC is working (EDCs are OFF).

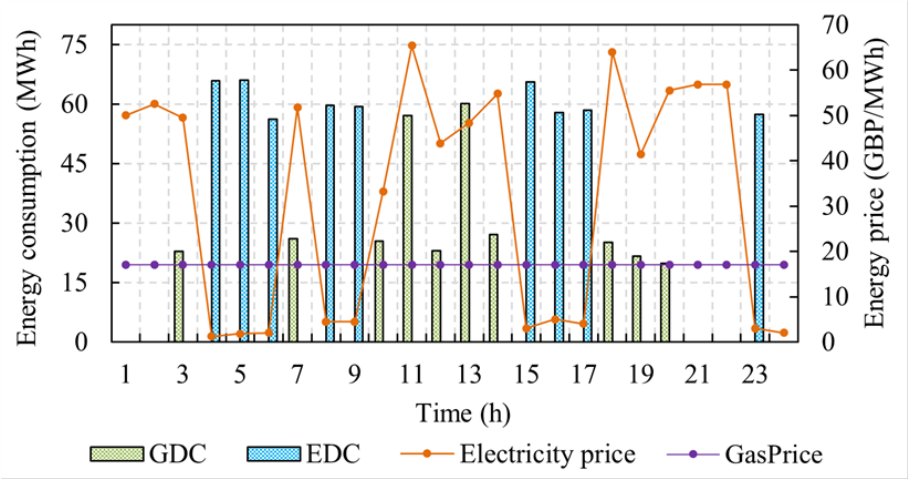

15**Figure 3.10** Energy consumption of compressors in Scenario 3

It can be additionally found that in all three scenarios, the compressors work close to their rated capacity in hour 23 to ensure the 'end-of-day' target for linepack will be met.

Different operation strategies for the compressor units result in different linepack pattern as Figure 3.11 shown. Generally, the linepack of Scenario 2 and Scenario 3 are higher than that of Scenario 1 because EDCs shift their operation in time to use low price electricity and therefore pressurise the network.

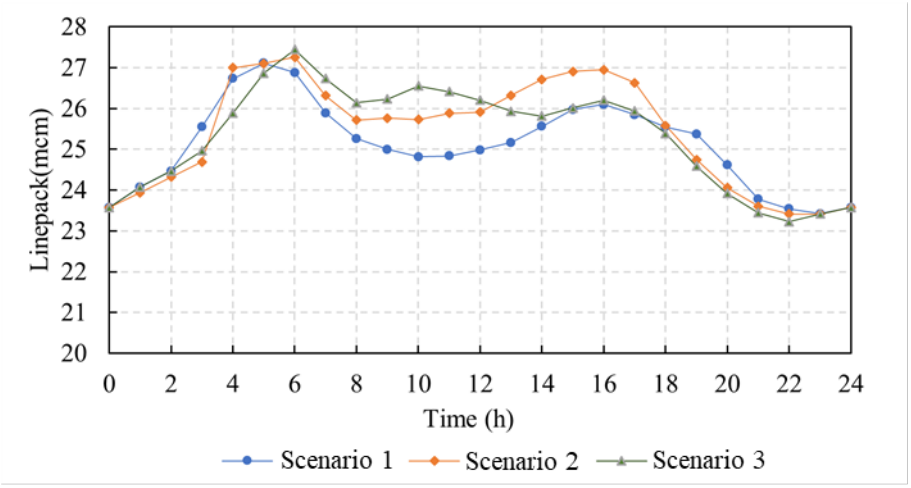

16**Figure 3.11** Linepack of the gas network in all scenarios

The operating costs for each scenario and emission of carbon dioxide from each operation schedule are listed below in Table 3.2 (1 m^3 natural gas produces 1.86 kg CO_2 [71]). It can be found that using EDC only produces no direct emission though, the cost of it is the highest among three scenarios. The operating cost of the system in Scenario 3 is the lowest due to the coordinated operation of EDCs and GDCs allows exploiting low energy price for operating the compressors. Scenario 3 also produces only 36% of the carbon dioxide emissions of Scenario 1.

3**Table 3.2** Cost of energy consumption and emissions in all scenarios

Scenario	**GDC cost (£/day)**	**GDC cost (£/day)**	**Total cost (£/day)**	**CO_2 Emissions (tone/day)**
Scenario 1	0	14461	14461	145.4
Scenario 2	19694	0	19694	0
Scenario 3	1741	5264	7006	52.9

3.5 Conclusion

The operation of a gas network with a combination of gas-driven and electric-driven compressor units was modelled to quantify the value of flexibility from compressor units. The mixed integer nonlinear optimisation problem was formulated as MISOCP. The problem was solved using an iterative bound-tightening algorithm to balance computational complexity and accuracy of the solution. It was found that the algorithm, which refines the boundaries of the SOCP, significantly enhances the model's accuracy (decreased average value of defined error from 14.5% to 2.7%) while not dramatically increasing the computation time.

The coordinated operation of GDCs and EDCs is highly sensitive to the relative prices of electricity and gas. The findings demonstrate that this coordinated approach can significantly lower operational costs to £7,006,

compared to £14461 when using GDCs alone and £19694 when relying solely on EDCs. Additionally, using a combined EDC and GDC system only produced 52.9 tonnes of emissions, a 64% reduction compared to the 145.4 tonnes generated in scenario that only the GDCs are employed only.

This chapter demonstrates the benefits of coordination across different types of compressors, considering the relative prices of gas and electricity. The next chapter will expand the analysis to the entire GB gas network, delving deeper into the benefits of coordinated compressor operations, such as their potential to provide flexibility to the power system.

Chapter 4 Assessing techno-economic and environmental impacts of gas compressor fleet as a source of flexibility to the power system

4.1 Introduction

The gas network in the GB delivered 881 TWh of energy and supplied almost 85% of households [72]. The national gas transmission system (NTS) is a significant source of flexibility to the power system by supplying fuel to power stations to meet peak electricity demand [73]. Moreover, with the development of low-carbon technologies (such as power-to-gas), the gas network is expected to provide more flexibility to maximise the use of renewables in the future [74].

For instance, flexibility can be provided by the gas network as gas stored in pipelines (linepack) can be adjusted to some extent. In the GB gas network, the linepack can provide more than 400 GWh diurnal storage [75]. However, many studies have neglected the benefits of linepack [76–79]. There are also some studies that took the linepack into account. Mi, et al. [80] optimised the operation of an

integrated gas and electricity network considering the fluctuation of linepack, and found that linepack is helpful for reducing the operational cost. Other research that highlighted the value of linepack can be found in [81–84].

Nevertheless, linepack cannot provide flexibility on its own as the adjustment of linepack needs the operation of compressor units. Although, compressor units play an important role in the gas transmission system, their role in providing flexibility has been neglected in a large volume of existing research that investigate the integrated operation of gas and electricity systems [83,85–88], Only few researchers took the compressor units into account when modelling the gas network. However, rather than considering detailed characteristics of compressors, most of the studies simplified them to a compressing ratio. Energy consumed by the compressor units was considered in some studies [77], [89–91], however, their operational flexibility was not investigated.

The operation of compressor units was optimised in Chapter 3. However, due to using two sets of compressor units as a case study, the benefits of the coordinated operation of multiple compressor stations distributed across a large-scale gas network could not be captured. In this chapter, the optimal operation of hybrid compressor stations (compressor stations in which both electric-driven and gas-driven compressor units exist) across the GB gas transmission system was analysed, to develop a better understanding of the role of compressor units.

First, the optimal operation of the whole GB gas network considering the flexible operation of compressor units under different scenarios was investigated. Next, the magnitude of flexibility offered by electric-driven compressors was quantified. The response of compressor units to variations of electricity prices and gas demand was then explored. This was followed by an examination of the role of linepack in exploiting the flexibility provided by compressors. Finally, a cost-benefit analysis was conducted to assess the profitability of installing new electric-driven compressors.

4.2 Flexibility from compressor stations

4.2.1 Flexibility from switching between gas and electric driven compressors

In GB, prices of gas and electricity can be different during a day which could impact the operational strategy of the compressors. A hybrid compressor station comprises both GDCs and EDCs and either of these compressors can be operated depending on the operational cost and other considerations (e.g., provide flexibility to the power grid from EDCs via regulating their electricity consumption). The configuration of two types of compressor units within a hybrid compressor station can be found in Figure 3.4 (Chapter 3, section 3.2.1).

Three valves were modelled in each hybrid compressor station to control the direction of gas flow. As gas flows to the compressor station from the suction

node, two decisions need to be made by the system. Firstly, valve 1 which is installed along the bypass line, is employed to determine whether the compressor is required to work. If valve 1 is opened, valve 2 and value 3 are closed and gas will flow through the bypass line rather than being pressurised by compressor units. However, if compressor units are required to work, valve 1 is closed while one of the other two valves is opened, which means one of the compressor units is working. When the gas price is lower than that of electricity, valve 3 is opened and gas is pressurised by the GDC, otherwise, valve 2 is opened to pressurise gas via EDC. Note that minimising the operational cost of gas compressors is also subject to meeting gas demand and ensuring operational constraints of the system.

4.2.2 Flexibility from upward/downward regulation of electric-driven compressors

Electric-driven compressors can provide flexibility to the power grid as they are able to adjust their electricity consumption in response to the needs of the power system, subject to the pressure and flow requirements from the gas network operator. Note that upward regulation means an increase in the electricity consumed by EDCs, while downward regulation denotes a decrease in the electricity consumption of EDCs (it is worth noting that a different naming convention might be in use in the power sector).

An approach for quantifying flexibility of the compressor units is graphically described in Figure. 4.1. The upward/downward regulation of EDCs (i.e. increase/decrease in their electricity consumption) was calculated at each time step by quantifying the difference between the optimum electricity consumption* and maximum/minimum amount of electricity that EDCs can consume without violating any operational limits or network constraints.

For instance, to calculate the upward/downward regulation of EDCs at t1, the optimum electricity consumption of each EDC was fixed at all the other time steps except t1, then the objective function was updated to maximise/minimise the value of electricity consumption of all EDCs at t1. Then the upward/downward regulation was obtained by calculating the difference between maximum/minimum value of electricity consumption and the optimum value. The same process was used to calculate the upward/downward regulation of EDCs for 24 hours.

* The optimal electricity consumption of EDCs is determined through baseline optimisation, which aims to minimise the operational cost of the gas network.

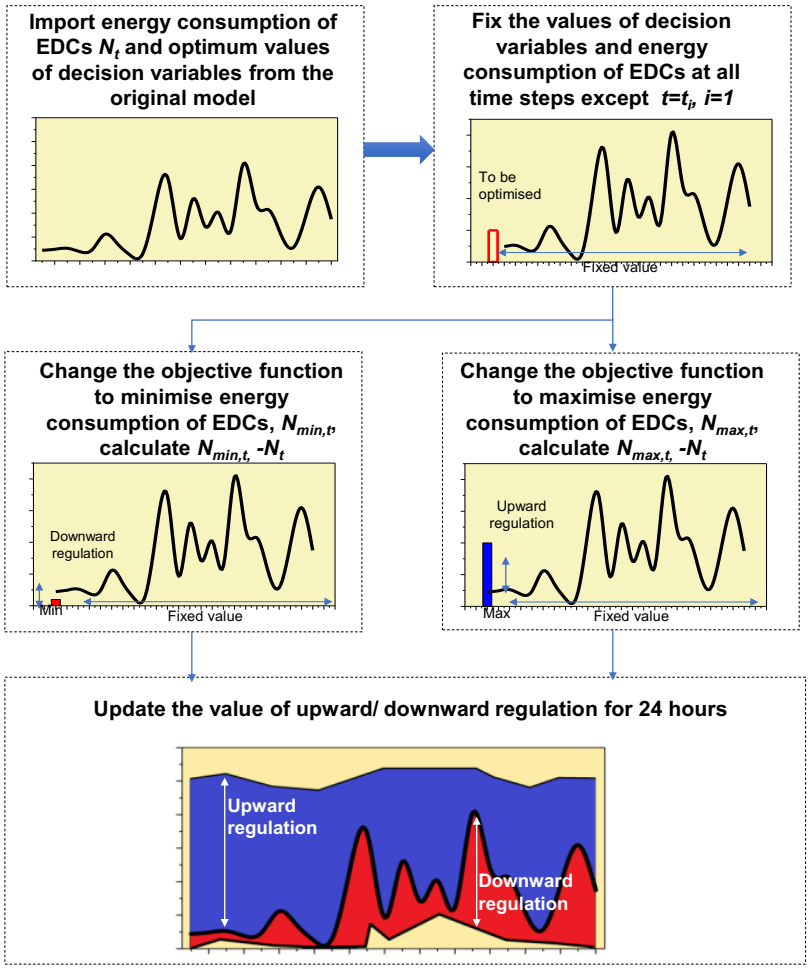

17Figure 4.1 Quantification of EDCs' flexibility

4.3 Key objectives and methodology

The primary objective of this investigation is to elucidate the role of coordinated compressor operations in reducing operational costs and enhancing system flexibility. As in Chapter 3, the analysis of this chapter focuses solely on

the modelling of the gas system, with the baseline optimisation aiming to minimise its operational cost.

The flexibility magnitude of EDCs was quantified as a post-analysis, derived from the solution of the least cost optimisation. In this phase, the model's objective function was adjusted to either maximise the energy consumption of EDCs for upward regulation or minimise it for downward regulation. The operational cost of the system was no longer the primary focus during this stage.

The sensitivity of the compressor operation to variations of the energy price, gas demand and linepack was further explored. In these analytical cases, the objective function of the model remains focused on minimising the operational cost of the system. Switching between case studies requires only changes to the input data, without needing to adjust the model itself. For instance, when analysing the impact of electricity prices on compressor operations, only changing the electricity prices in the input data is required.

Additionally, the profitability of installing new compressor units over their life cycles was clarified through a Cost Benefit Analysis. In this phase, the least cost optimisation was performed for various scenarios to determine the cost savings achieved by hybrid compressor stations. These cost savings were then compared with the capital costs to assess whether the installation of new compressor units is financially viable.

4.4 Case study

4.4.1 National gas transmission system in GB

The high-pressure gas transmission system in GB comprises 7600 km of pipelines (more than 400 pipes) and hundreds of offtake points [92]. It is challenging to optimise the operation of such a large gas network, as a large number of variables (especially the binary variables representing flow directions) dramatically increase the computational complexity. Due to this, using the method described in [93], a reasonable simplification of the GB gas network was conducted in this paper. The simplified gas network which retains the basic features (e.g., supply and demand values, volume of linepack, etc) of the original system, is shown in Figure 4.2. The simplified 67-node gas network has 76 pipelines, 8 gas terminals and 24 compressor stations. Each compressor station was assumed to have two parallel compressor units with capacity of 50 MW each – it is worth noting that, in reality, each compressor station has different number of units, and their arrangement is also distinct, however, accounting for this level of detail was not within the scope of this study.

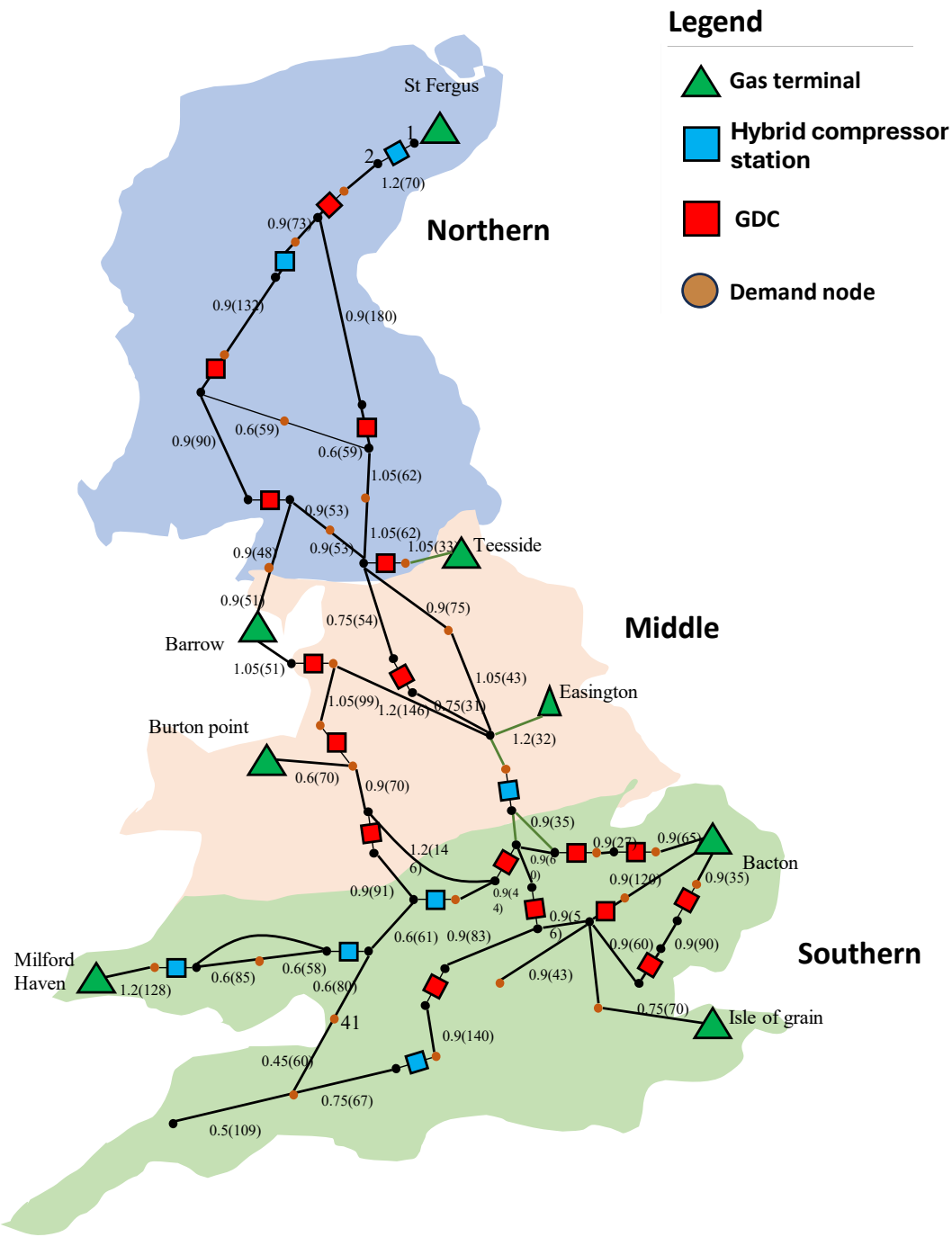

18Figure 4.2 Simplified GB gas network. (Number outside the basket is the diameter of pipelines (m) while number inside it is the length of the pipe (km))

The aggregate gas demand for a typical winter day shown in Figure 4.3 was used in the model after distributing the gas demand across different nodes. The electricity prices were assumed to be exogenous in this analysis. Therefore, the prices are known in advance and used in optimal scheduling of the compressors.

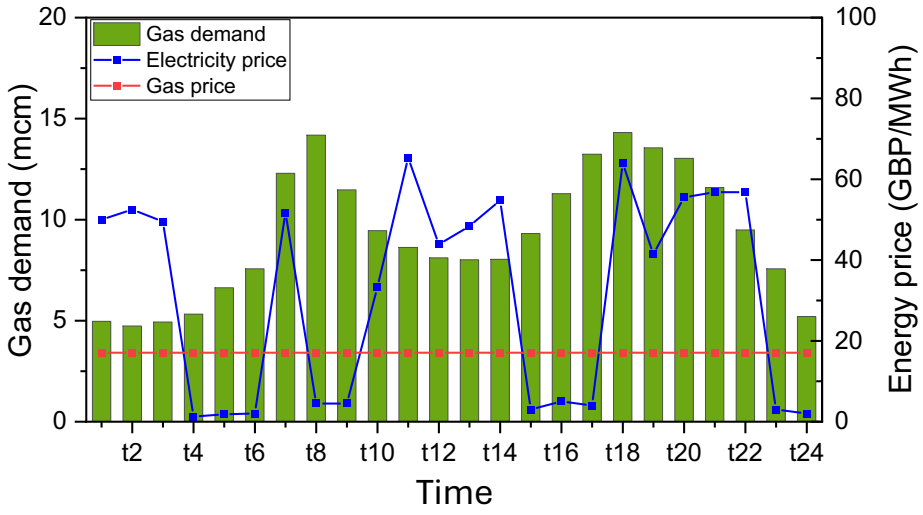

19Figure 4.3 Profile of gas demand data and energy prices

4.4.2 Optimisation scenarios

To demonstrate the benefits of the hybrid compressor station from an economic and environmental perspectives, along with the potential for providing flexibility to the power grid, three scenarios were defined.

Scenario 1: This scenario presents the current situation in the GB gas network in which there are 7 hybrid compressor stations, and 17 compressor stations have only gas-driven compressor units.

Scenario 2: In this scenario it was assumed that all 24 compressor stations in the GB gas network only have electric-driven compressor units.

Scenario 3: This scenario assumes all 24 compressor stations have both electric-driven and gas-driven compressors, i.e., they are all hybrid compressor stations.

For each of the above scenarios, the optimal operation of compressor units was analysed, and flexibility of compressor units was quantified.

4.5 Results and discussion

4.5.1 Optimal operation of compressor units

Optimal operation profiles of compressor units in each scenario were shown in Figure 4.4. Figure 4.4 (a) and Figure 4.4 (c) show that the operation of compressor units is sensitive to the relative prices of gas to electricity; EDCs were employed when electricity price is lower than that of gas (e.g., at t5 and t16) while GDCs is working when gas price is relatively lower (e.g., at t13 and t22). In Figure 4.4 (b), in which there are only EDC units, it can be seen that EDCs work harder

when electricity price is relatively lower. This is why the hourly energy consumption of EDCs in Scenario 2 is more variable during the day. Therefore, the maximum hourly energy consumption in Scenario 2 can be up to 320 MWh while in Scenario 1 only reaches 190 MWh. The operational cost and emissions for each scenario is shown in Table 4.1 (1 m3 natural gas at standard temperature and pressure produces 1.86 kg CO2). It is worth noting that in this study, we only considered the emission at the sites (rather than the emission from the whole system, e.g. emission associated with the electricity used by electric-driven compressors), because this is the emission that is required to be reduced to comply with Industrial Emission Directive[94].

As shown in Table 4.1, if all GDCs are replaced by EDCs (i.e. Scenario 2), the operational cost will increase by 36% based on the specific profile of electricity prices used in this study. However, it brings environmental benefits as EDCs do not emit GHG directly. Employing hybrid compressor stations reduces the operational cost of compressor units significantly and it reduces emissions as well, as gas consumption of GDCs in Scenario 3 is lower than that of Scenario 1.

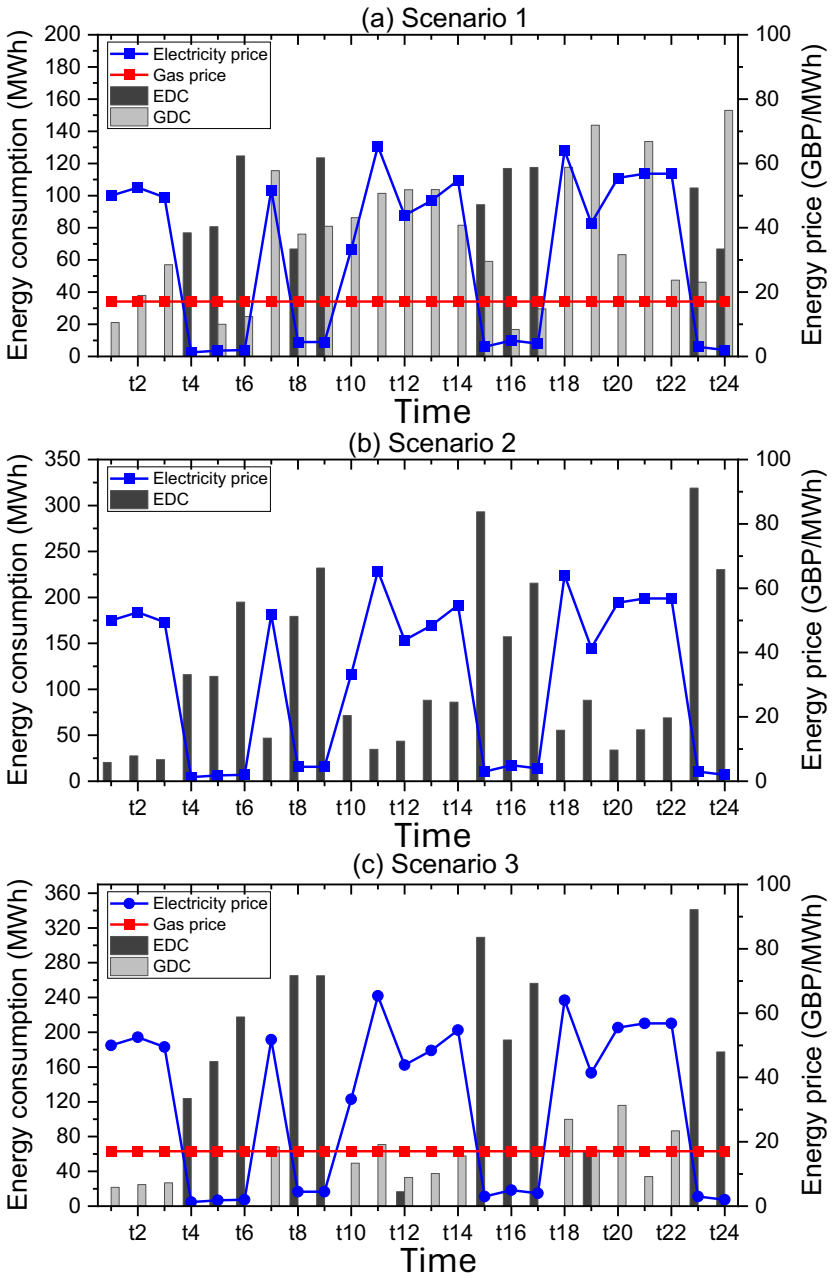

20Figure 4.4 Optimal operation of compressor units in three scenarios.

Scenario 1 represents the existing mix of compressor units, i.e. 7 compressor stations have both EDC and GDC, and the rest of the compressor stations only

have GDCs. In Scenario 2, all compressor stations only have EDCs. In Scenario 3, all compressor stations have both EDCs and GDCs.

4**Table 4.1** Operational cost (£) and emissions (tone) of compressor units in three scenarios

Scenario	Cost of operating EDC (£/day)	Cost of operating GDC (£/day)	Total cost of operating compressors (£/day)	Emissions from compressor sites (tone/day)
1	3808	26990	30798	290
2	44297	0	44297	0
3	10931	13506	24437	145

The linepack of NTS under the three scenarios are different due to the various operation schedule of compressor units. The hourly linepack profile for each scenario is shown in Figure 4.5 (linepack at t0 is the initial value of linepack). It can be observed that linepack in Scenario 1 is generally lower than that in other scenarios, since the number of EDCs in scenarios 2 and 3 are more than that in Scenario 1, and more EDCs are able to use more electricity with lower price. For instance, EDCs in Scenarios 2 and 3 work more and increase the linepack from t8 due to the low electricity price at t8 and t9.

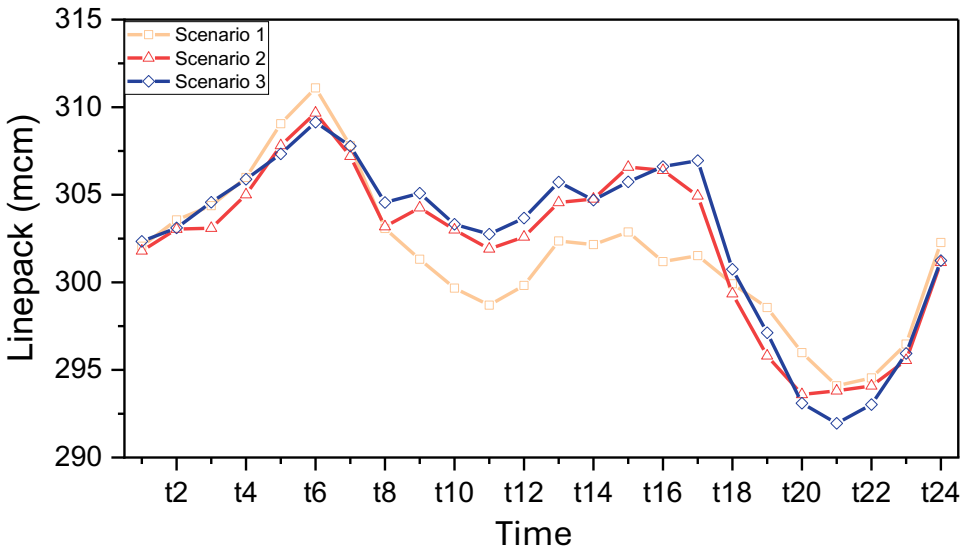

21Figure 4.5 Linepack for three scenarios with different mix of compressor units

4.5.2 Flexibility analysis of compressor units

The number of compressors is different in various regions of the existing GB gas network due to the length of pipelines and level of gas flow are different. Owing to this, the level of flexibility provided by EDCs distributed in different regions (Northern, Middle, and Southern as shown in Figure 4.2) can be distinct. The number of hybrid compressor station and gas-driven compressor station for each part is listed in Table 4.2. The flexibility of EDCs in each region (under Scenario 1) was quantified based on the approach presented in Figure 4.1. The results were shown in Figure 4.6.

5**Table 4.2** Number and type of compressor stations in each region of GB gas network. 'hybrid' compressor stations include one GDC and one EDC, 'gas-driven compressor stations' include two GDCs that operate in parallel.

Region	Hybrid compressor station	Gas-driven compressor station
Northern	2	5
Middle	1	4
Southern	4	8

It can be seen from Figure 4.6 that due to the support from GDCs during the coordinated operation, EDCs can be flexibly regulated at each time step. The flexibility provided by EDCs in the Southern region is much higher than that in the Middle and Northern regions, as a majority of EDCs were located in the Southern region.

To highlight the benefit of the hybrid compressor stations, the flexibility of EDCs in Scenarios 2 and 3 was quantified as shown in Figure 4.7. It can be observed that, in Scenario 2, in which only EDCs were employed, the downward regulation of EDCs is limited during the day as without the support from GDCs there is no potential for fuel switching. Besides during some periods, e.g., at t15 and t23, the upward regulation of their operation is also limited. In contrast, the

flexibility of EDCs in Scenario 3 is much higher since the GDCs can be employed when EDCs were switched off.

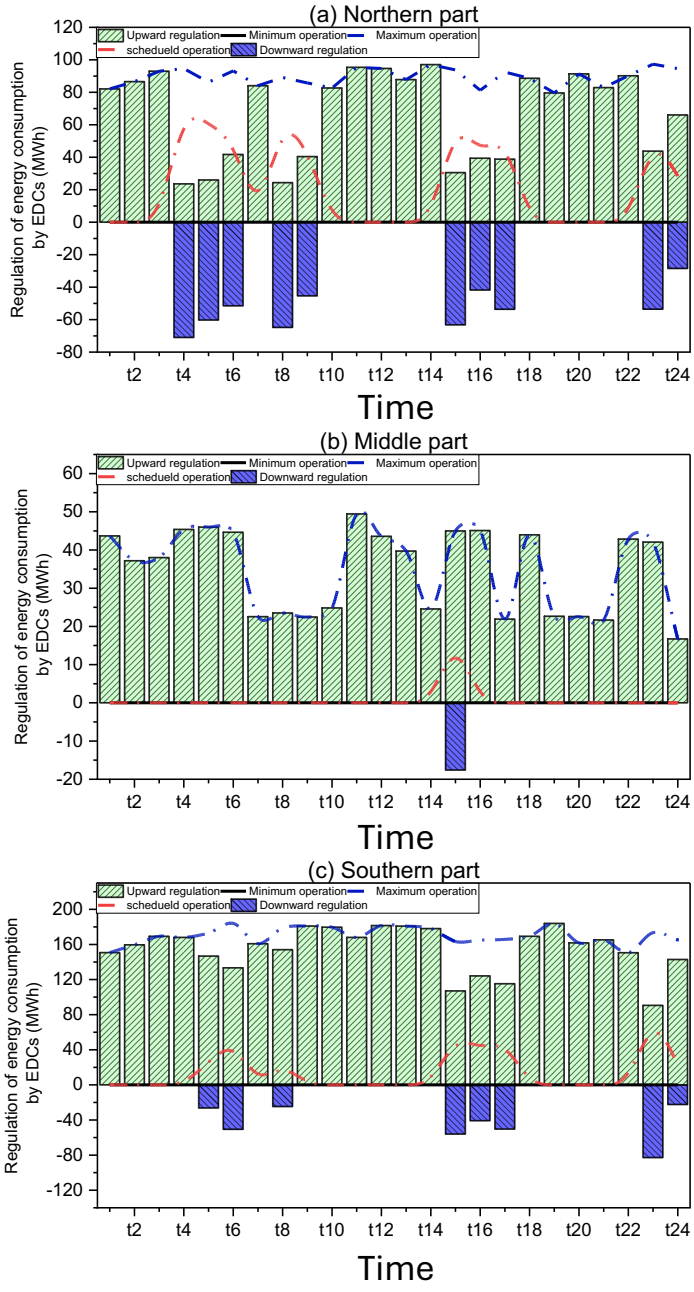

22**Figure 4.6** Upward and downward regulation of electricity consumption by compressor units in different regions in Scenario 1

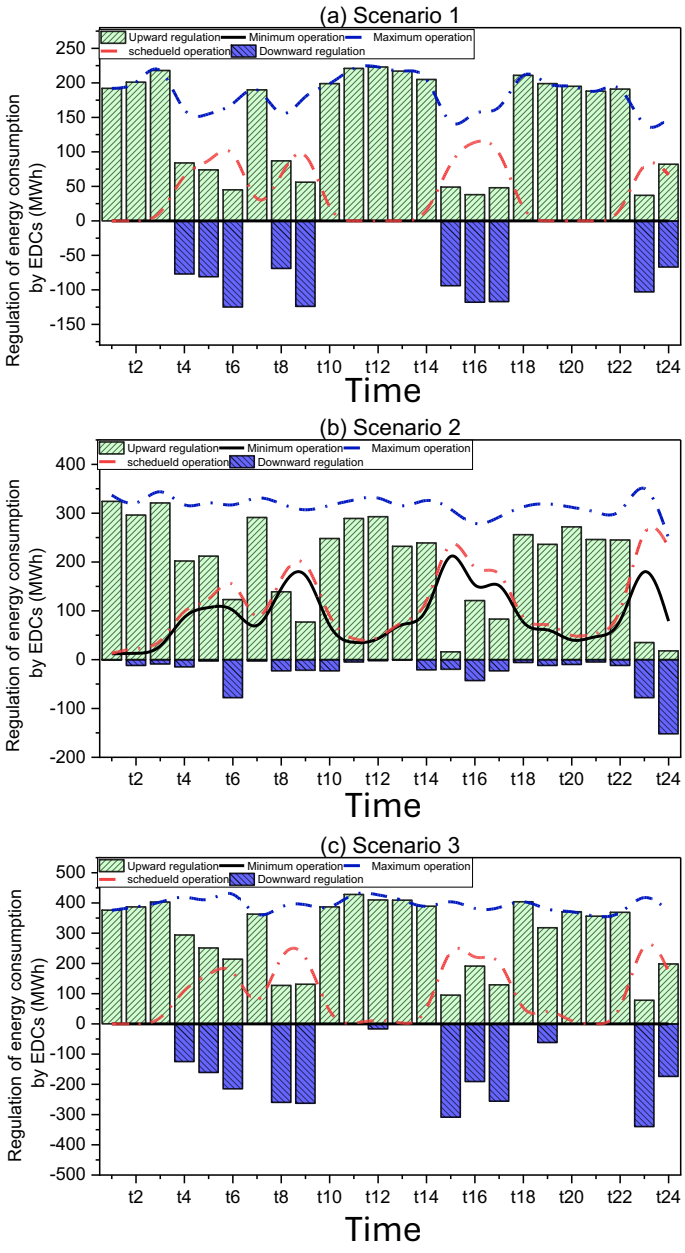

23**Figure 4.7** Upward and downward regulation of compressor units in all scenarios

4.5.3 Adjusting the operating schedule of compressor units in response to changes in gas demand and electricity prices

In the above sections, the optimal operation of compressor units was analysed assuming ‘perfect foresight’, i.e., both gas demand and energy prices are known for the whole operating horizon (in the case of energy prices, it makes sense to assume these prices are cleared in day-ahead market). In this section, the response of compressor units to unpredicted variations in gas demand and energy prices was analysed.

Firstly, it was assumed that at t12 gas demand is 30% higher than its predicted value as shown in Figure 4.8 (a). To model the sudden change at t12, solution of the optimisation for the baseline gas demand were fixed before t12, and then effects of the gas demand change on the operation of compressor units in the three scenarios are studied.

As shown in Figure 4.8 (b) and (d), the increase of gas demand mainly affects GDCs’ operation whilst EDCs are only slightly adjusted. This is because of the higher electricity price at t12. However, in Scenario 2 as shown in Figure 4.8 (c), more power is required to increase the operation of EDCs since no GDC is available in this scenario. The increasing cost of operating compressor stations due to the change of gas demand in each scenario was listed in Table 4.3. It can be seen that coordination of GDCs and EDCs are important in saving cost as the

increasing cost in Scenario 2 is the highest when met a sudden increase in gas demand.

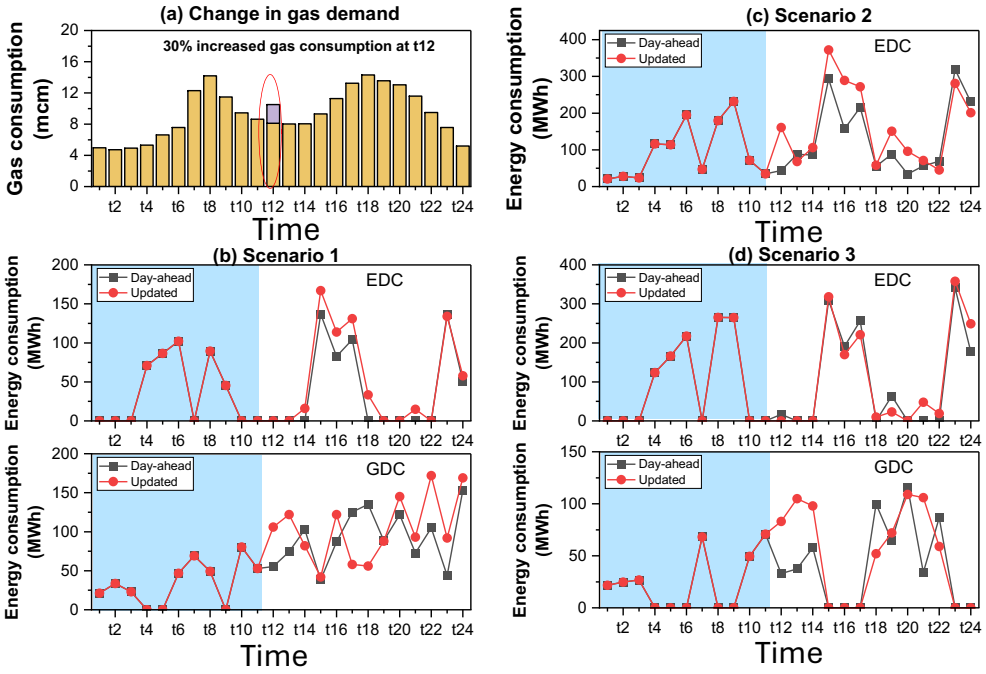

24**Figure 4.8** Effects of gas demand change on the operation of compressor units

6**Table 4.3** Increasing operational cos of compressor units in three scenarios (under the change in gas demand) (£)

Scenario	EDC	GDC	Total
1	1301	2716	4017
2	15189	0	15 189
3	1282	2095	3377

Moreover, the effect of unpredicted rise in the electricity price on the operation of compressor units was also analysed. The price of electricity at t16 was changed from 5 £/MWh to 51 £/MWh as shown in Figure 4.9 (a). The decision variables for time steps before t16 were fixed using the solution obtained for the baseline electricity price.

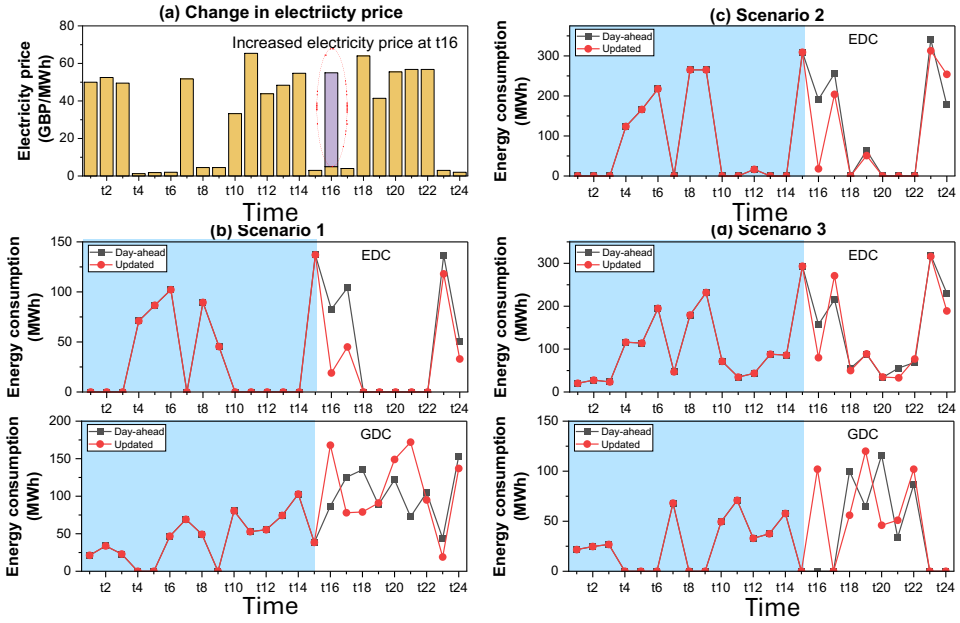

25**Figure 4.9** Effects of electricity price change on the operation of compressor units

As Figure 4.9 (b)-(d) show, to achieve the minimum operational cost, GDCs are increasingly employed at t16 to reduce the operation of EDCs in Scenario 1 and Scenario 3. However, reduction of electricity consumption by EDCs in Scenario 2 is not as much as that in Scenarios 1 and 3 as no support can be provided by GDCs. The rising costs of operating compressor units in all scenarios due to the change of electricity price were shown in Table 4.4. In all the three scenarios, flexibility from compressor stations (in the form of fuel switching between electricity and gas, and also shifting the operation of electric driven compressors in time) were employed to minimise the impacts of the rise in

electricity price on the operational cost of compressors. Since there are more hybrid compressor stations in Scenario 3, the total increase of cost is the lowest, in comparison with the other two scenarios.

7**Table 4.4** Increase of operational cost of compressor units in three scenarios compared with the baselines (under the change in electricity price) (£)

Scenario	EDC	GDC	Total
1	321	1128	1449
2	2990	0	2990
3	32	1071	1103

4.5.4 Role of linepack in exploiting the flexibility from compressor unit

To achieve a minimum operational cost, the compressor units work hard when the hourly price of energy is relatively lower. Then the compressor units may not be required to operate in the next few hours when the energy price becomes higher, as the increased linepack can be employed to contribute to meeting the gas demand. In this section, the effect of limiting the linepack variation (the range within which linepack can be varied) on the operational cost of compressor units was analysed and the results were shown in Figure 4.10.

In Scenario 1, operational cost of compressor units reduced rapidly, as the limited variation in linepack increased from 1% to 5% (increase or decrease compared to the opening linepack), and then it changes very slightly after linepack variation exceeds 5%. Compared with Scenario 1, operational cost of compressors in Scenario 2 keeps decreasing until the linepack variation exceeds 15%, which means using linepack is a key enabler to shift the operation of EDCs in time. In Scenario 3, the operational cost of compressor units declines slightly along with the increase in the linepack variation, as more hybrid compressor stations can be employed and the main source of flexibility is fuel switching in the compressor stations.

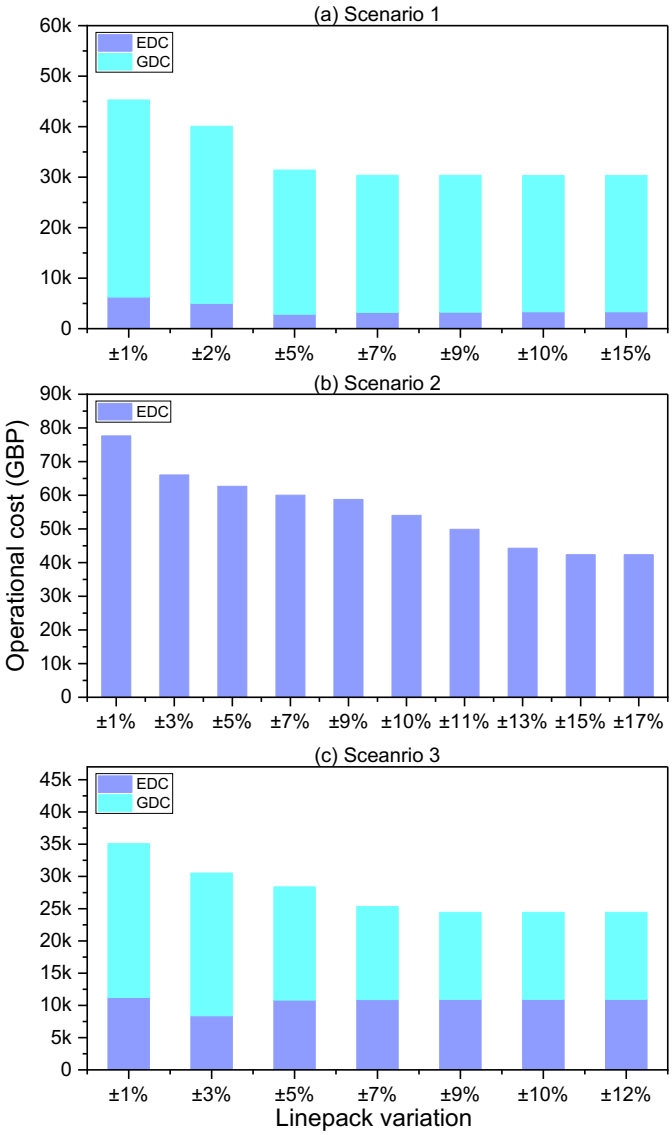

26**Figure 4.10** Operational cost of compressor units under different limits for linepack variations

4.5.5 Cost-benefits analysis (CBA) of hybrid compressor station in the GB gas network

Daily optimal operation of compressor units in different scenarios was analysed and it was demonstrated that using hybrid compressor stations in the GB gas network results in reducing the operational costs. However, whether the cost saving offered by EDCs during their service lifetime can cover their capital cost is necessary to be clarified. In this section, a CBA was carried out to evaluate the Net Present Value (NPV) of the investment in installing new EDCs. The calculation of NPV is denoted by Eq. (4.1), where C_{yc}^{op} is operational cost savings, C_{yc}^{em} is cost savings due to reduction in GHG emissions, C_{yc}^{ac} is the annualised investment cost for new EDCs, yc represents the yearly timestep for CBA, and r is the discount rate. The overview of methodology used was shown in Figure 4.11.

$$NPV = \sum_{yc=1}^{n} \frac{C_{yc}^{op} + C_{yc}^{em} - C_{yc}^{ac}}{(1+r)^{yc}} \quad (4.1)$$

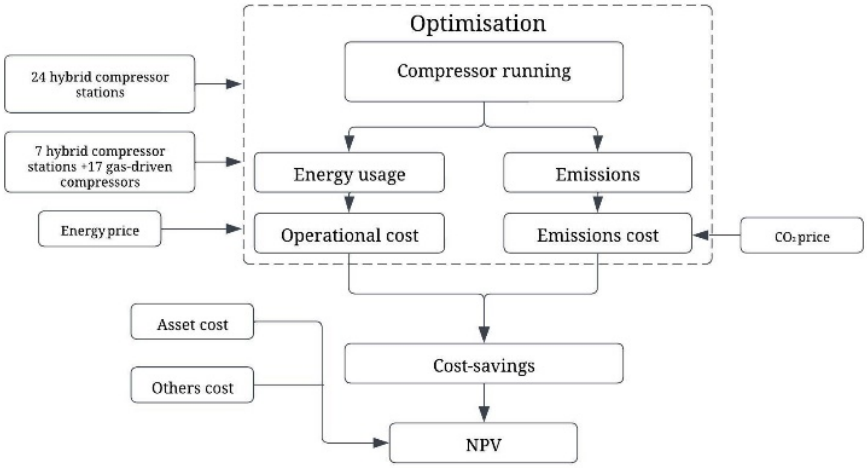

27**Figure 4.11** Overview of cost-benefit analysis (CBA)

We recognise that when carrying out a CBA, there are significant uncertainties around long-term technical and economic performance of proposed investments, however, this analysis attempts to provide insights into influential factors affecting the economic viability of investing in hybrid compressor stations. Therefore, following assumptions were made:

(1) Six typical days over a year were used to represent different level of gas demand. Long term changes in energy prices and demand were neglected.

(2) The life of compressor units was assumed to be 20 years.

(3) Three projections for CO2 prices provided by GOV.UK[94] were used as shown in Figure 4.12.

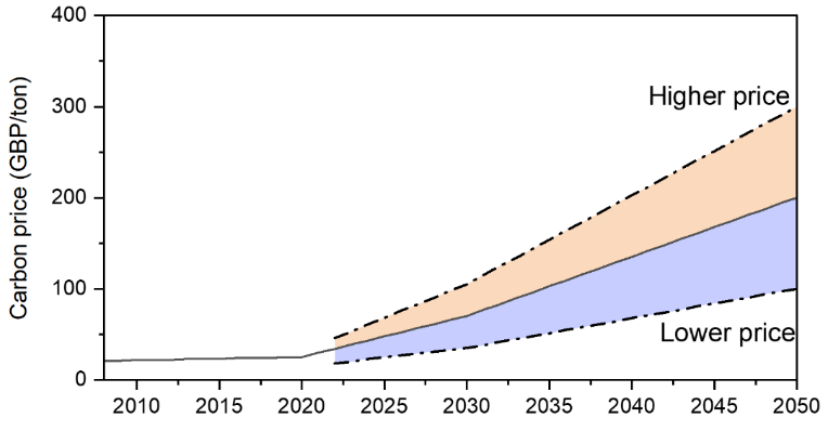

28**Figure 4.12** CO2 price projections

Firstly, the operational cost of the system under Scenario 1 and Scenario 3 was analysed as shown in Figure 4.13. The cost savings achieved by coordinated operation of EDCs and GDCs during a year was calculated then. The annual cost-saving in GHG emissions was calculated under different CO_2 prices. The annualised cost for installing 15 electric-driven compressor units in compressor stations that do not currently have an EDC was calculated considering Capital Recovery Factor (CRF) as denoted by Eq. (4.2).

$$CRF = \frac{r(1+r)^n}{(1+r)^n - 1} \tag{4.2}$$

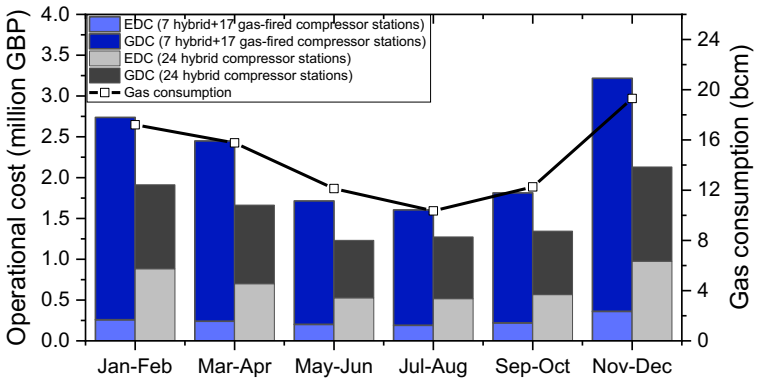

29**Figure 4.13** Operational cost of compressor units

The NPVs under different CO_2 prices were analysed and shown in Figure 4.14(a), after analysing the cost savings associated with the investment in electric-driven compressor units as shown in Figure 4.14(b). The NPV is negative when carbon prices are low, but when carbon prices are higher, installing new EDCs is profitable.

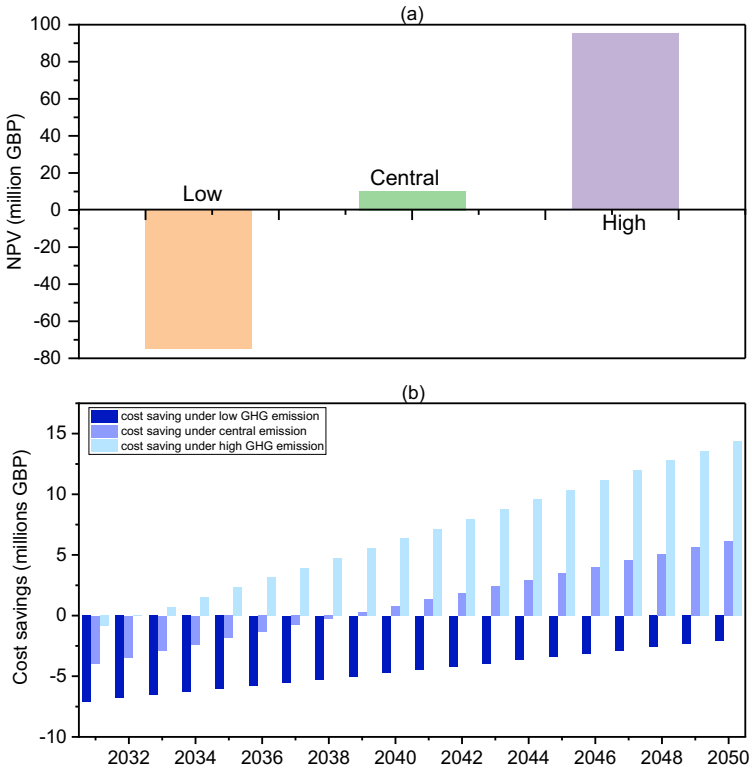

30**Figure 4.14** NPV (a) and Cumulative cost savings (b)

4.6 Conclusion

The operation of the GB gas transmission system including different types of compressor units (EDC and GDC) was modelled as a MISOCP optimisation problem. The role of compressor units in providing flexibility and subsequently offering economic and environmental benefits were investigated.

The optimal operation of the compressors under different scenarios was analysed. Evidenced by the modelling results, using hybrid compressor stations

can reduce the operational cost, as the compressor units are able to optimally respond to the gas and electricity price fluctuations. Meanwhile, installing larger number of EDCs considerably reduces CO_2 emissions from the compressor station fleet.

Moreover, the responses of the compressor units to the changes in both gas demand and electricity price were studied. The hybrid compressor stations show a better performance in minimising the impacts of these changes of the operational cost of the compressor stations.

The impact of limiting the linepack variations on the operational cost of compressor units was analysed. It was demonstrated that insufficient allowance of linepack variation weaken the ability of the compressors to provide operational flexibility and therefore increase the operational cost of the compressor units. However, the impact of limiting linepack variations on hybrid compressor stations is less significant, as these compressor stations are more flexible due to fuel switching capability between EDCs and GDCs.

Finally, the Cost-Benefits Analysis was performed to evaluate whether the capital cost of installing new EDCs can be covered by expected cost-savings they can achieve during their service lifetime. The results showed high sensitivity of the net present value of the proposed investments to the future CO_2 prices – i.e.

the investment in hybrid compressor stations is profitable as long as the future CO_2 is not low.

The main focus of this work was to quantify the flexibility of hybrid compressor stations in a gas transmission network that potentially could be used to support the operation of the power grid. In the following chapters, an integrated gas and electricity network will be modelled to assess the ‘whole-system’ value of flexibility from different sources, such as battery storage, electrolysers, etc.

Chapter 5 Value of flexibility through energy system integration

5.1 Introduction

Energy systems integration is a process that strategically combines diverse energy infrastructures to enhance efficiency, reliability and sustainability within energy systems. This integration allows the coordinated operation of various energy facilities to maximise flexibility* across the entire system. However, the operational characteristics of different energy infrastructures vary significantly, thereby complicating the management of the integrated energy system.

Some research has analysed the operation of the integrated energy system, primarily focusing on aspects such as emission reductions [95–98] and operational costs [97,99,100]. Other studies have focused on the provision of flexibility to electric

* Flexibility in this context refers to the ability of the energy system to swiftly balance supply and demand. Flexibility providers within the system are the energy facilities capable of operating flexibly to either absorb surplus energy or serve as backup to compensate for any gaps in supply.

power systems from specific energy vectors, e.g., the flexibility from linepack of the gas network [101], thermal energy systems of buildings, and storage technologies (thermal storage [102], battery storage [103,104]). These studies demonstrate the potential and value of providing flexibility through energy systems integration.

Due to the complex interactions between various energy vectors, the availability of cross-vector flexibility is affected by constraints governing the operation of the energy vectors as well as the coupling components linking them. Therefore, providing flexibility to electric power system from different energy vectors requires detailed consideration of the operational characteristics of the energy systems and the trade-offs between various sources of flexibility across the integrated system.

In this chapter, the benefits of using flexibility from energy system integration were investigated. Using an integrated electricity, hydrogen and heat supply system for Great Britain in 2050 as a case study, the impacts of flexibility on the operations of the integrated energy system were investigated.

Initially, this chapter designed various scenarios to clarify the roles of different sources, such as hydrogen infrastructures, residential heating systems, and storage facilities, in enhancing the energy system's flexibility. Furthermore, the system's operation with flexibility provided by all these sources was compared

to its operation without such flexibility, highlighting the economic benefits of unlocking the whole system's flexibility.

5.2 Motivations

Flexibility can be provided in different ways, as graphically described in Figure 5.1. Within the hydrogen system, linepack can swing up and down through adjusting pressure within the pipelines, to accommodate fluctuations in supply and demand of hydrogen.

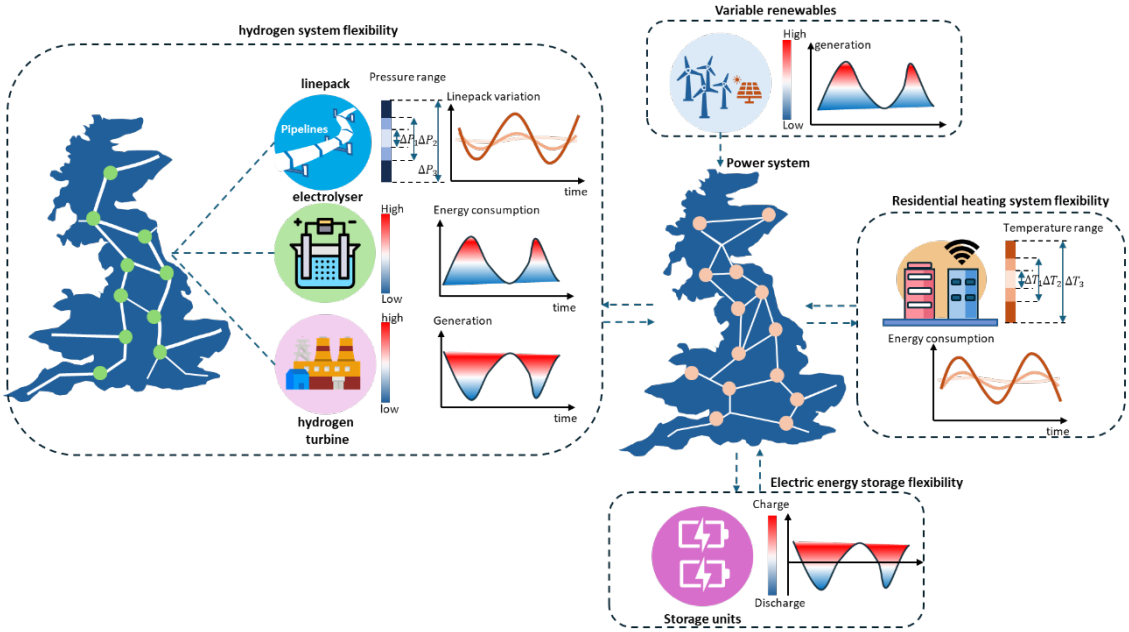

31**Figure 5.1** Flexibility provider within the integrated energy system

Linkage between the hydrogen system and the electricity system through electrolysers plays a pivotal role in offering flexibility by harnessing excess energy from the electricity grid to generate hydrogen. Furthermore, hydrogen-fired power plants serve as a valuable resource to compensate for times when renewable energy generation falls short of meeting electricity demand.

The residential heating system presents another avenue for enhancing system flexibility. Using thermal inertia of fabric, buildings are capable of storing heat which can be leveraged to manage energy consumption and maintain indoor comfort more efficiently. Moreover, electrical energy storage units like batteries and pump storage facilities offer additional flexibility to the electrical power system through their ability to charge and discharge power as needed.

While these facilities hold considerable potential to enhance flexibility within the whole energy system, their effectiveness is restricted by both their capacity and operational constraints. For example, variations in linepack are limited by the allowable pressure range necessary to maintain system safety. Likewise, the need to maintain indoor temperatures within a comfortable range restricts the operational flexibility of heat pumps or hydrogen boilers. Additionally, economic considerations often deter frequent switching on and off of energy facilities like hydrogen power plants, further limiting their ability to provide flexibility.

Understanding the intricate interdependencies among these energy facilities within the integrated energy system (IES) is paramount for strategically managing their operations and maximising their potential to offer flexibility to the entire system.

5.3 Methodology and scenarios definition

5.3.1 Methodology

The IES model introduced in Chapter 2 is applied to an integrated hydrogen-electricity-heating system projected for 2050 in Great Britain (GB). The interactions among the components considered in this model are graphically illustrated in Figure 5.2. The objective function aims to minimise the operation cost of the entire system, as detailed in Eq. (2.1). The detailed formulation of the constraints for each component can be found in Chapter 2.

Figure 5.2 illustrates the interactions among the components of the integrated energy system, along with their classification within the optimisation framework. Components shown in dark blue blocks, such as hydrogen supply, represent decision variables, while components shown in light blue blocks, such as wind and PV generation, represent parameters.

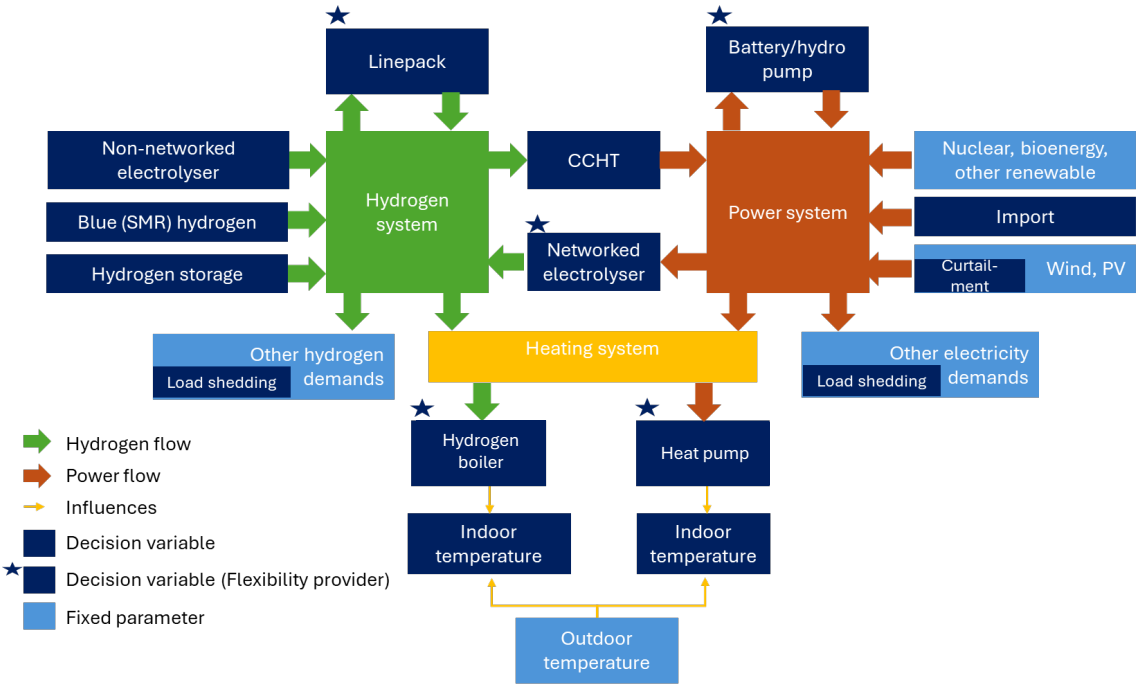

32**Figure 5.2** Interactions between each component within the whole energy system

5.3.2 Scenarios definition

To determine the value of the flexibility from the different resources, a total of ten scenarios have been defined to assess the effectiveness of different sources of flexibility in impacting the operation of the integrated energy system. The least-cost optimisation is carried out for each scenario.

It is notable that, the flexibility provided by different resources is distinct. Linepack of the hydrogen network is restricted by the pressure level and size of the network, by employing compressor units to adjust pressure, linepack can vary to provide flexibility to the system. The heating system could use the thermal

inertia of buildings to provide demand-side flexibility to the electricity and hydrogen supply system. Electrolysers are modelled to convert electricity to hydrogen when required. The model considers both pump hydro and battery storage, those units can provide flexibility to the electric power system directly, via charging and discharging within their capacities.

Scenario 1 serves as a baseline scenario, representing the energy system with minimal flexibility. In this scenario, the linepack can only vary by 1% compared to its closing value at the end of the day (no allowance on linepack variation results in model infeasibility). Eq. (5.1) is utilised to restrict the variation of linepack. Where $L_{p,t}$ is the volumetric value of linepack, and L_a^0 is the closing linepack (also the linepack at initial timestep before the optimisation).

$$(1+1\%)\mathrm{L}_p^0 \geq L_{p,t} \geq (1-1\%)\mathrm{L}_p^0, \forall p \in P, t \in T \tag{5.1}$$

Eq. (5.2) is employed to restrict the variation of indoor temperature and thereby limiting flexibility provide by the heating system. Where $T_{bd,t}^{\mathrm{in}}$ is the indoor temperature (K).

$$T_{bd,t}^{\mathrm{in}} = 294, \forall bd \in BD, t \in T \tag{5.2}$$

Eq. (5.3) is employed to restrict the operational regulation of the electrolyser, ensuring the production of hydrogen remains consistent across every two consecutive timesteps. Where $Q_{gp,t}^{\mathrm{GP}}$ is the production of hydrogen from the electrolyser.

$$Q_{gp,t}^{\mathrm{GP}} = Q_{gp,t-1}^{\mathrm{GP}}, gp \in EL, t \in T \backslash t_1 \tag{5.3}$$

Eq. (5.4) is used to limit the operational flexibility of the electric storage unit. Where $P_{es,t}^{\mathrm{ES}}$ denotes the amount of electrical energy being either charged into or discharged from the unit.

$$P_{es,t}^{\mathrm{ES}} = P_{es,t-1}^{\mathrm{ES}}, es \in ES, t \in T \backslash t_1 \tag{5.4}$$

Scenario 2-4 were designed to specify the value of flexibility provided by linepack within the hydrogen network. While constraints specified by Eq. (5.2) - Eq. (5.4) remain unchanged, Eq. (5.1) has been updated to Eq. (5.5) – Eq. (5.7), for Scenarios 2, 3, and 4, respectively as shown in Table 5.1.

8**Table 5.1** Updated constraints for scenario 2 - 4

Flexible sources		Related constraints
Linepack	Scenario 2	$(1+7\%)\mathrm{L}_p^0 \geq L_{p,t} \geq (1-7\%)\mathrm{L}_p^0,$ $\forall p \in P, t \in T$ (5.5)
	Scenario 3	$(1+13\%)\mathrm{L}_p^0 \geq L_{p,t} \geq (1-13\%)\mathrm{L}_p^0,$ $\forall p \in P, t \in T$ (5.6)
	Scenario 4	$L_{p,t} \geq 0, \forall p \in P, t \in T$ (5.7)
Heating system		$T_{bd,t}^{\mathrm{in}} = 21, \forall bd \in BD, t \in T$ (5.2)
Electrolysers		$Q_{gp,t}^{\mathrm{GP}} = Q_{gp,t-1}^{\mathrm{GP}}, gp \in GP, t \in T$ (5.3)
Electrical energy storage unit		$P_{es,t}^{\mathrm{ES}} = P_{es,t-1}^{\mathrm{ES}}, es \in ES, t \in T$ (5.4)

To explore the value of the flexibility from the heating systems of the residential buildings, the limit on the indoor temperature range is gradually widened (within a comfortable range) in Scenarios 5 to 7. In this scenario, the constraints specified by Eq. (5.1) – (5.3), and (5.4) remain unchanged, while Equation (5.2) has been updated to Eq. (5.8) – (5.10) for Scenarios 5, 6, and 7, respectively, as detailed in Table 5.2.

9**Table 5.2** Updated constraints for scenario 5-7

Flexible sources		Related constraints
Linepack		$(1+1\%)\mathrm{L}_p^0 \geq L_{p,t} \geq (1-1\%)\mathrm{L}_p^0,$ $\forall p \in P, t \in T$ (5.1)
Heating system	Scenario 5	$295 \geq T_{bd,t}^{\mathrm{in}} \geq 293, \forall bd \in BD, t \in T$ (5.8)
	Scenario 6	$296 \geq T_{bd,t}^{\mathrm{in}} \geq 292, \forall bd \in BD, t \in T$ (5.9)
	Scenario 7	$297 \geq T_{bd,t}^{\mathrm{in}} \geq 291, \forall bd \in BD, t \in T$ (5.10)
Electrolysers		$Q_{gp,t}^{\mathrm{GP}} = Q_{gp,t-1}^{\mathrm{GP}},\ gp \in GP, t \in T$ (5.3)
Electrical energy storage unit		$P_{es,t}^{\mathrm{ES}} = P_{es,t-1}^{\mathrm{ES}}, es \in ES, t \in T$ (5.4)

Scenario 8 was designed to specify the value of flexibility provided by the networked electrolysers. The updated constraints denoted by Eq. (5.1), Eq. (5.2) and Eq. (5.4) remain the same, while the constraint denoted by Eq. (5.3) is removed. The updated constraints are outlined in Table 5.3.

10**Table 5.3** Updated constraints for scenario 8

Flexible sources	Related constraints
Linepack	$(1+1\%)\mathrm{L}_p^0 \geq L_{p,t} \geq (1-1\%)\mathrm{L}_p^0,$ $\forall p \in P, t \in T$ (5.1)
Heating system	$T_{bd,t}^{\mathrm{in}} = 294, \forall bd \in BD, t \in T$ (5.2)
Electrolysers	Remove the constraint (5.3).
Electrical energy storage unit	$P_{es,t}^{\mathrm{ES}} = P_{es,t-1}^{\mathrm{ES}}, es \in ES, t \in T$ (5.4)

Scenario 9 was designed to specify the value of flexibility provided by the electrical energy storage units. The updated constraints denoted by Eq. (5.1) - Eq. (5.3) remain the same, while the constraint denoted by Eq. (5.4) is removed. The updated constraints are outlined in Table 5.4.

11**Table 5.4** Updated constraints for scenario 9

Flexible sources	Related constraints
Linepack	$(1+1\%)\mathrm{L}_p^0 \geq L_{p,t} \geq (1-1\%)\mathrm{L}_p^0,$ $\forall p \in P, t \in T$ (5.1)
Heating system	$T_{bd,t}^{\mathrm{in}} = 294, \forall bd \in BD, t \in T$ (5.2)
Electrolysers	$Q_{gp,t}^{\mathrm{GP}} = Q_{gp,t-1}^{\mathrm{GP}}, gp \in GP, t \in T$ (5.3)
Electrical energy storage unit	Remove the constraint (5.4).

Scenario 10 was designed to specify the value of flexibility provided by all flexible sources. The updated constraints are outlined in Table 5.5. In this scenario, the flexibility of linepack, residential heating systems, electrolysers, and electrical energy storage units is fully unlocked.

12**Table 5.5** Updated constraints for scenario 10

Flexible sources	Related constraints
Linepack	$L_{p,t} \geq 0, \forall p \in P, t \in T$ (5.7)
Heating system	$297 \geq T_{bd,t}^{\text{in}} \geq 291, \forall bd \in BD, t \in T$ (5.10)
Electrolysers	Remove the constraint (5.3).
Electrical energy storage unit	Remove the constraint (5.4).

For each optimisation except for scenario 10, only one type of flexible unit is allowed. For example, in scenarios 2 - 4 only linepack can vary within a specific relative range in each scenario, while the operation of all the other sources of flexibility is set to be fixed over all time steps. Additionally, all other inputs and assumptions such as, hydrogen cost, ambient temperature, and wind and PV generation, are the same across all optimisations.

In all scenarios, the input parameters for the model remain fixed, (e.g., such as energy demands excluding heating, availability of wind and PV generation, etc). The decision variables, such as hydrogen supply from electrolysers and linepack volume, are determined through optimal system operation.

5.4 Case study

Great Britain (GB) in the year 2050 was used as a case study to investigate the value of flexibility provided by different flexible sources and the optimal mix of flexibility in an integrated electricity, hydrogen and heat system.

Table 5.6 shows the capacities of technologies, interconnectors and storage units in 2050. These assumptions are based on the 'System Transformation Scenario' proposed by National Grid's Future Energy Scenarios (FES) [105]. In the System Transformation Scenario, it is assumed that hydrogen will have widespread uses across different sectors including industry, heating and transport. Wind and solar generation are projected to contribute approximately 68% of the total annual electricity generation in 2050. The future capacity of heating technologies comes from the literature [106].

Note that the simplified GB electricity network established in this work has 30 Busbars, based on the Electricity Ten Year Statement (ETYS) [107] map. It is assumed that the hydrogen network has a similar structure as the current gas network (see Figure 4.2 in Chapter 4, section 4.3.1), but uses electric-driven compressors only. The detailed network map of both the electric power grid and hydrogen network can be found in Figure 5.3 and 5.4.

13**Table 5.6** Capacity of technologies in 2050

Sectors	**Technologies**	**Installed capacity (GW)**
Hydrogen production	Blue hydrogen production (Methane reformation with CCUS)	26
	Green hydrogen (via networked electrolysers)	38
	Green hydrogen (via non-networked electrolysers)	15
Electricity generation	Hydrogen-fired power plant	22
	Onshore wind	34
	Offshore wind	97
	PV	57
	Nuclear	13
	Bioenergy	11
	Other renewable (made up of waste, hydro, marine)	13
	Interconnector	16
Heating supply	Air Source Heat Pump (ASHP)	34
	Hydrogen boiler	67

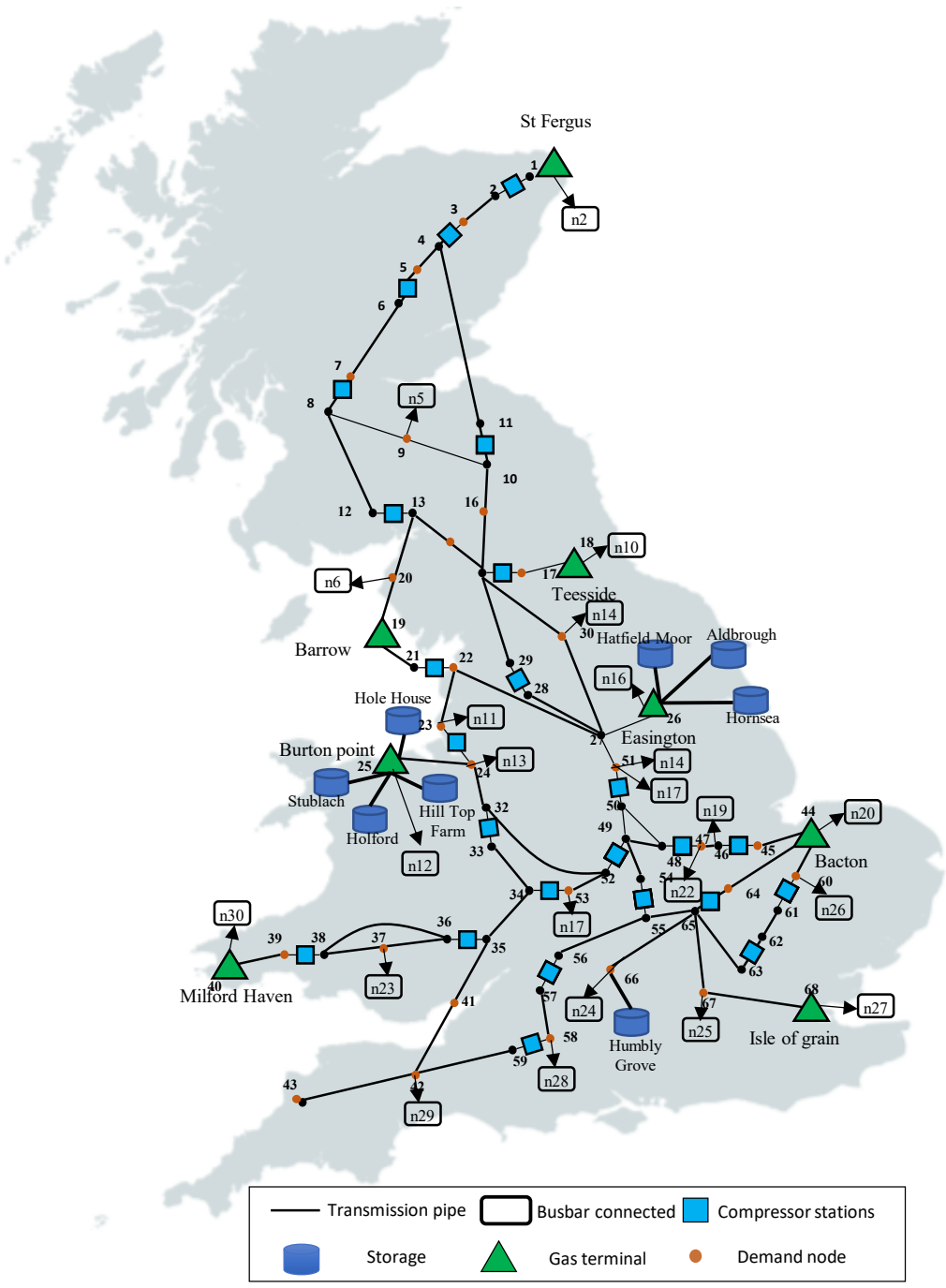

33Figure 5.2 A simplified hydrogen transmission system

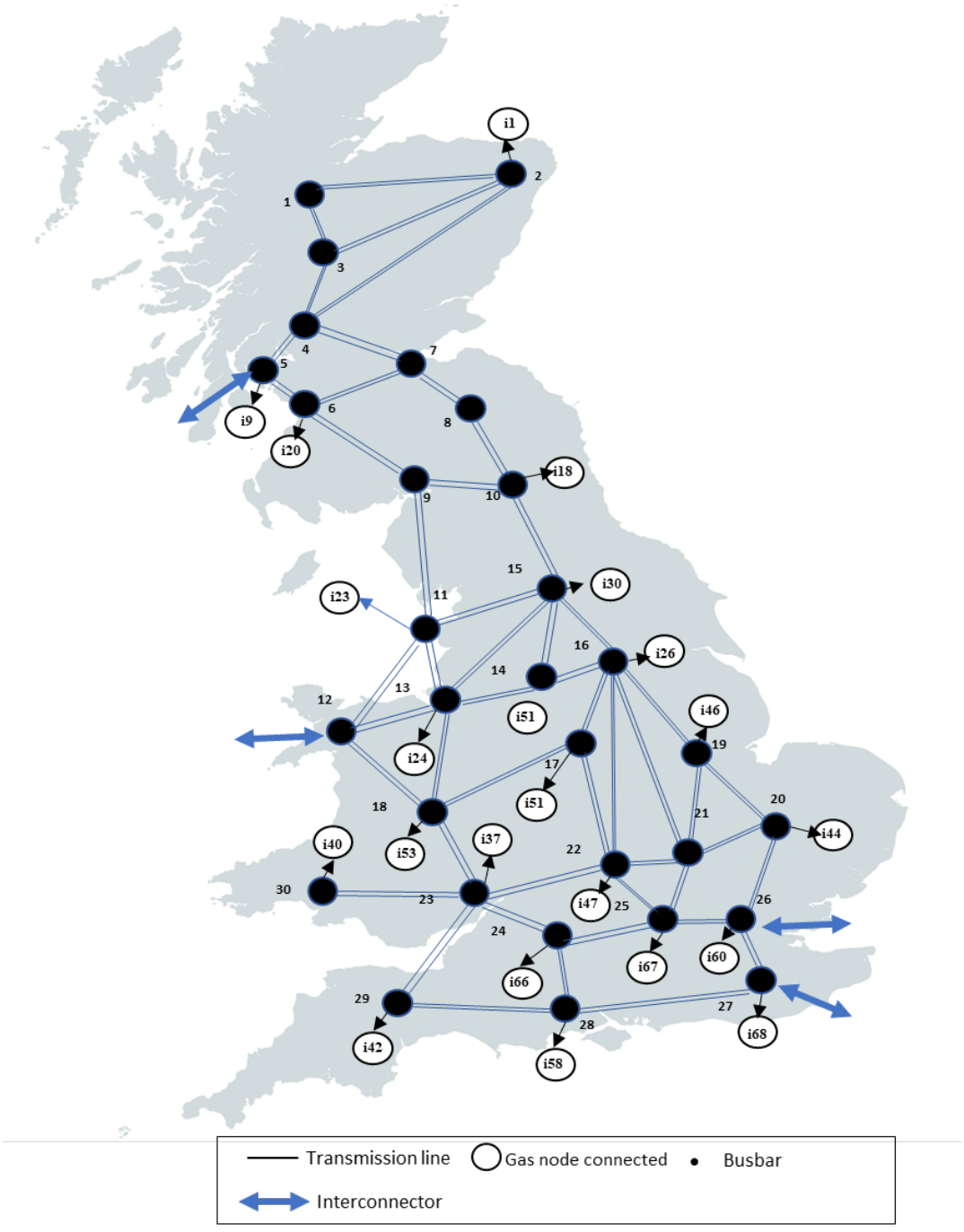

34Figure 5.3 A simplified electricity transmission system

The electricity generation from renewable sources and non-flexible energy demands (base demand) are shown in Figure 5.4. These profiles are predefined as input data to the model.

To derive the time-series demand profile of hydrogen, several assumptions are used due to the lack of actual data. Initially, the daily baseline demand of hydrogen (excluding hydrogen demand for heating) is calculated by averaging the projected annual hydrogen demand for 2050 for each day (data sourced from [105]). Subsequently, the profile of current gas demand is employed as a proxy for the trend in hydrogen demand. The same approach is also used for generating profile of the based demand of future electricity demand.

The current wind and PV generation profiles at each busbar are acquired from Renewables. ninja, an online tool offering hourly Variable Renewable Energy (VRE) generation and weather data (accessible at: https://www.renewables.ninja/). To update the profiles of the future wind/PV generation, a ratio reflecting the variance between the installed wind/PV capacity in 2050 and the present capacity is taken into account.

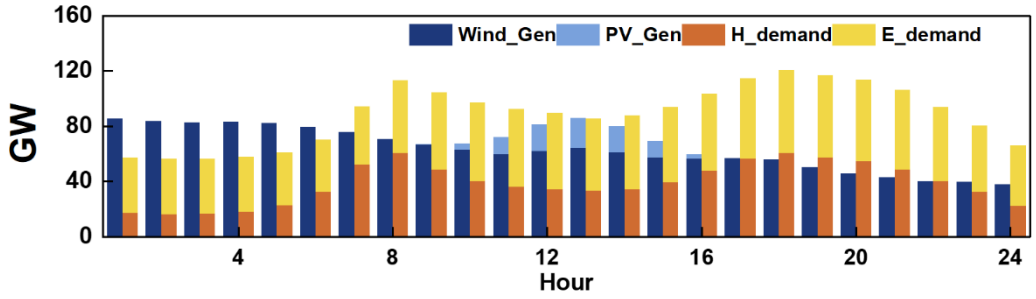

35**Figure 5.4** predefined renewable generation and base energy demand (H_demand is base hydrogen demand and E_demand is base electricity demand).

Additionally, some parameters associated with operating the energy system considered in the model (such as operational cost, ramping rate of turbines, etc) are outlined in the Table 5.7 and Table 5.8. Note that, the networked green hydrogen (hydrogen produced by networked electrolysers) is assumed zero since the networked electrolysers serve as the flexibility provider, and their operation are determined by the optimal operation of system. There might be additional cost related to water consumption and materials usage, but they are beyond the scope of this study. Additionally, the fuel cost of hydrogen-fired generation is zero as it will be calculated when the hydrogen is produced, so it is not double counted. The cost of load shedding is assumed to be very high, so it will be minimised in the optimisation, except in extreme cases where it is necessary to match supply.

Table 5.7 Details of the costs associated with operating the energy system

Cost (£/MWh)	SMR hydrogen	Non-networked green hydrogen	Networked green hydrogen	Hydrogen-fired generation
	62	124	0	0
	Others	Electricity import	Renewable curtailment	Load shedding
	0	500	40	50000
	Nuclear	Bioenergy	start-up cost of hydrogen turbine	
	44	10	418-92021	

Table 5.8 Operational rate of hydrogen turbine

Operational rate of hydrogen turbine (MW/h)	Spinning-up rate	Spinning-down rate	Start-up rate	Shut-down rate
	500	500	500	500
Time (h)	Min-up time	Min-down time	Min-up time at t1	Min-down time at t1
	4	4	4	0

5.4 Results and discussion

5.4.1 Value of flexibility from different sources within the integrated energy system

Without sufficient operational flexibility, the energy system struggles to balance supply and demand economically. For instance, to satisfy the nodal balance (see Eq. 2.8 and Eq. 2.41 in Chapter 2) for both the hydrogen and electricity networks, various interventions may be necessary. These could include curtailing large volumes of renewable energy, reducing energy demand through load-shedding, or utilising energy from costly sources such as importing electricity from other countries.

To identify the value of flexibility comes from different sources, the least-cost optimisation is carried out for all scenarios defined in section 5.3.2.

5.4.1.1 Value of flexibility from linepack

As a within-pipe storage, linepack can provide flexibility through swing up and down to match hydrogen supply and demand. Without sufficient flexibility from linepack, meaning limited variation in linepack, the hydrogen system's ability to balance supply and demand is significantly compromised. This could consequently impact the operation of the electric power system. This section explores the value of flexibility provided by linepack in enhancing the whole

system's operation by optimising the integrated energy system across Scenarios 1 to 4.

The linepack variations in different scenarios are shown in Figure 5.5, as well as their impacts on the total amount of hydrogen-fired generation, renewable curtailment, hydrogen load-shedding and electricity import over a day. It can be found that, by gradually relaxing the limits for variation of linepack in the hydrogen network, the occurrence of hydrogen load shedding is significantly reduced.

This is attributed to the enhanced capacity for within-pipe hydrogen storage within the hydrogen network, which serves to mitigate imbalances between hydrogen supply and demand. The linepack acts as a buffer to balance the supply and the base hydrogen demand, i.e. Figure 5.5 (a) indicating that linepack increases when the base hydrogen demand is low (e.g., from hour 1 to hour 6 as shown in Figure 5.4) as the excess hydrogen supply causes accumulation of hydrogen in the pipes, and linepack decreases when the base hydrogen demand reaches its peak (e.g., at hour 8).

Consequently, hydrogen can be utilised more flexibly during the time it is needed the most, such as when increasing hydrogen-fired generation can decrease the need for more expensive electricity import, as shown in Figure 5.5 (b).

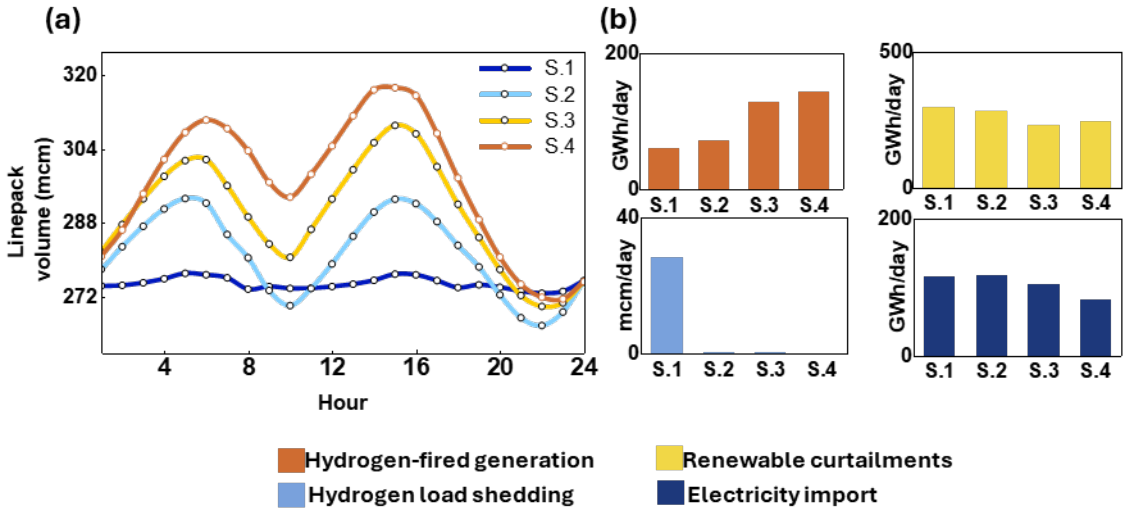

36**Figure 5.5** Variations of linepack under different limits and their impacts

5.4.1.2 Flexibility from the heating system

The residential heating system can offer significant flexibility by operating heat pumps and hydrogen boilers adaptively, using the building fabric as a buffer. The energy consumption of these heating devices is influenced by both the indoor and ambient temperatures. Therefore, restricting the range of allowable indoor temperatures can reduce the heating system's ability to provide flexibility to the whole energy system, potentially leading to negative impacts such as load shedding. This section investigates the optimal operation of the whole system under different indoor temperature limitations (scenarios 5 - 7) to explore the value of flexibly operating heat pumps and hydrogen boilers.

Figure 5.6 demonstrates the benefits of flexibility from the residential heat sector. As Figure 5.6(a) shows, when indoor temperatures are allowed to vary within a range, representing the comfort temperature, electricity and hydrogen consumptions by heat pumps and hydrogen boilers can be adjusted to avoid energy usage during peak periods.

The flexible operation of heat pumps is mainly influenced by the gap between renewable generation and the base electricity demand, while that of hydrogen boilers is primarily affected by the profile of base hydrogen demand. By operating them flexibly, the occurrence of hydrogen load shedding and electricity import is greatly reduced, with a slight decrease in renewable curtailment, as illustrated by Figure 5.6(b).

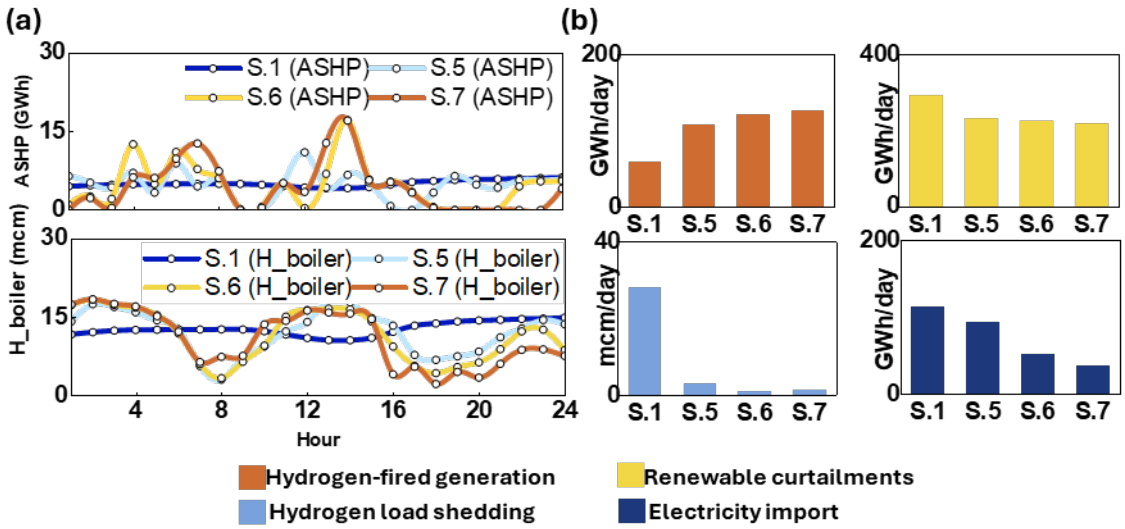

37**Figure 5.6** Variations of the energy consumption of heat pumps and hydrogen boilers and their impacts

5.4.1.3 Flexibility from electrolysers and electric energy storage units

Unlike linepack and the heating system, electrolysers and electric energy storage units (such as battery storage and pump storage) within the electric power system can provide flexibility directly to the energy system. This is because their operation is not constrained by external factors—for instance, linepack flexibility is limited by within-pipe pressure, and heating system flexibility is determined by the temperature range.

The flexible operation of electrolysers can utilise surplus electrical energy to produce hydrogen, while the flexible charging and discharging of storage units can help balance electricity supply and demand. The impact of the flexible operation of these units on the optimal operation of the whole system is analysed in this section.

Figure 5.7 demonstrates that by harnessing the flexibility of electrolysers, there is a substantial reduction in the renewable energy curtailment and costly hydrogen-fired generation, since the flexible electrolysers are more capable of leveraging the renewable generation, compared to the case that those units are only allowed to working consistently. Additionally, the hydrogen load shedding is high when the flexibility of electrolysers is minimised, since the restricted variation hampers electrolysers' ability to provide a steady hydrogen supply. However, with adjustable electrolysers, more hydrogen could be offered by them and thereby reducing hydrogen load shedding.

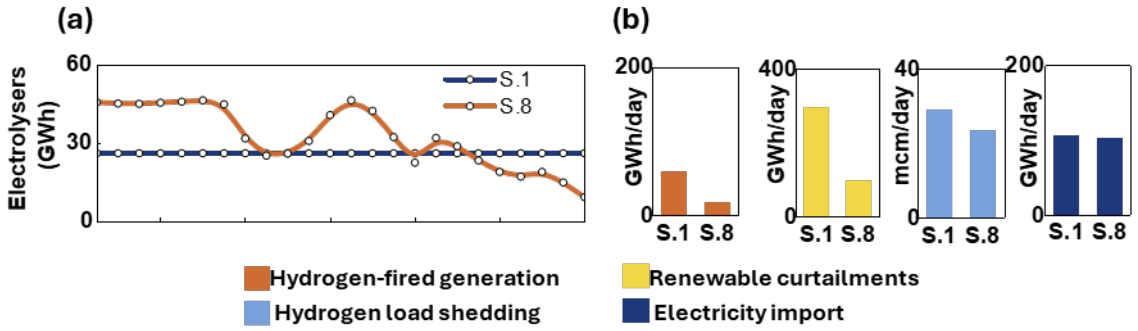

38**Figure 5.7** Operation of electrolysers with and without flexibility

Figure 5.8 outlines the impact of flexible operation of electric energy storage units on the optimal operation of the whole system. As depicted in Figure 5.8, when energy storage units are allowed to operate flexibly, they cause reductions in both renewable curtailment and hydrogen load shedding. Yet, to minimise hydrogen load shedding, there is a slight uptick in electricity imports and hydrogen-fired generation. This is because the electric-side storage units can swiftly adjust their operations, facilitating a more dynamic interaction with the grid or alternative power sources for hydrogen production or consumption, thus imparting flexibility to the hydrogen network.

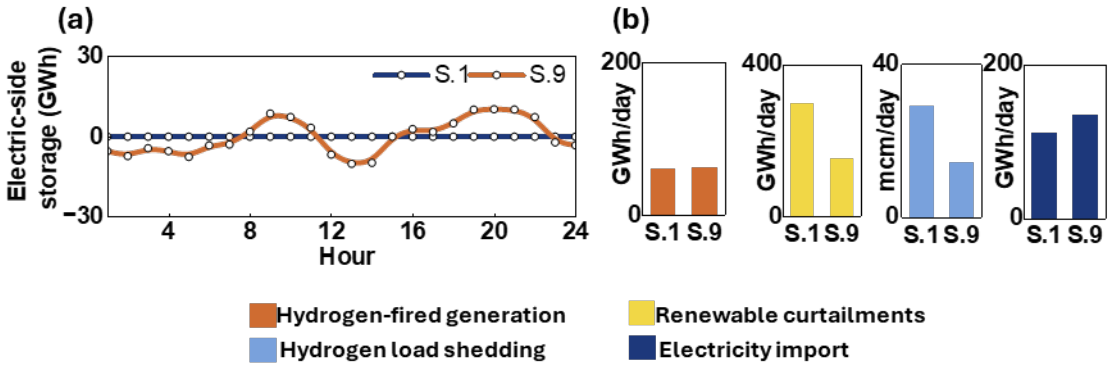

39**Figure 5.8** Operation of electric-storage units with and without flexibility

5.4.2 Impacts of unlocking flexibility on the operation of the integrated energy system

The operation of the integrated energy system with and without flexibility was investigated and compared, as shown in Figure 5.9. Figure 5.9(a) highlights the operational range of flexibility sources in both scenario 1 (with minimal available flexibility) and scenario 10 (where all flexibility sources are accessible). Electrolysers appear to offer greater system flexibility than electric-side storage units and heat pumps, attributed to their higher capacity. Furthermore, hydrogen boiler energy consumption can vary between 10 GWh and 60 GWh while the linepack volume can range from 825 GWh to 880 GWh, suggesting they have the potential to offer ample system flexibility.

Figure 5.9(b) reveals that upon activating the flexibility of these flexibility resources, the integrated energy system becomes capable of accommodating significantly higher levels of renewable energy generation. This results in a reduction of approximately 70% in renewable curtailment, thereby reducing the need for electricity from interconnectors and hydrogen-fired power plants. Additionally, the requirement for hydrogen load shedding is also significantly reduced.

The breakdown of the operating costs for both hydrogen and electricity are presented in Figure 5.9(c). It is evident that in the absence of a sufficient level of flexibility, the overall cost is substantially higher. This is primarily attributed to the expensive nature of hydrogen load shedding and electricity import.

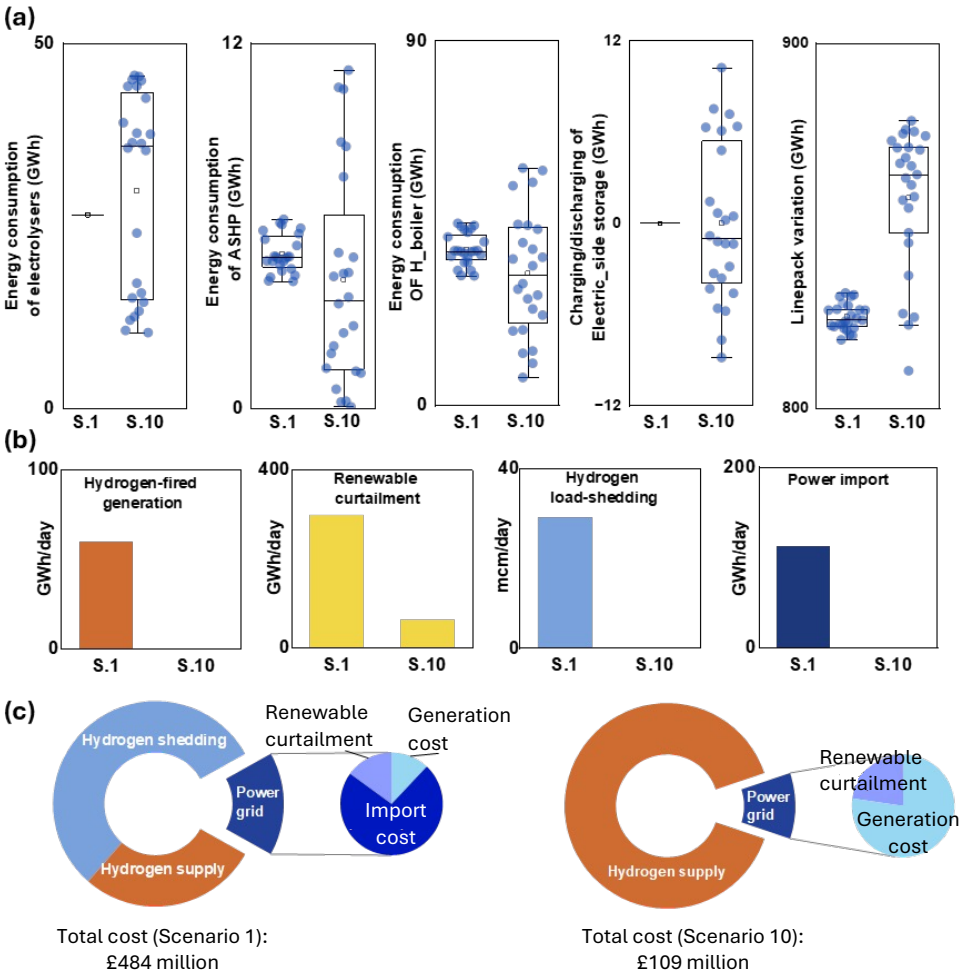

40**Figure 5.9** (a) variations of different flexibility resources with/without flexibility. (b), the impact of unlocking the flexibility of each type of unit on the operation of hydrogen-fired power plants, renewables curtailment, hydrogen load shedding and electricity import. (c), the operational cost of the energy systems integration with/without flexibility

5.5 Conclusions

As the penetration of variable renewable generation continues to increase while the capacity of unabated fossil-fuelled power stations is required to be reduced, the need for alternative sources of flexibility to support the operation of the electric power system becomes increasingly crucial.

In this chapter, flexibility available through energy systems integration was quantified, and the value of flexibility in supporting cost-effective operation of integrated energy systems was investigated. It can be found that, leveraging flexibility from different flexible sources could help reduce renewable curtailments and load shedding. Additionally, it helps in reducing dependence on costly electricity generation from hydrogen-fired power plants and electricity imports. As a consequence, the operational cost is significantly decreased after unlocking flexibility from the integrated system, from 484 million £ to 109 million £ over 24 hours.

Notably, while this chapter focuses on illustrating the value of flexibility from a whole-system perspective, achieving flexibility requires coordination across various locations. To maximise the economic benefits for the entire system, the operation of local energy systems may be affected, potentially leading to social challenges such as energy inequity. Future work will address these factors by integrating them into the IES model.

Chapter 6 Impacts of flexibility on the locational marginal prices in the electricity system

6.1 Introduction

In Chapter 5, the benefits of harnessing flexibility from various sources were explored, emphasizing how their ability to adjust output within operational boundaries enhances the system's overall efficiency. Nonetheless, it is crucial to quantify the extent to which these operations can vary within those limits—essentially, determining the magnitude of available flexibility. This illustrates how well the system can adapt to unforeseen fluctuations in energy demands and supplies.

Additionally, understanding the level of flexibility within the electric power system can inform policymakers and investors about where to allocate resources and investments. It can guide the development of infrastructure projects, such as energy storage systems, demand response programs, and flexible generation sources, to enhance its flexibility.

Some investigations have focused on accessing flexibility from single sources, e.g., buildings [108–110] and electrolysers [111], etc. Nonetheless, it is complicated to quantify the flexibility of integrated energy systems since diverse

flexibilities provided by different units have unique characteristics and constraints. To date, there is a lack of comprehensive investigation on quantifying the magnitude of flexibility from integrated energy systems.

In this chapter, a method was proposed to quantify the operational margin of the integrated energy system by focusing on maximising flexibility rather than minimising costs. This approach determines the maximum flexibility achievable at each time step, considering the operational constraints of technologies and interdependent energy vectors.

Locational Marginal Price (LMP), a key indicator of the value of electricity across different locations, was analysed to highlight the benefits of flexibility. As LMP reflects the cost impact of increased electricity demand and the electric power system’s upward flexibility showcase its capacity to maximise the supply minus demand, it is reasonable to expect a relationship between LMP and upward flexibility. To further clarify their relationship, a correlation analysis was conducted in this chapter.

6.2 Approach to quantifying electric power system’s flexibility

The quantification of the electric system's flexibility was conducted as a post-analysis, as shown in Figure 6.1. The results from the least-cost optimisation

were used as the input portfolio for this flexibility assessment as shown in Figure 6.1 (a). In this phase, the primary focus shifts from minimising operational costs to maximising the system's potential flexibility.

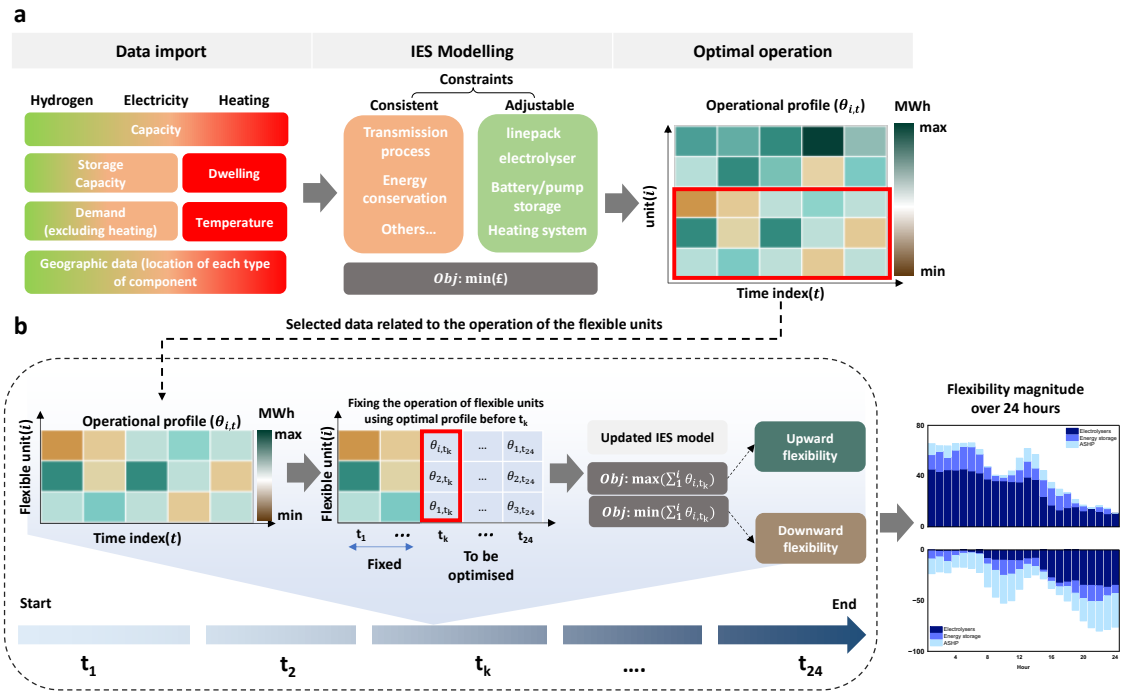

41**Figure 6.1** (a) Modelling framework of the IES. (b) approach for quantifying flexibility of the system.

In order to calculate the maximum level of flexibility for a specific hour, certain variables (include renewable curtailments, electricity import, hydrogen-fired generation and load shedding for both hydrogen and electricity) must be fixed for all time steps, since those variables are changeable and could affect quantifying the system flexibility if they are not fixed.

Some other variables associate with the basic operational constraints of the system such as pressure value of the hydrogen transmission system, pipe flow, electricity flow cannot be fixed, since they have to be adjustable to help different units providing flexibility. Additionally, the operation of each flexibility resource needs to be fixed for all time steps before the hour being optimised. This ensures that the optimisation process focuses solely on determining the flexibility provision of the flexibility resources during the target hour while keeping other variables and resource operations constant throughout the previous time steps.

The original power balance equation Eq. (2.41) was formulated to Eq. (6.1), by introducing a set of auxiliary variables $ax_{b,t}$. This enables flexible units to provide flexibility. Then we update the objective of IES model to maximise the upward or downward flexibility starting from the first timestep and continuing to the last. The Figure 6.1 (b) provides an example on how flexibility is quantified at timestep *k*. To quantify upward flexibility at t_k, it is require to fix the energy consumption $\theta_{b,t}$ of all flexible units before t_k, then maximise $\sum_{b\in B}\ \theta'_{b,t_k}$ and the upward flexibility can be calculated by $\sum_{b\in B}\ (\theta'_{b,t_k} - \theta_{b,t_k})$. The downward flexibility can be quantified using the same approach but minimise the $\sum_{b\in B}\ \theta'_{b,t_k}$.

$$P_{b,t}^{\mathrm{sup}} - P_{b,t}^{\mathrm{dem}} + \sum_{l\in l^{\mathrm{up}}} P_{l,t} - \sum_{l\in l^{\mathrm{down}}} P_{l,t} = ax_{b,t}, \forall b \in B, \forall t \in T \quad (6.1)$$

6.3 Locational Marginal Prices calculation

Locational marginal price (LMP), also known as nodal pricing, serves as a crucial method for setting electricity prices within managed wholesale markets [112]. It reflects the real-time cost of meeting additional demand at each location, factoring in forecasted system conditions and outcomes from the most recent, approved real-time security-constrained economic dispatch. LMP accounts for various constraints, including transmission limitations and reliability requirements, ensuring that the price of electricity accurately represents the cost of generating and delivering power to that specific point in the network [113].

LMP consists of three distinct components, as defined in Eq. (6.2). CE represents the energy component and accounts for the cost associated with energy consumption. CL signifies the loss component, capturing the cost attributed to energy losses occurring along the transmission lines. CG represents the congestion cost.

$$LMP = CE + CL + CG \tag{6.2}$$

The calculation of LMP is carried out as a post analysis, based on the results derived from the least-cost optimisation. To capture the value of LMP at each Busbar, it is required to get the dual value of the energy balance constraints. A simple example is given below to present the way to calculate the LMP of each

Busbar. Eq. (6.3) is the Lagrangian formulation of the of original problem, where $P_b^{\mathrm{sup}} - P_b^{\mathrm{dem}} + \sum_{l \in L^{\mathrm{up}}} P_{l,t} - \sum_{l \in L^{\mathrm{down}}} P_{l,t}$ is the nodal balance, $f(x_b)$ denotes other constraints at b. Then the LMP value λ_b can be calculated by Eq. (6.4).

$$L = C + \lambda_b \left(P_b^{\mathrm{sup}} - P_b^{\mathrm{dem}} + \sum_{l \in L^{\mathrm{up}}} P_{l,t} - \sum_{l \in L^{\mathrm{down}}} P_{l,t} \right) + \mu f(x_b) \quad (6.3)$$

$$\lambda_b = \frac{\partial L}{\partial P_b^{\mathrm{dem}}} \quad (6.4)$$

6.3 Case study

The results derived from the least-cost optimisation for scenario 10 (see Chapter 5) were used as input data in this case study, to quantify the magnitude of available flexibility of the electric power system. In this case, networked electrolysers, heat pumps and electric-side energy storage units, which can directly provide flexibility to the electric power system, were severed as flexibility providers. The optimisation aims to maximise the total flexibility offered by them to the electric power system, subjected to distinct operational constraints.

The locational distribution of flexibility at each Busbar derived from the output containing the magnitude of flexibility of the entire system was visualised spatiotemporally. Five regions were defined including Middle region, North region, Scottland region, Southeast region, Southwest and Wales region. Additionally, to

capture the intrinsic value of electric energy at diverse geographical locations, LMP analysis was carried out for the electric power system with sufficient flexibility (scenario 10) and without such (scenario 1), based on primal-dual optimisation approach.

Moreover, since LMP is a notable indicator reflecting the influence of the increase in electricity demand on the overall cost of the system, and the electric power system's upward flexibility showcases its capacity to maximise the supply minus demand, it is reasonable to expect a relationship between LMP and upward flexibility. In this chapter, a correlation analysis was carried to examine the interplay between LMP and flexibility each Busbar over all timesteps.

6.4 Results and discussions

6.4.1 Quantification of the electric power system flexibility

The flexibility for the entire system under scenario 10 was quantified and the results was visualised spatiotemporally in each region as Figure 6.2 shows. The distribution of locational flexibility reveals that each Busbar is distinct in terms of type and magnitude of flexibility. For instance, certain Busbars like London and those in the Midlands tend to offer downward flexibility (downward flexibility refers to the system's capacity to reduce energy supply while increase energy demand) due to relatively higher demand in those areas. On the other hand, Busbars in Scotland, characterised by higher renewables generation, find it easier to provide

upward flexibility (upward flexibility refers to the system's capacity to augment energy supply or reduce energy demand), mainly by decreasing the workload of the electrolysers.

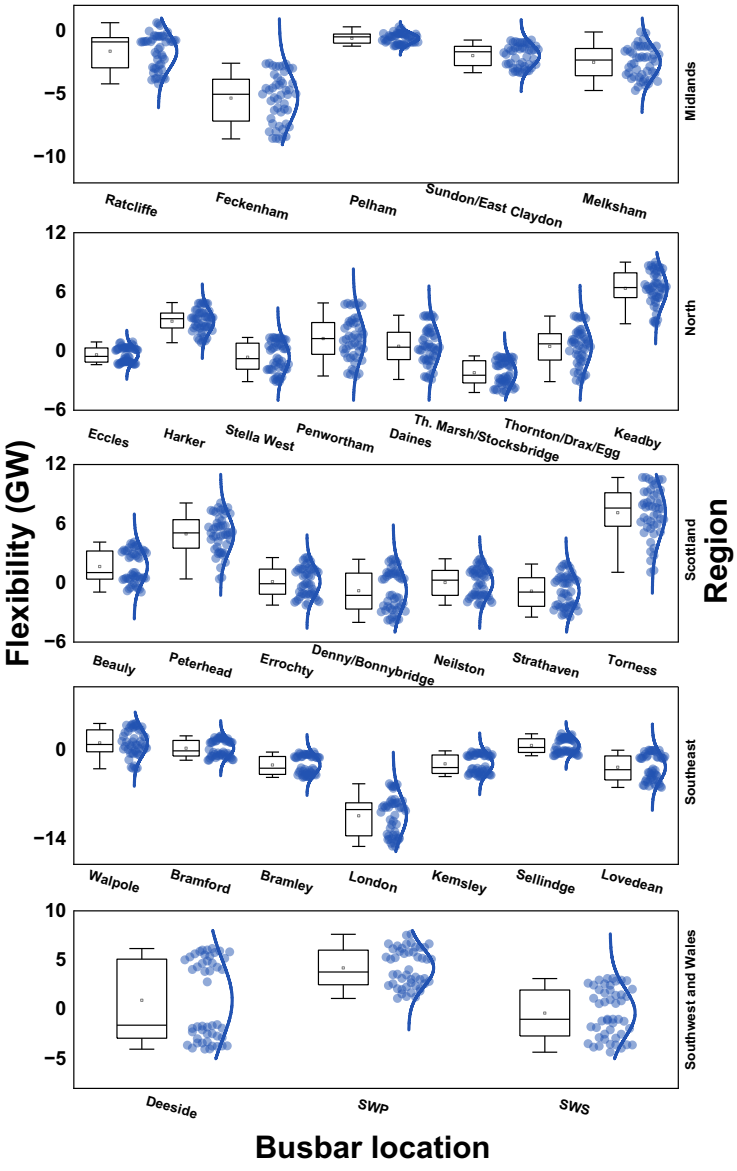

42**Figure.6.2** Flexibility offered by each Busbar in different regions

The upward Figure 6.3 (a) is the profile of the optimal operation of each flexibility resource in scenario 10 while 6.3 (b) and 6.3 (c) show the share of flexibility from each flexible unit in the mix. Figure 6.3 (b) reveals that electrolysers play a predominant role in offering upward flexibility since hydrogen storage in the linepack can be used to meet the hydrogen demand. In contrast, heat pumps only provide limited upward flexibility (i.e. reducing their electricity consumption), since their energy consumption was optimised to reach the minimum operational cost of the system.

However, the manner in which each flexibility resource provides downward flexibility differs from their provision of upward flexibility, as depicted in Figure 6.3 (c). During the initial hours, it is challenging for all flexibility resources to offer downward flexibility. This can be attributed to the higher renewable generation and lower electricity demand during this period (as illustrated in Figure 5.4, see Chapter 5) which caused the electrolysers and ASHP to already maximise their consumption in the day ahead schedule (i.e. Scenario 10). The total downward flexibility gradually increases from hour 1 to hour 11, as renewable generation decreases, and electricity demand rises. However, at hour 12, the total downward flexibility experiences a slight decrease due to the peak in renewable generation, particularly from solar sources. Subsequently, from hour 13 onwards, the downward flexibility mix provided by all flexibility resources begins to rise again, as their operation in the optimal profile remains far below their upper operational limit. This figure specifically shows flexibility directly offered to the electricity

system through adjusting electricity demand and supply, therefore, other flexibility resources such as linepack and hydrogen boilers are not included in the quantification analysis of system flexibility magnitude.

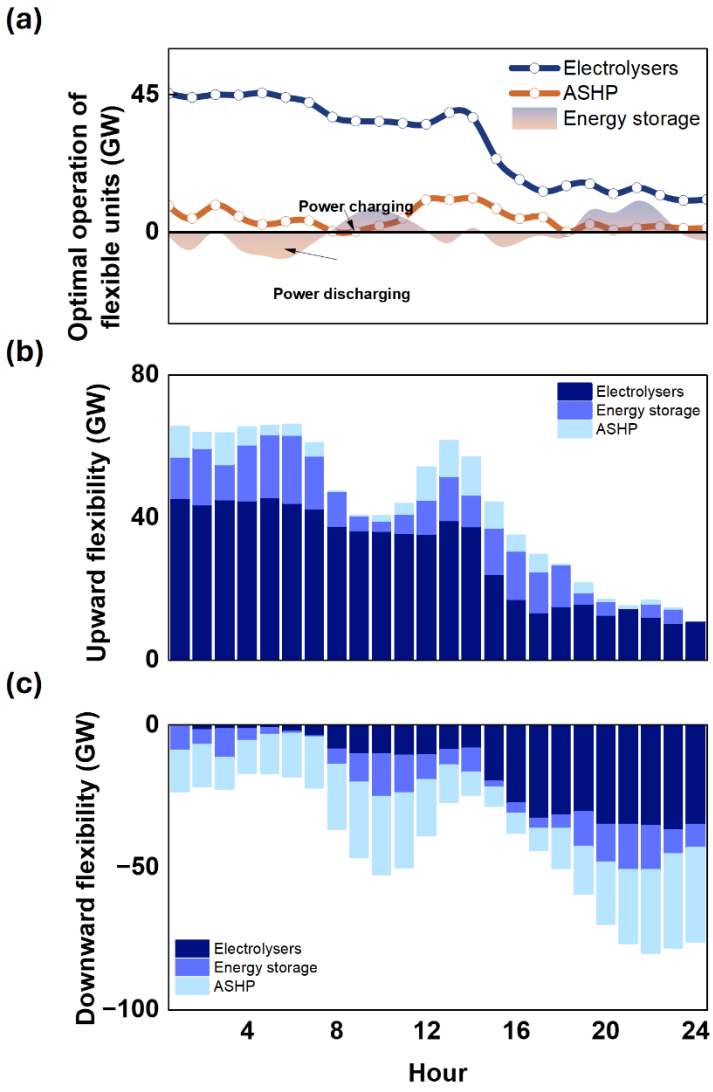

43**Figure 6.3** (a), the optimal operation of electrolysers, ASHP and power storages; (b), the upward flexibility mix of the system; (c), downward flexibility mix of the system

6.4.2 LMP of the system with and without sufficient flexibility

The LMP value of the electric power system in scenario 1 was captured. The result for each Busbar over 24 hours was visualised as Figure 6.4 (a). Additionally, the results for renewable curtailment, electricity import, and hydrogen load shedding were presented as shown in Figure 6.4 (b), to demonstrate the economic value of flexibility for the electric power system.

It is evident that the LMP value for the inflexible system peaks significantly during hours 19-22, as shown in Figure 6.4 (a). This surge can largely be attributed to hydrogen load shedding and electricity imports as Figure 6.4 (b) shows. Conversely, during hours 1-8 and 10-16, the LMP value dips into the negatives, due to a consequence of substantial renewable curtailment.

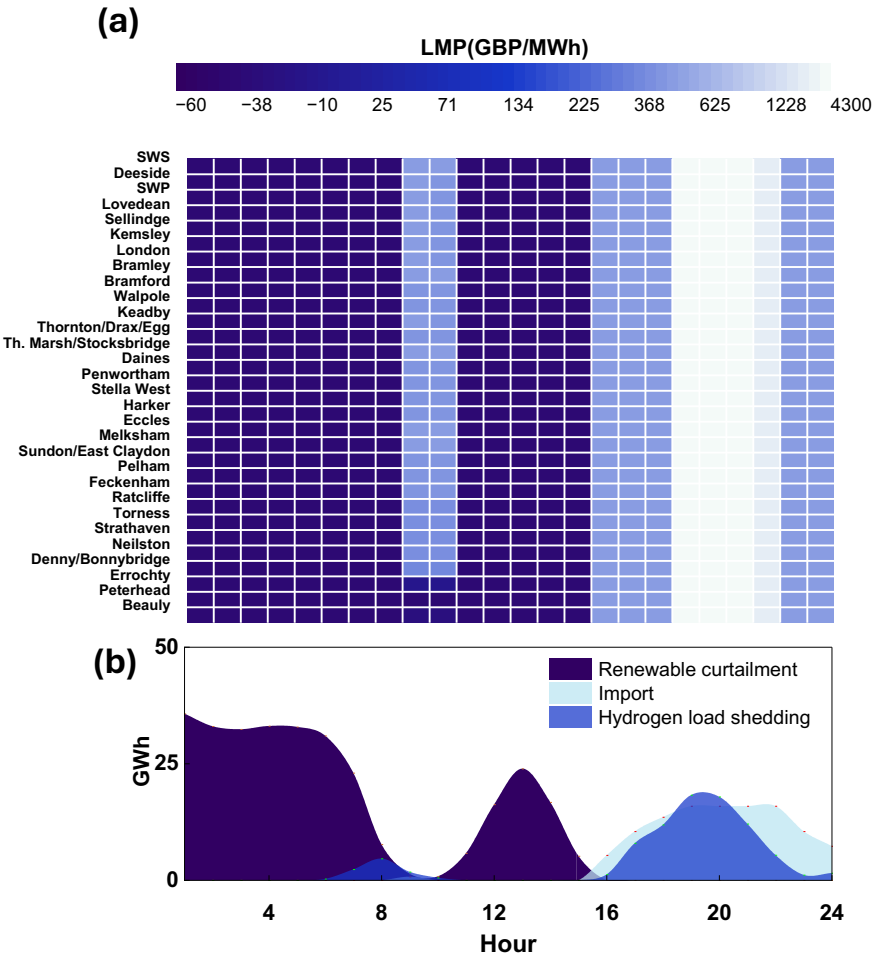

44**Figure 6.4** (a), LMP of the non-flexible electric power system in scenario 1. (b), renewable curtailment, electricity import and hydrogen load shedding over 24 hours in scenario 1.

In comparison, Figure 6.5 shows such results for the electric power system in scenario 10. The system with ample flexibility exhibits a much-reduced LMP during hours 19-22. Moreover, due to the diminished renewable curtailment, only a handful of Busbars have negative LMP values at specific intervals.

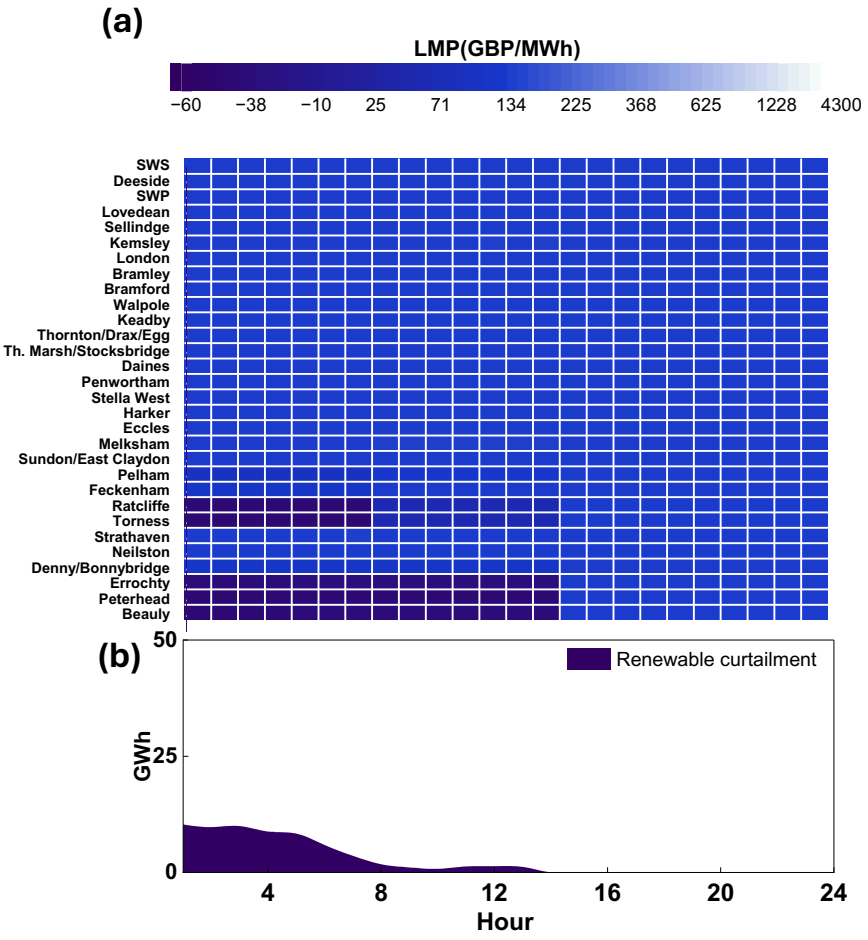

45**Figure 6.5** (a), LMP of the non-flexible electric power system in scenario 10. (b), renewable curtailment, electricity import and hydrogen load shedding over 24 hours in scenario 10.

6.4.3 Correlations between Locational Marginal Price and magnitude of available flexibility

Given that the LMP is a notable indicator reflecting the influence of the increase in electricity demand on the overall cost of the system, and the electric

power system's upward flexibility showcases its capacity to maximise the supply minus demand, it is reasonable to expect a relationship between LMP and upward flexibility. To examine the interplay between these two factors, 30 profiles were used showing correlations between them at each Busbar over all timesteps in Figure 6.6.

By fitting linear curves, the correlations between Locational Marginal Price (LMP) and upward flexibility were visualised illustrated. The result of analysis demonstrates a prevailing negative correlation across the majority of the plots, signifying that an increase in the system's capability to provide upward flexibility corresponds to a decrease in LMP.

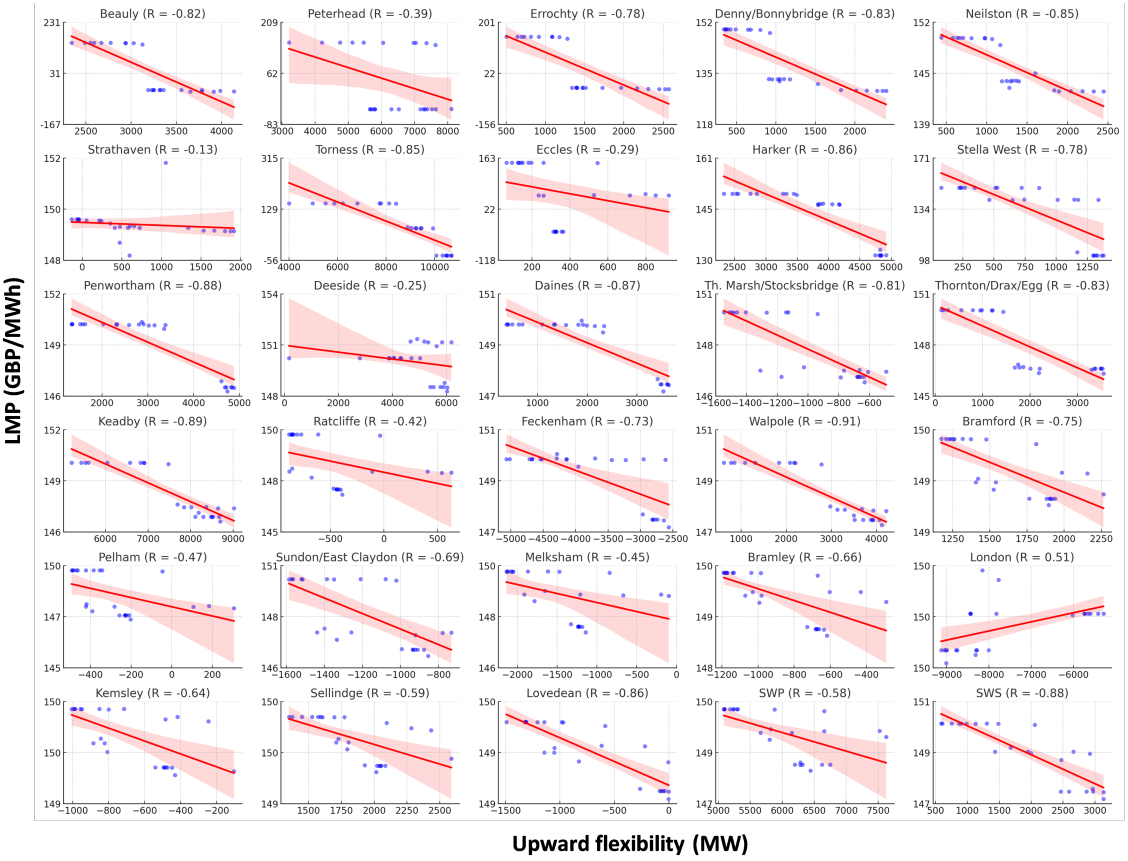

46**Figure 6.6** Matrix of correlations between LMP and upward flexibility at each Busbar

6.4 Conclusions

A comprehensive approach to quantify magnitude of the available flexibility is provided in this Chapter, using the output from least-cost optimisation as an input. To identify the potential economic benefits of the system flexibility, locational marginal price of the electric power system was calculated, using primal and dual optimisation.

The quantified flexibility of the entire power grid was visualised spatiotemporally, which illustrated the ability of each Busbar to provide both upward and downward flexibility. It is demonstrated by the results that Busbars with a higher electricity demand are more likely to offer downward flexibility while some other Busbars equipped with higher amount of renewable generation tend to provide upward flexibility.

Moreover, the share of flexibility from different flexible sources in mix was visualised, to show their ability in providing flexibility to the electric power system. It was found that, electrolysers could play a predominate role in offering upward flexibility with the coordination of linepack to meet the hydrogen demand. Heat pumps tended to provide downward flexibility rather than providing upward flexibility, since their energy consumption was optimised to minimise the operational cost.

Additionally, LMP value of the electric power system with and without flexibility was quantified. The results demonstrated that the electric power system equipped with sufficient flexibility, can be operated more effectively, with mitigated congestions with the transmission, and hence resulting in a lower renewable curtailment and load shedding. Furthermore, the relationship between LMP and system flexibility was investigated through carrying out a correlation analysis. The negative correlation indicating that an increase in the system’s capability to provide upward flexibility corresponds to a decrease in LMP.

Chapter 7 Conclusions and future work

7.1 Conclusions

A modelling framework for an integrated energy system (IES) was developed to optimise its operation by considering the complex interactions between diverse energy facilities. Initially, the model was applied to the gas network in South Wales and the Southwest, focusing on the optimal operation of compressor units. Subsequently, it was extended to the entire gas transmission system in Great Britain to demonstrate the potential of electric-driven compressors in providing flexibility to the electric power system. Additionally, the model was applied to an integrated hydrogen-electricity-heating system in Great Britain in 2050. The value of flexibility provided by different facilities or technologies was analysed, and the magnitude of flexibility available within the energy system was quantified based on a post-analysis.

7.1.1 Flexibility through coordinated operation of GDCs and EDCs in the gas network

Compressor units within the gas network can enhance flexibility by utilising linepack as a buffer. This study analysed the optimal operation of these units through case studies in South Wales, Southwest England, and across Great Britain.

The findings revealed that hybrid compressor stations—comprising both gas-driven compressors (GDCs) and electric-driven compressors (EDCs)—are cost-effective. Operational strategies adapt based on the relative costs of gas and electricity: EDCs are deployed when electricity is less expensive than gas, and conversely, GDCs are used when gas prices are lower.

Additionally, hybrid stations have shown a better performance in minimising the impact of cost fluctuations on the operation of compressor stations. The findings also indicate that the investment in new EDC units can be offset by the cost savings accrued over their lifetime, provided that future CO2 prices do not remain low.

7.1.2 Flexibility from an integrated energy system

The IES model was applied to an integrated hydrogen-electricity-heating network, with Great Britain in 2050 serving as the case study. It was shown by

the results that, by integrating various energy sectors, greater flexibility can be achieved through the coordinated use of diverse technologies and facilities.

A series of scenarios were defined to elucidate the role of distinct flexible resources in optimising the operation of the whole system. For instance, by allowing variations in linepack within the pipes, the hydrogen system's ability to balance the hydrogen demand and supply is enhanced.

The thermal inertia of building materials serves as a buffer, enabling residential heating systems to offer significant demand-side flexibility. Indoor temperatures can be adjusted flexibly within an acceptable range based on the discrepancy between renewable energy generation and base electricity demand.

Electrolysers can contribute additional flexibility by using excess electricity to produce hydrogen, which can then be supplied to the hydrogen network for immediate use or stored in pipelines. Furthermore, electrical energy storage units directly enhance the power system's flexibility through charging and discharging cycles.

Leveraging these forms of flexibility helps mitigate issues such as renewable energy curtailment, load shedding, and reliance on costly generation methods, significantly reducing the operational costs of the system. The results demonstrated that the operational costs of a system with sufficient flexibility were only about 25% of those of a comparable system lacking such capabilities.

7.1.3 Relationship between the flexibility magnitude and LMP of the electric power system

A post-analysis was conducted to quantify the flexibility of the electric power system. The results highlighted that the type and magnitude of flexibility vary significantly across different regions. For instance, busbars in London and the Midlands tend to offer downward flexibility in response to higher local demand, whereas those in Scotland generally provide upward flexibility, supported by higher renewable generation and lower demand.

Additionally, the results reveal that different components contribute to system flexibility in distinct ways. For example, Electrolysers predominantly offer upward flexibility, whereas heat pumps provide limited upward flexibility. However, heat pumps excel in offering downward flexibility, while electrolysers can only provide sufficient downward flexibility during specific hours.

A correlation analysis was conducted to determine the relationship between upward flexibility and the Locational Marginal Price (LMP) of the electric power system. The results indicated that Busbars with higher amounts of upward flexibility tend to have relatively lower LMPs, suggesting that upward flexibility plays a role in reducing the potential for congestion within the electric power system.

7.2 Future work

In this investigation, an effective model framework for the integrated energy system (IES) was developed. This framework is applicable to a variety of cases and scenarios, enabling the exploration of complex interactions between different sectors within the energy system.

However, the complexity of the mathematical model, which includes a large number of binary variables and nonlinear constraints to represent the operational status of certain facilities and hydraulic flow within various pipelines, limits its application for long-term optimisation. To avoid further complexify the optimisation, the representation of some facilities such as gas storge and battery storage units is simplified. For example, operational modes are not considered, as including them would introduce additional integer variables.

Furthermore, the system's operation was optimised under a set of specific scenarios without accounting for uncertainties such as renewable generation and ambient temperature.

Future improvements could involve embedding advanced approaches, such as physics-aware data-driven methods, into the IES model to enhance its performance. By doing this, it becomes more feasible to implement long-term expansion analysis that considers uncertainties. This enables the model to

provide additional insights, such as more efficient pathways to achieve Net Zero and informed investment decisions for installing new low-carbon technologies.

Reference

1. REBECCA LINDSEY & LUANN DAHLMAN. Climate Change: Global Temperature. https://www.climate.gov/news-features/understanding-climate/climate-change-global-temperature (2023).
2. Santosh Rao. *Carbon Tech Industry Poised for Transformative Growth*. https://drive.google.com/uc?export=download&id=1S5rrb423i5vF6SymxaHuoNOo8flObid6 (2023).
3. Department for Energy Security & Net Zero & Department for Business, E. & I. S. *Net Zero Strategy: Build Back Greener*. https://assets.publishing.service.gov.uk/media/6194dfa4d3bf7f0555071b1b/net-zero-strategy-beis.pdf.
4. Department for Energy Security & Net Zero. *Energy Trends December 2023 - GOV.UK*. https://www.google.com/url?sa=t&rct=j&q=&esrc=s&source=web&cd=&cad=rja&uact=8&ved=2ahUKEwjmtuTo4d6DAxULATQIHagTALEQFnoECA0QAw&url=https%3A%2F%2Fassets.publishing.service.gov.uk%2Fmedia%2F6582da2d23b70a0013234cef%2FEnergy_Trends_December_2023.pdf&usg=AOvVaw03yTfXJNOmbXA-yGBLYDM6&opi=89978449 (2023).
5. Climate Change Committee. *The Sixth Carbon Budget – Electricity Generation*. https://www.theccc.org.uk/wp-content/uploads/2020/12/Sector-summary-Electricity-generation.pdf (2020).
6. National Grid. *Future Energy Scenarios 2023 Report*. https://www.nationalgrideso.com/document/283101/download (2023).
7. National Grid. *Future Energy Scenarios: Pathways at a Glance*. https://www.neso.energy/document/321046/download (2024).

8. National Grid. *Introduction to Energy System Flexibility*. https://www.neso.energy/document/189851/download#:~:text=What%20is%20flexibility?,to%20achieve%20that%20energy%20balance.

9. LCP. *Renewable Curtailment and the Role of Long Duration Storage*. https://www.drax.com/wp-content/uploads/2022/06/Drax-LCP-Renewable-curtailment-report-1.pdf.

10. Bojan Lepic. UK losing over $1bn a year from wasted offshore wind power. https://splash247.com/uk-losing-over-1bn-a-year-from-wasted-offshore-wind-power/ (2024).

11. National Grid ESO. *Potential Electricity Storage Routes to 2050*. https://www.nationalgrideso.com/document/273166/download.

12. Department for Energy Security & Net Zero. *Transitioning to a Net Zero Energy System*. https://assets.publishing.service.gov.uk/media/60f575cd8fa8f50c7f08aecd/smart-systems-and-flexibility-plan-2021.pdf (2021).

13. Hannah Ritchie. The price of batteries has declined by 97% in the last three decades. https://www.google.com/url?sa=t&rct=j&q=&esrc=s&source=web&cd=&cad=rja&uact=8&ved=2ahUKEwjanKeqmv2DAxWFU0EAHTasBVIQFnoECCcQAQ&url=https%3A%2F%2Fourworldindata.org%2Fbattery-price-decline&usg=AOvVaw2hzdd9OcEZrJBxK6oGevU9&opi=89978449 (2021).

14. Michelle Lewis. Solar and battery storage prices have dropped almost 90% in 10 years. https://electrek.co/2023/09/25/solar-battery-storage-prices-dropped-almost-90-percent-in-10-years/ (2023).

15. Lithium-Ion Battery Pack Prices Hit Record Low of $139/kWh. https://about.bnef.com/blog/lithium-ion-battery-pack-prices-hit-record-low-of-139-kwh/ (2023).

16. Peters, J. F., Baumann, M., Zimmermann, B., Braun, J. & Weil, M. The environmental impact of Li-Ion batteries and the role of key

parameters – A review. *Renewable and Sustainable Energy Reviews* **67**, 491–506 (2017).

17. Notter, D. A. *et al.* Contribution of Li-Ion Batteries to the Environmental Impact of Electric Vehicles. *Environ Sci Technol* **44**, 6550–6556 (2010).

18. McManus, M. C. Environmental consequences of the use of batteries in low carbon systems: The impact of battery production. *Appl Energy* **93**, 288–295 (2012).

19. Majeau-Bettez, G., Hawkins, T. R. & Strømman, A. H. Life Cycle Environmental Assessment of Lithium-Ion and Nickel Metal Hydride Batteries for Plug-In Hybrid and Battery Electric Vehicles. *Environ Sci Technol* **45**, 4548–4554 (2011).

20. García, A., Monsalve-Serrano, J., Martinez-Boggio, S. & Soria Alcaide, R. Carbon footprint of battery electric vehicles considering average and marginal electricity mix. *Energy* **268**, 126691 (2023).

21. Fagiolari, L. *et al.* Integrated energy conversion and storage devices: Interfacing solar cells, batteries and supercapacitors. *Energy Storage Mater* **51**, 400–434 (2022).

22. Wali, S. Bin *et al.* Battery storage systems integrated renewable energy sources: A biblio metric analysis towards future directions. *J Energy Storage* **35**, 102296 (2021).

23. Karimi, H. & Jadid, S. Multi-layer energy management of smart integrated-energy microgrid systems considering generation and demand-side flexibility. *Appl Energy* **339**, 120984 (2023).

24. Gilson Dranka, G., Ferreira, P. & Vaz, A. I. F. Co-benefits between energy efficiency and demand-response on renewable-based energy systems. *Renewable and Sustainable Energy Reviews* **169**, 112936 (2022).

25. Hunter, C. A. *et al.* Techno-economic analysis of long-duration energy storage and flexible power generation technologies to support high-variable renewable energy grids. *Joule* **5**, 2077–2101 (2021).

26. Guerra, O. J., Eichman, J., Kurtz, J. & Hodge, B.-M. Cost Competitiveness of Electrolytic Hydrogen. *Joule* **3**, 2425–2443 (2019).

27. Sepulveda, N. A., Jenkins, J. D., Edington, A., Mallapragada, D. S. & Lester, R. K. The design space for long-duration energy storage in decarbonized power systems. *Nat Energy* **6**, 506–516 (2021).

28. Glenk, G. & Reichelstein, S. Economics of converting renewable power to hydrogen. *Nat Energy* **4**, 216–222 (2019).

29. Peng, P. *et al.* Cost and potential of metal–organic frameworks for hydrogen back-up power supply. *Nat Energy* **7**, 448–458 (2022).

30. Huang, J. *et al.* Decoupled amphoteric water electrolysis and its integration with Mn–Zn battery for flexible utilization of renewables. *Energy Environ Sci* **14**, 883–889 (2021).

31. Canet, A. & Qadrdan, M. Quantification of flexibility from the thermal mass of residential buildings in England and Wales. *Appl Energy* **349**, 121616 (2023).

32. Qin, H., Yu, Z., Li, T., Liu, X. & Li, L. Energy-efficient heating control for nearly zero energy residential buildings with deep reinforcement learning. *Energy* **264**, 126209 (2023).

33. Zhang, Y., Johansson, P. & Sasic Kalagasidis, A. Feasibilities of utilizing thermal inertia of district heating networks to improve system flexibility. *Appl Therm Eng* **213**, 118813 (2022).

34. Jansen, J., Jorissen, F. & Helsen, L. Optimal control of a fourth generation district heating network using an integrated non-linear model predictive controller. *Appl Therm Eng* **223**, 120030 (2023).

35. Quirosa, G., Torres, M. & Chacartegui, R. Analysis of the integration of photovoltaic excess into a 5th generation district heating and cooling system for network energy storage. *Energy* **239**, 122202 (2022).

36. Chen, Q., Zhao, Y., Qadrdan, M. & Jenkins, N. Optimal Operation of Compressors in an Integrated Gas and Electricity System—An Enhanced MISOCP Method. *IEEE Access* **10**, 131489–131497 (2022).

37. Chen, Q., Zhang, T. & Qadrdan, M. Assessing Techno-Economic and Environmental Impacts of Gas Compressor Fleet as a Source of Flexibility to the Power System. *IEEE Transactions on Energy Markets, Policy and Regulation* **1**, 274–285 (2023).

38. Rostami, A. M., Ameli, H., Ameli, M. T. & Strbac, G. Secure Operation of Integrated Natural Gas and Electricity Transmission Networks. *Energies (Basel)* **13**, 4954 (2020).

39. Zhang, Z. *et al.* Day-Ahead Optimal Dispatch for Integrated Energy System Considering Power-to-Gas and Dynamic Pipeline Networks. *IEEE Trans Ind Appl* **57**, 3317–3328 (2021).

40. Faraji, H. & Hemmati, R. Centralized Multifunctional Control of Integrated Electricity–Gas Network in District Energy System Considering Resilience. *IEEE Trans Industr Inform* **20**, 649–658 (2024).

41. Tan, H., Yan, W., Ren, Z., Wang, Q. & Mohamed, M. A. A robust dispatch model for integrated electricity and heat networks considering price-based integrated demand response. *Energy* **239**, 121875 (2022).

42. Li, X. *et al.* Collaborative scheduling and flexibility assessment of integrated electricity and district heating systems utilizing thermal inertia of district heating network and aggregated buildings. *Appl Energy* **258**, 114021 (2020).

43. Martinez Cesena, E. A., Loukarakis, E., Good, N. & Mancarella, P. Integrated Electricity– Heat–Gas Systems: Techno–Economic Modeling, Optimization, and Application to Multienergy Districts. *Proceedings of the IEEE* **108**, 1392–1410 (2020).

44. Farrokhifar, M., Nie, Y. & Pozo, D. Energy systems planning: A survey on models for integrated power and natural gas networks coordination. *Appl Energy* **262**, 114567 (2020).

45. Zhang, S. & Chen, W. Assessing the energy transition in China towards carbon neutrality with a probabilistic framework. *Nat Commun* **13**, 87 (2022).

46. Schilt, U. *et al.* Modelling of multi-energy systems of residential buildings with Calliope and validation of results. *J Phys Conf Ser* **2600**, 032005 (2023).

47. CE-080 Natural Gas Pipeline Flow Calculations | PDH STAR. *CE-080 Natural Gas Pipeline Flow Calculations | PDH STAR*. https://pdhstar.com/wp-content/uploads/2019/04/CE-080-Natural-Gas-Pipeline-Flow-Calculations.pdf.

48. Wang, D. *et al.* Optimal scheduling strategy of district integrated heat and power system with wind power and multiple energy stations considering thermal inertia of buildings under different heating regulation modes. *Appl Energy* **240**, 341–358 (2019).

49. National Grid. *Gas Ten Year Statement 2020*. https://www.nationalgas.com/document/133851/download#:~:text=We%20have%20published%20the%202020,GTYS)%20as%20an%20interactive%20document.&text=We%20are%20in%20the%20midst,ever%20before%20for%20our%20industry. (2020).

50. OFGEM. *Compressor Emissions Compliance Strategy Guidance*. https://www.ofgem.gov.uk/sites/default/files/docs/2019/06/compressor_emissions_compliance_guidance.pdf (2019).

51. Zhao, Y., Xu, X., Qadrdan, M. & Wu, J. Optimal operation of compressor units in gas networks to provide flexibility to power systems. *Appl Energy* **290**, 116740 (2021).

52. MIT. *Nonlinear Programming*.

53. Hochbaum, D. S. Complexity and algorithms for nonlinear optimization problems. *Ann Oper Res* **153**, 257–296 (2007).

54. Mu, Y. *et al.* A two-stage scheduling method for integrated community energy system based on a hybrid mechanism and data-driven model. *Appl Energy* **323**, 119683 (2022).

55. Fleschutz, M., Bohlayer, M., Braun, M., Henze, G. & Murphy, M. D. The effect of price-based demand response on carbon emissions in

European electricity markets: The importance of adequate carbon prices. *Appl Energy* **295**, 117040 (2021).

56. Chen, L. *et al*. Communication reliability-restricted energy sharing strategy in active distribution networks. *Appl Energy* **282**, 116238 (2021).

57. Guzmán-Feria, J. S., Castro, L. M., Tovar-Hernández, J. H., González-Cabrera, N. & Gutiérrez-Alcaraz, G. Unit commitment for multi-terminal VSC-connected AC systems including BESS facilities with energy time-shifting strategy. *International Journal of Electrical Power & Energy Systems* **134**, 107367 (2022).

58. Rigo-Mariani, R., Chea Wae, S. O., Mazzoni, S. & Romagnoli, A. Comparison of optimization frameworks for the design of a multi-energy microgrid. *Appl Energy* **257**, 113982 (2020).

59. Hurwitz, Z. L., Dubief, Y. & Almassalkhi, M. Economic efficiency and carbon emissions in multi-energy systems with flexible buildings. *International Journal of Electrical Power & Energy Systems* **123**, 106114 (2020).

60. Chen, S., Conejo, A. J., Sioshansi, R. & Wei, Z. Unit Commitment With an Enhanced Natural Gas-Flow Model. *IEEE Transactions on Power Systems* **34**, 3729–3738 (2019).

61. Schwele, A., Arrigo, A., Vervaeren, C., Kazempour, J. & Vallée, F. Coordination of Electricity, Heat, and Natural Gas Systems Accounting for Network Flexibility. *Electric Power Systems Research* **189**, 106776 (2020).

62. Chen, Y., Yao, Y. & Zhang, Y. A Robust State Estimation Method Based on SOCP for Integrated Electricity-Heat System. *IEEE Trans Smart Grid* **12**, 810–820 (2021).

63. Sharma, A. & Padhy, N. P. Towards the Decentralized Energy Optimization of Active Unbalanced Distribution Systems Integrated with Natural Gas Systems. in *2022 IEEE International Conference on*

Power Electronics, Drives and Energy Systems (PEDES) 1–5 (IEEE, 2022). doi:10.1109/PEDES56012.2022.10080268.

64. Han, H., Zhang, H., Yang, J. & Su, H. Distributed Model Predictive Consensus Control for Stable Operation of Integrated Energy System. *IEEE Trans Smart Grid* **15**, 381–393 (2024).

65. Chowdhury, M. M.-U.-T., Kamalasadan, S. & Paudyal, S. A Second-Order Cone Programming (SOCP) Based Optimal Power Flow (OPF) Model With Cyclic Constraints for Power Transmission Systems. *IEEE Transactions on Power Systems* **39**, 1032–1043 (2024).

66. Huang, G., Wang, J., Wang, C. & Guo, C. Cascading imbalance in coupled gas-electric energy systems. *Energy* **231**, 120846 (2021).

67. McCormick, G. P. Computability of global solutions to factorable nonconvex programs: Part I — Convex underestimating problems. *Math Program* **10**, 147–175 (1976).

68. Zhang, C., Jiao, Z., Liu, J. & Ning, K. Robust planning and economic analysis of park-level integrated energy system considering photovoltaic/thermal equipment. *Appl Energy* **348**, 121538 (2023).

69. Sun, B. *et al.* An Effective Spinning Reserve Allocation Method Considering Operational Reliability With Multi-Uncertainties. *IEEE Transactions on Power Systems* **39**, 1568–1581 (2024).

70. Fernandes, L. M., Júdice, J. J., Sherali, H. D. & Antunes, A. P. Siting and Sizing of Facilities under Probabilistic Demands. *J Optim Theory Appl* **149**, 420–440 (2011).

71. *Conversion Guidelines - Greenhouse Gas Emissions -*. https://www.eeagrants.gov.pt/media/2776/conversion-guidelines.pdf.

72. National grid. *HyNTS: Hydrogen in the NTS*. https://www.nationalgas.com/document/133841/download.

73. BEIS. *Gas Security of Supply: A Strategic Assessment of Great Britain's Gas Security of Supply*.

https://assets.publishing.service.gov.uk/media/5c376d9d40f0b67c362849ec/gas-security-supply-assessment.pdf (2017).

74. Jamie Speirs, Francisca Jalil Vega, Pedro Gerber Machado University & Sara giarola. *The Flexibility of Gas: What Is It Worth?* DOI:10.13140/RG.2.2.20219.13602 (2020).

75. Quarton, C. J. & Samsatli, S. Should we inject hydrogen into gas grids? Practicalities and whole-system value chain optimisation. *Appl Energy* **275**, 115172 (2020).

76. Yamchi, H. B., Safari, A. & Guerrero, J. M. A multi-objective mixed integer linear programming model for integrated electricity-gas network expansion planning considering the impact of photovoltaic generation. *Energy* **222**, 119933 (2021).

77. Li, X. *et al.* Security region of natural gas network in electricity-gas integrated energy system. *International Journal of Electrical Power & Energy Systems* **117**, 105601 (2020).

78. Cui, Z., Chen, J., Liu, C. & Zhao, H. Time-domain continuous power flow calculation of electricity–gas integrated energy system considering the dynamic process of gas network. *Energy Reports* **8**, 597–605 (2022).

79. AlHajri, I., Ahmadian, A. & Elkamel, A. Techno-economic-environmental assessment of an integrated electricity and gas network in the presence of electric and hydrogen vehicles: A mixed-integer linear programming approach. *J Clean Prod* **319**, 128578 (2021).

80. Mi, J. & Khodayar, M. E. Operation of natural gas and electricity networks with line pack. *Journal of Modern Power Systems and Clean Energy* **7**, 1056–1070 (2019).

81. Dvorkin, V., Mallapragada, D., Botterud, A., Kazempour, J. & Pinson, P. Multi-stage linear decision rules for stochastic control of natural gas networks with linepack. *Electric Power Systems Research* **212**, 108388 (2022).

82. Bao, Z., Chen, D., Wu, L. & Guo, X. Optimal inter- and intra-hour scheduling of islanded integrated-energy system considering linepack of gas pipelines. *Energy* **171**, 326–340 (2019).

83. Rabiee, A., Kamwa, I., Keane, A. & Soroudi, A. Gas Network's Impact on Power System Voltage Security. *IEEE Transactions on Power Systems* **36**, 5428–5440 (2021).

84. Shabazbegian, V., Ameli, H., Ameli, M. T., Strbac, G. & Qadrdan, M. Co-optimization of resilient gas and electricity networks; a novel possibilistic chance-constrained programming approach. *Appl Energy* **284**, 116284 (2021).

85. Fang, J., Zeng, Q., Ai, X., Chen, Z. & Wen, J. Dynamic Optimal Energy Flow in the Integrated Natural Gas and Electrical Power Systems. *IEEE Trans Sustain Energy* **9**, 188–198 (2018).

86. Wang, C., Wei, W., Wang, J., Wu, L. & Liang, Y. Equilibrium of Interdependent Gas and Electricity Markets With Marginal Price Based Bilateral Energy Trading. *IEEE Transactions on Power Systems* **33**, 4854–4867 (2018).

87. Mirzaei, M. A. *et al.* A Novel Hybrid Framework for Co-Optimization of Power and Natural Gas Networks Integrated With Emerging Technologies. *IEEE Syst J* **14**, 3598–3608 (2020).

88. Isam Saedi, Sleiman Mhanna, Han Wang & Pierluigi Mancarella. Integrated Electricity and Gas Systems Modelling: Assessing the Impacts of Electrification of Residential Heating in Victoria. in *Australasian Universities Power Engineering Conference* (2020).

89. Wu, Q. H. *et al.* Optimal operation of integrated energy systems subject to the coupled demand constraints of electricity and natural gas. *CSEE Journal of Power and Energy Systems* (2019) doi:10.17775/CSEEJPES.2018.00640.

90. Zheng, J. H., Wu, Q. H. & Jing, Z. X. Coordinated scheduling strategy to optimize conflicting benefits for daily operation of integrated electricity and gas networks. *Appl Energy* **192**, 370–381 (2017).

91. Qadrdan, M., Ameli, H., Strbac, G. & Jenkins, N. Efficacy of options to address balancing challenges: Integrated gas and electricity perspectives. *Appl Energy* **190**, 181–190 (2017).

92. National grid. *Gas Ten Year Statement*. https://www.nationalgas.com/document/137861/download (2021).

93. Qadrdan, M., Chaudry, M., Wu, J., Jenkins, N. & Ekanayake, J. Impact of a large penetration of wind generation on the GB gas network. *Energy Policy* **38**, 5684–5695 (2010).

94. Ofgem. *Compressor Emissions Compliance Strategy Guidance*. https://www.ofgem.gov.uk/sites/default/files/docs/2019/06/compressor_emissions_compliance_guidance.pdf (2019).

95. GOV. U.K. *Guidance on Estimating Carbon Values beyond 2050: An Interim Approach*. https://assets.publishing.service.gov.uk/media/5a756347ed915d6faf2b297a/1_20100120165619_e____carbonvaluesbeyond2050.pdf (2011).

96. Borasio, M. & Moret, S. Deep decarbonisation of regional energy systems: A novel modelling approach and its application to the Italian energy transition. *Renewable and Sustainable Energy Reviews* **153**, 111730 (2022).

97. Gonzalez, J. M. *et al.* Designing diversified renewable energy systems to balance multisector performance. *Nat Sustain* **6**, 415–427 (2023).

98. Zeyringer, M., Price, J., Fais, B., Li, P.-H. & Sharp, E. Designing low-carbon power systems for Great Britain in 2050 that are robust to the spatiotemporal and inter-annual variability of weather. *Nat Energy* **3**, 395–403 (2018).

99. Zantye, M. S., Arora, A. & Hasan, M. M. F. Renewable-integrated flexible carbon capture: a synergistic path forward to clean energy future. *Energy Environ Sci* **14**, 3986–4008 (2021).

100. Pickering, B., Lombardi, F. & Pfenninger, S. Diversity of options to eliminate fossil fuels and reach carbon neutrality across the entire European energy system. *Joule* **6**, 1253–1276 (2022).

101. Guo, F. *et al.* Implications of intercontinental renewable electricity trade for energy systems and emissions. *Nat Energy* **7**, 1144–1156 (2022).

102. Clegg, S. & Mancarella, P. Integrated Electrical and Gas Network Flexibility Assessment in Low-Carbon Multi-Energy Systems. *IEEE Trans Sustain Energy* **7**, 718–731 (2016).

103. de Chalendar, J. A., Glynn, P. W. & Benson, S. M. City-scale decarbonization experiments with integrated energy systems. *Energy Environ Sci* **12**, 1695–1707 (2019).

104. Seward, W., Qadrdan, M. & Jenkins, N. Revenue stacking for behind the meter battery storage in energy and ancillary services markets. *Electric Power Systems Research* **211**, 108292 (2022).

105. Mimica, M., Boras, I.-P. & Krajačić, G. The integration of the battery storage system and coupling of the cooling and power sector for increased flexibility under the consideration of energy and reserve market. *Energy Convers Manag* **286**, 117005 (2023).

106. National Grid. Future energy scenarios 2023 Data workbook. (2023).

107. Canet, A., Qadrdan, M., Jenkins, N. & Wu, J. Spatial and temporal data to study residential heat decarbonisation pathways in England and Wales. *Sci Data* **9**, 246 (2022).

108. National grid ESO. *Electricity Ten Year Statement*. https://www.nationalgrideso.com/document/275611/download (2022).

109. Bai, Y. *et al.* Flexibility quantification and enhancement of flexible electric energy systems in buildings. *Journal of Building Engineering* **68**, 106114 (2023).

110. Carlucci, F., Negendahl, K. & Fiorito, F. Energy flexibility of building systems in future scenarios: optimization of the control strategy of a dynamic shading system and definition of a new energy flexibility metric. *Energy Build* **289**, 113056 (2023).

111. Triolo, R. C., Rajagopal, R., Wolak, F. A. & de Chalendar, J. A. Estimating cooling demand flexibility in a district energy system using temperature set point changes from selected buildings. *Appl Energy* **336**, 120816 (2023).

112. Firdous, A., Prakash Barala, C., Mathuria, P. & Bhakar, R. Extended power to hydrogen operations for enhanced grid flexibility in low carbon systems. *Energy Convers Manag* **301**, 117982 (2024).

113. SARP OZKAN. An Intro to Locational Marginal Pricing. https://www.enverus.com/blog/an-intro-to-locational-marginal-pricing/ (2022).

114. Simon Gill, Keith Bell & Callum MacIver. The Potential Impact of Locational Marginal Pricing. https://ukerc.ac.uk/news/potential-lmp-impacts/ (2023).